Accepted Manuscript

Synthesis and structure-activity relationship of trisubstituted thiazoles as Cdc7 kinase inhibitors

Andreas Reichelt, Julie M. Bailis, Michael D. Bartberger, Guomin Yao, Hong Shu, Matthew R. Kaller, John G. Allen, Margaret F. Weidner, Kathleen S. Keegan, Jennifer H. Dao

PII: S0223-5234(14)00332-8

DOI: 10.1016/j.ejmech.2014.04.013

Reference: EJMECH 6884

To appear in: *European Journal of Medicinal Chemistry*

Received Date: 22 January 2013

Revised Date: 1 April 2014

Accepted Date: 4 April 2014

Please cite this article as: A. Reichelt, J.M. Bailis, M.D. Bartberger, G. Yao, H. Shu, M.R. Kaller, J.G. Allen, M.F. Weidner, K.S. Keegan, J.H. Dao, Synthesis and structure-activity relationship of trisubstituted thiazoles as Cdc7 kinase inhibitors, *European Journal of Medicinal Chemistry* (2014), doi: 10.1016/j.ejmech.2014.04.013.

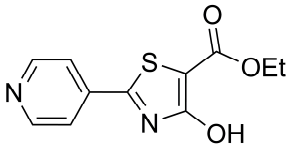

>130 analogues

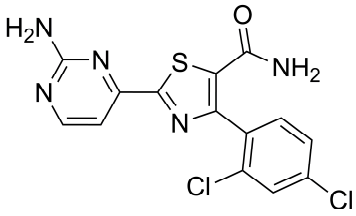

HTS hit **1**
Cdc7 IC_{50} = 0.323 μM
pMCM2 IC_{50} > 50 μM

74
Cdc7 IC_{50} = 0.00377 μM
pMCM2 IC_{50} = 0.501 μM

Synthesis and structure-activity relationship of trisubstituted thiazoles as Cdc7 kinase inhibitors

Andreas Reichelt[a,*], *Julie M. Bailis*[b], *Michael D. Bartberger*[c], *Guomin Yao*[a], *Hong Shu*[a], *Matthew R. Kaller*[a], *John G. Allen*[a], *Margaret F. Weidner*[b], *Kathleen S. Keegan*[b], *Jennifer H. Dao*[c]

[a]*Departments of Medicinal Chemistry, Amgen, Inc., One Amgen Center Drive, Thousand Oaks, California 91320.* [b]*Oncology Research, Amgen, Inc., 1201 Amgen Court West, Seattle, Washington 98119.* [c]*Molecular Structure and Characterization, Amgen, Inc., One Amgen Center Drive, Thousand Oaks, California 91320.*

ABSTRACT: The Cell division cycle 7 (Cdc7) protein kinase is essential for DNA replication and maintenance of genome stability. We systematically explored thiazole-based compounds as inhibitors of Cdc7 kinase activity in cancer cells. Our studies resulted in the identification of a potent, selective Cdc7 inhibitor that decreased phosphorylation of the direct substrate MCM2 *in vitro* and *in vivo*, and inhibited DNA synthesis and cell viability *in vitro*.

KEYWORDS: Cdc7; MCM2; kinase inhibitor; DNA replication; thiazole

* Corresponding Author. Phone: +1 (805) 313-5225. Fax: +1 (805) 480-3015. E-mail: Andreas.Reichelt@amgen.com

1. Introduction

The complete, accurate replication of the DNA in each cell cycle is fundamental to maintaining genomic stability. In cancer cells, oncogene activation or loss of tumor suppressor function can lead to increased replication stress and deregulation of cell cycle controls. Proteins that control key transitions in DNA replication and cell cycle progression therefore represent potential nodes for therapeutic intervention in cancer.

The serine/threonine protein kinase Cdc7 is essential for the activation of individual origins of replication and the initiation of DNA synthesis.[1,2] Cdc7 activation depends on the bipartite binding of a subunit, Dbf4.[2] Cdc7/Dbf4 phosphorylates proteins associated with the replication origin, such as the minichromosome maintenance (MCM) complex, to trigger origin firing.[2] In particular, direct phosphorylation of the MCM2 subunit by Cdc7/Dbf4 promotes a conformational change in the MCM complex that activates its helicase activity and initiates local DNA unwinding.[2] This allows the association of other proteins required for DNA synthesis, such as DNA polymerase, to the exposed regions of single-stranded DNA.[2]

Cdc7 plays a key role not only in activating origins to initiate synthesis, but also in regulating ongoing replication. Cdc7 promotes the phosphorylation and activation of Chk1 and the replication checkpoint,[3] which responds to blocks of replication fork progression or limiting amounts of nucleosides by arresting cells in S phase. Checkpoint activation may downregulate Cdc7 kinase, preventing additional replication origins from firing,[4] or Cdc7 may be required for recovery from replication fork arrest.[5]

Given its essential function in cell proliferation, Cdc7 has been considered as a novel target for cancer therapy.[6,7,8] Cdc7 inhibition with siRNA or small molecule inhibitors arrests normal cells at G1/S after activation of a cell cycle checkpoint, but is lethal to cancer cells that cannot activate this checkpoint due to defects in the DNA damage response pathway.[9,10,11,12,13] Expression levels of Cdc7 and Dbf4 are increased in cancer cells, and amplification of Dbf4 has been identified in some breast and ovarian cancer cell lines.[14,15,16] Although interfering with the DNA replication process is

a proven strategy for cancer therapy, efficacy of current drugs that target this pathway is limited by cytotoxicity to normal cells and inherent or acquired drug resistance. Compounds that inhibit Cdc7 kinase activity provide a potential advantage in that they target the initiation step of DNA replication, rather than replication fork progression, and that toxicity may be decreased due to activation of a cellular checkpoint response in normal cells. The interest in Cdc7 as a target for cancer therapy is demonstrated by the report of several potent Cdc7 inhibitors by different research groups[17,18,19,20,21,22,23,24] but clinical trials with Cdc7 inhibitors have not yet moved past Phase I studies.

In our laboratories, high-throughput screening (HTS) efforts aimed at the discovery of inhibitors of Cdc7 kinase activity led to the identification of compounds bearing a thiazole core. In particular, thiazole **1** (Figure 1) was found to be a sub-micromolar inhibitor of Cdc7 kinase activity and showed no detectable activity in our primary counter screen against the structural and functional homolog, cyclin-dependent kinase CDK2. The synthetic approach to this compound allowed for the rapid synthesis of analogues with variations at all substituents on the thiazole ring. Herein, we describe the synthesis and structure-activity relationship (SAR) of compounds based on the thiazole scaffold of **1**, eventually leading to **74**, a potent and selective Cdc7 inhibitor.

[Please, insert Figure 1 here]

2. Chemistry

The thiazole cores of the compounds described in this paper were generally formed by reaction of thioamides with diethyl bromomalonate (**3**) as demonstrated by the synthesis of compound **1** (Scheme 1). The hydroxyl substituent in **1** was further elaborated by alkylation to form ether **4** or was transformed into the corresponding triflate **5**. Reaction of **5** with ammonia as well as primary or secondary amines led to the 4-amino substituted thiazoles **6**–**10**. Compound **13** that lacks a substituent at C4 of the thiazole was synthesized by Suzuki coupling of commercially available ethyl 2-

bromothiazole-5-carboxylate (**12**) with 4-pyridineboronic acid (**11**), while the synthesis of 4-methyl thiazole **15** was achieved by reaction of pyridine-4-carbothioamide (**2**) with ethyl 2-chloro-3-oxobutanoate (**14**). Suzuki-coupling of triflate **5** with a variety of boronic acids and esters gave convenient access to compounds **16**–**24**, which bear aromatic substituents at the 4-position of the thiazole.

[Please, insert Scheme 1 here]

Amide **27** was synthesized analogously to its corresponding ester **1** by condensation of pyridine-4-carbothiamide (**2**) with bromide **26** (Scheme 2). Saponification of the ester moiety in **1** delivered the hydrochloride salt of acid **28**, which was transformed into the corresponding acid chloride. Reaction of the crude acid chloride with a variety of amines gave amides **29**–**31**. Activation of acid **32**, prepared by saponification of ester **16**, with HATU followed by treatment with ammonia, hydrazine, or hydroxylamine hydrochloride delivered the primary amide **33**, hydrazide **34**, and hydroxamic acid **35**, respectively. Other amides bearing different functional groups at the 4-position of the thiazole were prepared analogously.

[Please, insert Scheme 2 here]

The syntheses of thiazoles bearing heterocyclic carbonyl replacements at the 4-position are illustrated in Scheme 3. Dehydration of amide **33** under Swern oxidation conditions[25] gave nitrile **38**, which was transformed into tetrazole **39** by reaction with sodium azide in the presence of zinc bromide.[26] Oxadiazole **40** was obtained by reaction of hydrazide **34** with trimethyl orthoformate under acidic conditions. Displacement of the triflate moiety in **5** with 1,2-phenylenediamine followed by cyclization gave lactam **41**.

[Please, insert Scheme 3 here]

Our general strategy for the formation of the thiazole core was also applicable to the synthesis of analogues of **1** with diverse substituents at the 2-position of the thiazole (Scheme 4). Thus, reaction of a variety of thioamides **42** with bromides **3** or **52** gave easy access to compounds **43**–**51** and **53**–**54**, respectively. Thioamides that were not commercially available were synthesized from the corresponding chlorides as shown in Scheme 4.

[Please, insert Scheme 4 here]

The complete reaction sequence to 2-(2-amino-4-pyrinidyl)thiazole-5-carboxamides bearing aromatic or amino groups at the 4-position of the thiazole is outlined in Scheme 5. Transformation of 2-amino-4-chloropyrimidine (**55**) into the corresponding iodide followed by palladium-mediated cyanation gave 2-amino-4-cyanopyrimidine. Treatment with ammonium sulfite delivered thioamide **60**, which was cyclized to thiazole **46** following the standard protocol. The corresponding triflate was employed in Suzuki-reactions or displaced with dimethylamine to give access to the 4-substituted thiazoles **63**–**70**. A two-step transformation of the esters to the primary amides then afforded analogues **71**–**78**.

[Please, insert Scheme 5 here]

3. Pharmacology

Cdc7/Dbf4 biochemical activity was assessed through a Protein A Amplified Luminescent Proximity Homogenous Assay (AlphaScreen). Counter screens to determine the biochemical activity of related protein kinases CDK2/Cyclin E, CDK1/Cyclin B, CDK4/Cyclin D1, Pim1, Pim2, CDK9/Cyclin T1, CK2, and CK1 employed homogeneous time-resolved fluorescence (HTRF) assays. MCM2 phosphorylation was assessed by high content imaging in HCT-116 cells and with a Meso-Scale

Discovery (MSD) assay in tumor xenografts. Additional assays in HCT-116 cells were bromodeoxyuridine (BrdU) incorporation measured using a colorometric ELISA assay, cell viability assessed using a Cell Titer-glo assay, and DNA content evaluated by flow cytometry. See Experimental protocols for details.

4. Results and discussion

Intrigued by the arguments for Cdc7 as a potential novel target for cancer, we initiated a high-throughput screen of a library of approximately 250,000 compounds for Cdc7 kinase inhibitors. In this HTS campaign, we identified a high hit rate (1.1%) of Cdc7 inhibitors and we counter screened for compounds with selectivity against CDK2, a closely related kinase that shares both structural and functional homology with Cdc7.[1] Verified hits from the screen represented several, distinct chemical series with remarkably low molecular weights and high binding efficiencies for inhibitors of kinase activity. Prioritization of series based on drug-like properties led us to focus initially on a class of compounds featuring a thiazole core.

Compound **1** was the most promising hit in a series of thiazoles that was obtained from the HTS screen. In a biochemical assay for Cdc7 kinase activity (see Experimental protocols), the IC_{50} of **1** was determined to be 0.323 μM, with no activity (IC_{50} >125 μM) detected in the counter screen assay against CDK2. Mechanism of action studies indicated this compound to be ATP competitive (Supplementary Figure 1). Thiazole **1** appeared to be a very selective compound: in a panel of 100 kinases (KinomeSCAN, Ambit Bioscience, Inc.), compound **1** did not show any response with a percent of control (POC) <50 at 1 μM (Supplementary Figure 2), and no agonist or antagonist activity was detected in a panel of 13 receptors. The origin of this compound had been as an intermediate in a series of potential CDK5 inhibitors;[27] its low molecular weight combined with its potency corresponds to a binding efficiency of >0.5. It also exhibits other favorable characteristics including low intrinsic clearance in human liver microsomes (HLM) and rat liver microsomes (RLM), (17 and <14 μl/min/mg, respectively), good permeability and low efflux ratios ($P_{app} \geq 8.9 \times 10^{-6}$ cm/s, ER = 1 for parental,

MDR1- and rat mdr1-infected LLC-PK1 cells). The structure of **1** offered multiple points for diversification and its efficient synthetic scheme allowed for the rapid synthesis of analogues.

An X-ray crystal structure, while not available during the course of our medicinal chemistry campaign, has recently been reported for Cdc7 kinase and its activator Dbf4.[28] Although the structure-activity relationships reported in this manuscript were carried out in a ligand-based fashion in the absence of crystallographic information, the subsequent publication of the Cdc7/Dbf4 structure made it possible to retrospectively analyze the binding of compound **1** and subsequent analogs in the active site of Cdc7.

The predicted binding mode for the initial hit **1,** arising from docking of the lowest-energy conformation as determined by quantum mechanics into the ATP binding site, is depicted in Figure 2.[29,30,31,32] The pyridine nitrogen of **1** is engaged in a hydrogen bond to the backbone NH of the linker LEU137, whereas the ethyl ester functionality projects outward toward the exterior of the ATP binding site, with an intramolecular hydrogen bond predicted between the thiazole hydroxyl group and the carbonyl of the ethyl ester.

[Please, insert Figure 2 here]

Early SAR from our HTS campaign suggested that variations at the 4-position of the thiazole might lead to compounds with improved affinity for Cdc7 but extensive SAR studies disproved this hypothesis. Selected examples from a series of 2-(4-pyridyl)thiazole-5-carboxylates varying by the substituent at C4 are shown in Table 1. Alkylation of the 4-hydroxy group was not tolerated, as methyl ether **4** lost two orders of magnitude in its inhibitory activity against Cdc7 kinase compared with alcohol **1**. The precipitous loss of activity of ether **4** (17.2 μM) upon O-alkylation of compound **1** can be explained by disruption of the intramolecular H-bonding motif and likely resultant steric clash of the alkoxyl and/or ester function with nearby residues LEU195, ASP96, or LYS90.

Introduction of 4-amino substituents led to compounds with a wide range of potencies: the primary amine **6** showed micromolar activity as did compound **7** that bears a methyl amino group at the 4-position of the thiazole. Larger substituents at the amine as in **8** (NHBn) and in **9** (NHPh) were not tolerated. The dimethylamino analogue **10** however, showed activities comparable with **1**. Removal of the substituent at the 4-position of the thiazole in **13** or replacement with a small alkyl group (e.g. methyl in **15**) led to compounds with micromolar activities. Thiazoles bearing unsubstituted aryl moieties as C4-substituents (**16** and **23**) were 25–60-fold less potent than **1**; however, this loss of potency could be restored by introduction of substituents on the aromatic ring. In particular, compound **18** that bears an *ortho*-chloro phenyl group at the 4-position of the thiazole showed sub-micromolar levels of activity. Substituents on the phenyl ring in addition to *ortho*-chloro were tolerated as well (**19**–**22**). Large aromatic groups like the 2-naphthyl group in **24** were not tolerated at the 4-position of the thiazole. None of the compounds showed any detectable inhibitory activity against CDK2. Overall, the variations in the substituent on the 4-position of the thiazole ethyl esters depicted in Table 1 led to compounds with activities at best as good as our starting point **1** and we focused our attention toward the 5-substituent.

[Please, insert Table 1 here]

Exploration of the influence of substituents at C5 on the thiazole ring on the inhibitory activity against Cdc7 revealed some promising trends (Table 2). Acids were generally found to be one to two orders of magnitude more potent than their corresponding esters, as exemplified in the comparison of ester **16** (IC_{50} = 20.5 µM) with acid **32** (IC_{50} = 0.172 µM). However, we noticed an interesting relationship between the substituents at C4 and C5 in acid **28** as this compound, which was isolated as its hydrochloride salt, exhibited an IC_{50} of 6.13 µM, 20-fold less potent than ester **1**. Primary amides, on the other hand, were uniformly found to be more potent: compounds **27** and **33**, for example, showed IC_{50} values of 0.115 µM and 0.101 µM, respectively. The activities of secondary and tertiary amides

(e.g. **29**–**31)** were in the micromolar range. Hydrazide **34**, hydroxamic acid **35,** and nitrile **38** as well as the 5-heterocycle substituted thiazoles **39** and **40** showed improved activity compared to ethyl ester **16** but none of these compounds reached the activity level of primary amide **33**. Only lactam **41** showed an IC_{50} comparable with amides **27** and **33** but significantly reduced selectivity over CDK2 (11-fold vs. >300-fold).

[Please, insert Table 2 here]

Having established the primary amide as the optimal C5-substituent, several amides with different substituents at the 4-position of the thiazole were synthesized. These compounds showed activities around 0.1 µM, which in many cases equated to potency increases of two orders of magnitude compared to their corresponding esters (Table 3). In order to test whether the biochemical potency would translate into an effect on cells, phosphorylation of SER53 in MCM2, a Cdc7-dependent, Cdc7-specific phosphorylation site,[33,34] was analyzed in the colon cancer cell line HCT-116 using a high content imaging assay (see Experimental protocols). Potency in the Cdc7 biochemical assay did not result in comparable potency in the cellular assay: compound **27**, which bears a hydroxyl substituent at the 4-position, did not show measurable activity in the cellular assay, whereas compounds **33**, **36**, and **37** inhibited MCM2 phosphorylation at micromolar concentrations, a greater than 100-fold shift from the biochemical IC_{50} values. The shift in potency between the biochemical and cellular assays is consistent with data on Cdc7 inhibitors from other chemical series (Reference 10, and data not shown), and may be due in part to the low K_M(app) for ATP for Cdc7, which we determined as 0.4 µM (Supplementary Figure 3).

[Please, insert Table 3 here]

In analogy to general kinase inhibitors, we envisioned the 2-substituents on the thiazole to interact with the hinge region of the enzyme, a hypothesis that was retrospectively supported by the proposed binding of compound **1** in the active site of Cdc7. Hence, we expected variations at this position to have a pronounced effect on the inhibitory activity against Cdc7 kinase and focused our SAR studies towards the 2-position of the thiazole (Table 4). Indeed, compound **43**, which bears a 3-pyridyl moiety, lost 2 orders of magnitude in potency compared to **1**, and the corresponding 2-pyridyl analogue **44** did not show any inhibitory activity against Cdc7. We rationalize this decrease in activity of pyridyl regioisomers **43** and **44** by the loss of the key intermolecular hydrogen bonding contact between the pyridine nitrogen of **1** and the backbone NH of the linker LEU137 of Cdc7 (Figure 2). The importance of the ring-nitrogen *para* to the connection to the thiazole ring was further demonstrated by the high micromolar activities of compounds **48**–**51**. An alkyl substituent at the 2-position of the 4-pyridyl moiety in **45** led to 20-fold loss in potency, whereas an amino substituent at this position was tolerated (**53** was equipotent to **16**). When we explored other heterocycles at the 2-position of the thiazole our efforts were rewarded by the discovery of **46**. This compound features a 2-amino-4-pyrimidyl moiety and showed an 8-fold improvement in potency over our starting point **1**. Interestingly, its regioisomer **54** did not show any inhibitory activity against Cdc7. Again, a pyrazine ring in **47**, which lacks the ring-nitrogen *para* to the connection to the thiazole ring, was poorly tolerated.

[Please, insert Table 4 here]

So far, our SAR studies had established the 2-amino-4-pyrimidyl moiety as the optimal substituent at the 2-position of the thiazole and we had discovered that thiazole-5-carboxamides were exquisitely potent. Keeping these groups constant, we reevaluated the influence of substituents at the 4-position on the inhibitory activity against Cdc7 kinase as well as the cellular activity against MCM2 phosphorylation in HCT-116 cells. The compounds depicted in Table 5 showed cellular activities <10 μM, and sub-micromolar potency was observed for compounds **74** and **77** equating to shifts in potency

between the biochemical and cellular Cdc7 kinase assays of >30-fold. To further characterize these compounds, we tested their stability in microsomes *in vitro*, using HLM and RLM assays (see Experimental protocols). All compounds tested were stable in HLM and RLM assays, with clearance of <100 µl/min/mg for all but one (Table 5).

[Please, insert Table 5 here]

Compounds **74** and **77** were potent in the biochemical and cellular assays and displayed low (<100 µl/min/mg) clearance in both HLM and RLM assays. We also tested these compounds in a mouse liver microsome (MLM) assay (see Experimental protocols), because we intended to further test the best compound *in vivo* using a mouse model. The MLM assay resulted in intrinsic clearance of 57 µl/min/mg for **74,** and 155 µl/min/mg for **77**, showing a similar trend with the results of the RLM assay.

Additional profiling of these two compounds against a panel of 100 protein kinases (KinomeSCAN, Ambit Bioscience, Inc.) revealed similar overall selectivity, with a POC < 35 at 1 µM for 12/100 and 10/100 kinases for **74** and **77**, respectively (Supplementary Figure 2). As the KinomeSCAN used binding competition assays to assess kinase inhibition, and Cdc7 kinase was not included in that panel, we tested these and select other compounds in enzymatic assays for kinases of particular interest (Table 6).

Compounds **74** and **77** were not active against the cell cycle kinases CDK1 or CDK4, but did inhibit CDK9 (IC_{50} values of 0.75 µM and 0.73 µM, respectively), a kinase which primarily functions in cellular transcription through regulation of RNA polymerase II.[35] Cdc7/CDK9 inhibitors reported by Nerviano Medical Sciences have been shown to be efficacious in tumor models, in part because inhibition of CDK9 downregulates transcripts of anti-apoptotic proteins such as Mcl-1.[11,36] We also tested for activity of our Cdc7 inhibitors against protein kinases from the casein kinase family, which are structurally related to Cdc7 and have also been considered as anticancer targets.[37,38] Compounds **74** and **77** did not inhibit CK2, but did show activity against CK1 kinases. Compound **74** inhibited

CK1α with an IC_{50} of 0.69 μM, CK1γ with an IC_{50} of 0.76 μM, and CK1δ with an IC_{50} of 0.084 μM. Compound **77** inhibited CK1α with an IC_{50} of 0.55 μM, CK1γ with an IC_{50} of 1.9 μM, and CK1δ with an IC_{50} of 0.104 μM. We did not detect any inhibition of Pim1, another structurally related kinase, by compounds **74** and **77** in enzymatic assays. Compound **74** also did not show any agonist or antagonist activity in a panel of 13 receptors.

[Please, insert Table 6 here]

We further characterized compounds **74** and **77** in different cellular assays (Table 7 and Figure 3). The compounds inhibited DNA synthesis in HCT-116 cells, with IC_{50} values of 2.6 μM and 6.9 μM, for **74** and **77** respectively, in a colorometric bromodeoxyuridine (BrdU) assay (Figure 3A). Compounds **74** and **77** also inhibited cell proliferation, resulting in IC_{50} values of 4.2 μM and 4.6 μM in a Cell Titer-Glo assay, which measures cellular ATP metabolism (Figure 3B). The IC_{50} values for the BrdU and cell viability assays were similar to each other, but were 5- to 9-fold less potent than the IC_{50} values for the proximal assay, MCM2 phosphorylation. This suggests that inhibition of MCM2 close to the IC_{90} is required for maximal inhibition of cell proliferation (pMCM2 IC_{90} = 6.37 μM for **74**). Flow cytometry for DNA content of HCT-116 cells treated with compound **74** revealed an accumulation of cells in the S/G2/M phases of the cell cycle (Figure 3C), suggesting delayed progression through S phase following Cdc7 inhibition. Caspases 3 and 7 were not activated at the time points analyzed (Table 7), raising the possibility that the cells did not undergo apoptosis, although an increase in sub-G1 DNA content was observed at higher compound concentrations or at later time points (Figure 3 and data not shown). Imaging analysis of HCT-116 cells treated with compound **74**, as well as with Cdc7 inhibitors from other chemical series, suggested that loss of cell viability occurred following aberrant mitosis (Supplementary Figure 5).

[Please, insert Table 7 here]

[Please, insert Figure 3 here]

Mechanism of action studies demonstrated that **74**, like the initial thiazole **1** and other compounds from this series, showed ATP-competitive inhibition of Cdc7 (Supplementary Figure 4). Its predicted binding mode as determined in a manner analogous to that of compound **1** is shown in Figure **4.** The binding orientation of compound **74** displays a *syn* orientation of the sulfur atom of the thiazole with respect to the proximal nitrogen atom of the adjacent pyrimidine ring, predicted from our own quantum mechanical calculations as well as previous studies,[39,40] which demonstrate the *syn* preference of aromatic sulfur atoms to lone-pair donor atoms when oriented in a 2,2'-arrangement. This *syn* S-N arrangement, favored over the *anti* S-N conformer of **74** by greater than 4 kcal/mol, necessitates an outward orientation of the pendant 2,4-dichloroaryl group toward the solvent front. The 2,4-dichlorophenyl substituent may potentially engage in an electrostatic or van der Waals interaction with the sidechain of HIS139 (depending on protonation state) and/or the backbone carbonyl oxygen of SER181. [41] The aminopyridine moiety interacts with the linker residue in a manner typical of this functionality, with the ring nitrogen atom of **74** interacting with the NH of linker LEU137, augmented by an H-bonding contact between the pendant NH_2 and backbone C=O of PRO135 in the rear of the binding cavity. The carbonyl and NH_2 groups of the primary amide moiety of **74** are predicted to interact with the salt-bridged LYS90 and ASP196, respectively.

[Please, insert Figure 4 here]

Based on its potency, selectivity, and microsomal clearance *in vitro* (Tables 5–7), we prioritized compound **74** for *in vivo* studies. Pharmacokinetic (PK) studies in rat following intravenous (iv) administration of **74** resulted in a high clearance of 3890 ml/kg/h, and a high volume of distribution of 4430 ml/kg (Table 8). Following oral administration, the bioavailability of **74** was low (6.6%), as was

the C_{max} (13 ng/ml), although the terminal half-life was 3.73 h. Mouse plasma protein binding assays showed a free fraction (fu) of 9.0% for compound **74**.

[Please, insert Table 8 here]

Despite suboptimal PK, for proof of principle we investigated whether compound **74** inhibits Cdc7 kinase activity *in vivo*. Because of its low oral bioavailability, NCR/nude mice bearing HCT-116 tumor xenografts were administered compound **74** as a single iv dose at 50 mg/kg or 150 mg/kg, and blood plasma and tumor samples were collected at 1, 3, 6, and 16 h post dose for pharmacokinetic/pharmacodynamic (PK/PD) analysis (Figure 5). For the PD readout, we used a meso-scale discovery (MSD) assay to detect MCM2 serine 53 phosphorylation in tumor lysates (see Experimental protocols). The 50 mg/kg dose of **74** was well tolerated and resulted in partial inhibition of MCM2 phosphorylation in tumors. MCM2 phosphorylation was inhibited by 39% at the 3 h time point, but showed less of an effect at later time points, with 20% inhibition of the signal at the 6 h time point, and near control levels of MCM2 phosphorylation at the 16 h time point. The 50 mg/kg dose resulted in an unbound plasma concentration of >1 µM at 1 h, and decreased thereafter. The 150 mg/kg dose of compound **74** also inhibited MCM2 phosphorylation in tumors, with 30% inhibition at 1 h, 38% inhibition at 3 h, and 31% inhibition at 6 h following dosing. The 150 mg/kg dose resulted in unbound plasma levels of nearly 5 µM at the 1 h time point, and remained above 1 µM through 6 h post-dose. However, this high dose was not well tolerated: even at 6 h, mice appeared moribund and consequently, we did not test a 16 h time point. For both doses tested, inhibition of MCM2 phosphorylation occurred after the maximal plasma concentrations were observed, consistent with the idea that cells must pass through S phase for Cdc7 kinase activity and MCM2 phosphorylation to be inhibited. Compound **74** therefore demonstrated that a potent, selective inhibitor of Cdc7 kinase activity can decrease MCM2 phosphorylation *in vitro* as well as *in vivo*.

[Please, insert Figure 5 here]

5. Conclusions

Cdc7 presents a challenge as a target for drug discovery, because the presence of a kinase insert domain adjacent to the active site, together with dependence on binding of the Dbf4 subunit for kinase activity, are not straightforward for building homology models [1], and a crystal structure of the protein had not been revealed until very recently [28]. Our primary HTS screen identified a high hit rate of Cdc7 inhibitors that were remarkable, relative to previously described protein kinase inhibitors, for their low molecular weight and high binding efficiency. We focused on compounds bearing a thiazole moiety, systematically exploring SAR by building off the core of compound **1**. Rapid synthesis and characterization of analogs identified amide **74** as the most potent, selective Cdc7 inhibitor from our SAR studies with on-target activity demonstrated *in vitro* and *in vivo*.

Our studies demonstrated a large shift in potency between enzymatic activity and activity in cells. Additionally, we found that plasma exposure levels of compound **74** over the cellular IC_{50} for 3–6 h were not sufficient to cause 50% inhibition of MCM2 phosphorylation in tumors *in vivo*. Together, these observations suggest that *in vivo* inhibition of Cdc7 with small molecules may require constant inhibition of the target at levels much greater than the cellular IC_{50}.

Comparison of Cdc7 inhibitors from distinct chemical series, including thiazole-based compounds, will facilitate better understanding of on-target activity and the requirements for target coverage for efficacy.

6. Experimental protocols

6.1. Chemistry

All chemicals were used as received from the commercial sources. Reactions were performed without significant exclusion of moisture or air. Reaction temperatures describe the temperature of the bath surrounding the reaction vessel. Reactions under microwave irradiation were performed in a Biotage®

Initiator microwave reactor in sealed vessels. Column chromatography was conducted under medium pressure either on silica gel (Merck® Grade 9385, pore size 60 Å, 230–400 mesh) or on prepacked silica gel cartridges (Biotage®). Analytical HPLC and mass spectroscopy were conducted using a reverse-phase Agilent 1100 Series HPLC-mass spectrometer. Purities for final compounds were measured using UV detection at 215 nm and 254 nm as >95%. NMR spectra were acquired as solutions in the indicated solvents on Bruker Avance DRX400 or Bruker Avance DPX300 spectrometers at 400 and 300 MHz field strengths, respectively. Chemical shifts are reported in parts per million (ppm, δ), downfield from tetramethylsilane (TMS, δ = 0.00 ppm), and are referenced to the residual solvent. Coupling constants are reported in Hertz (Hz). Spectral splitting patterns are designated as s: singlet, d: doublet, t: triplet, q: quartet, quin: quintet, m: multiplet, br.: broad.

The general reaction sequence is demonstrated by the synthesis of lead compound **74** as depicted in Scheme 5:

*6.1.1. 2-Amino-4-iodopyrimidine (**55-iodide**).* 2-Amino-4-chloropyrimidine (**55**) (13.0 g, 100 mmol) was added to a 57 wt.% aqueous solution of hydriodic acid (115 ml, 1.00 mol) at 0 °C and the mixture was stirred at room temperature for 3 h. The mixture was cooled to 0 °C and the resulting precipitate was removed by filtration and taken up in cold 5N aqueous Na_2CO_3 (200 ml). The mixture was extracted with EtOAc (3 × 500 ml) and the combined organic layers were concentrated under reduced pressure to deliver 2-amino-4-iodopyrimidine (21.1 g, 95.0 mmol, 95% yield) as a white solid. ^{1}H NMR (400 MHz, DMSO-d_6) δ ppm 7.78 (d, J = 5.0 Hz, 1 H), 7.02 (br. s, 2 H), 7.00 (d, J = 5.0 Hz, 1 H). MS (ESI, pos. ion) *m/z*: 222.1 (M+1).

*6.1.2. 2-Aminopyrimidine-4-carbonitrile (**57**).* A flask containing a solution of **55-iodide** (4.09 g, 18.5 mmol) in NMP (75 ml) was purged with argon for 5 minutes. Zinc cyanide (2.28 g, 19.4 mmol) and tetrakis(triphenylphosphine)palladium (0) (1.71 g, 1.48 mmol) were added and the mixture was stirred at 80 °C for 2 h. The mixture was cooled to room temperature, EtOAc (200 ml) and 30% aqueous NH_4OH (200 ml) was added, and stirring was continued for 1 h. The layers were separated, the aqueous layer was extracted with EtOAc (4 × 200 ml), and the combined organic layers were concentrated under

reduced pressure. Et_2O (30 ml) was added and the precipitate was collected by filtration and washed with Et_2O to deliver 2-aminopyrimidine-4-carbonitrile (1.66 g, 13.8 mmol, 75% yield) as a white solid. ^{1}H NMR (400 MHz, DMSO-d_6) δ ppm 8.51 (d, *J* = 4.7 Hz, 1 H), 7.31 (br. s, 2 H), 7.08 (d, *J* = 4.7 Hz, 1 H). MS (ESI, pos. ion) *m/z*: 121.1 (M+1).

*6.1.3 2-Aminopyrimidine-4-carbothioamide (**60**).* 40-48 wt.% aqueous ammonium sulfide (8.27 ml, 48.5 mmol) was added to a mixture of **57** (5.3 g, 44.1 mmol), triethylamine (6.14 ml, 44.1 mmol), and pyridine (28.8 ml, 353 mmol) and the resulting suspension was stirred at 52 °C for 2 h. The mixture was concentrated under reduced pressure and H_2O was added to the residue. The mixture was chilled to 0 ºC and the resulting precipitate was removed by filtration to deliver 2-aminopyrimidine-4-carbothioamide (5.5 g, 35.7 mmol, 80% yield) as a yellow solid. ^{1}H NMR (400 MHz, DMSO-d_6) δ ppm 10.23 (br. s, 1 H), 9.58 (br. s, 1 H), 8.42 (d, *J* = 4.9 Hz, 1 H), 7.35 (d, *J* = 4.9 Hz, 1 H), 6.80 (br. s, 2 H). MS (ESI, pos. ion) *m/z*: 155.1 (M+1).

*6.1.4. Ethyl 2-(2-aminopyrimidin-4-yl)-4-hydroxythiazole-5-carboxylate (**46**).* A mixture of **60** (5.4 g, 35.0 mmol), pyridine (11.4 ml, 140 mmol), and diethyl bromomalonate (**3**) (8.84 ml, 52.5 mmol) in EtOH (15 ml) was heated under reflux for 16 h. The mixture was concentrated under reduced pressure and H_2O was added to the residue. The resulting precipitate was removed by filtration and washed with Et_2O to deliver ethyl 2-(2-aminopyrimidin-4-yl)-4-hydroxythiazole-5-carboxylate (5.30 g, 19.9 mmol, 57% yield) as a tan solid. ^{1}H NMR (400 MHz, DMSO-d_6) δ ppm 12.27 (s, 1 H), 8.46 (d, *J* = 4.9 Hz, 1 H), 7.11 (d, *J* = 4.9 Hz, 1 H), 7.01 (s, 2 H), 4.23 (q, *J* = 7.1 Hz, 2 H), 3.35 (br. s, 3 H), 1.27 (t, *J* = 7.1 Hz, 3 H). MS (ESI, pos. ion) *m/z*: 267.0 (M+1).

*6.1.5. Ethyl 2-(2-aminopyrimidin-4-yl)-4-(trifluoromethylsulfonyloxy)thiazole-5-carboxylate (**46-triflate**).* Trifluoromethanesulfonic anhydride (7.95 g, 28.2 mmol) was added to a mixture of **46** (5.0 g, 18.8 mmol) and pyridine (4.46 g, 56.3 mmol) in CH_2Cl_2 (80 ml) at 0 ºC and the mixture was stirred for 2 h at 0 °C. H_2O (200 ml) was added, the layers were separated, and the organic layer was washed with H_2O (4 × 200 ml). The organic layer was dried (Na_2SO_4) and concentrated under reduced pressure. The crude product was purified by a flash chromatography (silica gel, 0% to 40% EtOAc/hexanes) to deliver

ethyl 2-(2-aminopyrimidin-4-yl)-4-(trifluoromethylsulfonyloxy)thiazole-5-carboxylate (4.3 g, 10.8 mmol, 58% yield). ^{1}H NMR (400 MHz, DMSO-d_6) δ ppm 8.54 (d, J = 4.9 Hz, 1 H), 7.17 (s, 2 H), 7.14 (d, J = 4.9 Hz, 1 H), 4.39 (q, J = 7.1 Hz, 2 H), 1.34 (t, J = 7.1 Hz, 3 H). MS (ESI, pos. ion) *m/z*: 398.9 (M+1).

*6.1.6. Ethyl 2-(2-aminopyrimidin-4-yl)-4-(2,4-dichlorophenyl)thiazole-5-carboxylate (**66**).* A mixture of **46-triflate** (485 mg, 1.22 mmol), 2,4-dichlorophenylboronic acid (279 mg, 1.46 mmol), trans-dichlorobis(triphenyl-phosphine)palladium (ii) (85.0 mg, 0.122 mmol), and sodium carbonate monohydrate (453 mg, 3.65 mmol) in 1,4-dioxane/H_2O (1:1, 2.4 ml) was stirred at 60 °C for 1.5 h. The mixture was partitioned between H_2O (10 ml) and CH_2Cl_2 (15 ml), the layers were separated, and the aqueous layer was extracted with CH_2Cl_2 (2 × 15 ml). The combined organic layers were dried ($MgSO_4$) and concentrated under reduced pressure. The resulting brown oil was absorbed onto silica gel and purified by flash chromatography (silica gel, 20% to 60% EtOAc/hexanes) to deliver ethyl 2-(2-aminopyrimidin-4-yl)-4-(2,4-dichlorophenyl)thiazole-5-carboxylate (259 mg, 0.655 mmol, 54% yield) as a yellow solid. ^{1}H NMR (400 MHz, DMSO-d_6) δ ppm 8.47 (d, J = 4.9 Hz, 1 H), 7.78 (d, J = 2.0 Hz, 1 H), 7.59 (d, J = 8.2 Hz, 1 H), 7.55 (dd, J = 8.2, 2.0 Hz, 1 H), 7.22 (d, J = 4.9 Hz, 1 H), 7.06 (s, 2 H), 4.18 (q, J = 7.2 Hz, 2 H), 1.14 (t, J = 7.2 Hz, 3 H). MS (ESI, pos. ion) *m/z*: 395.0 (M+1).

*6.1.7. 2-(2-Aminopyrimidin-4-yl)-4-(2,4-dichlorophenyl)thiazole-5-carboxylic acid (**66-acid**).* Lithium hydroxide monohydrate (78.0 mg, 1.86 mmol) was added to a solution of **66** (245 mg, 0.620 mmol) in THF/H_2O (1:1, 1.2 ml) and the mixture was stirred at room temperature for 2 h and under reflux for 12 h. The THF was removed under reduced pressure and the mixture was diluted with H_2O (10 ml). The precipitate was collected by filtration and titurated in boiling MeOH to deliver 2-(2-aminopyrimidin-4-yl)-4-(2,4-dichlorophenyl)thiazole-5-carboxylic acid (180 mg, 0.490 mmol, 79% yield) as an off-white solid. ^{1}H NMR (400 MHz, DMSO-d_6) δ ppm 13.65 (br. s, 1 H), 8.45 (d, J = 5.0 Hz, 1 H), 7.76 (d, J = 1.9 Hz, 1 H), 7.57 (d, J = 8.3 Hz, 1 H), 7.53 (dd, J = 8.3, 1.9 Hz, 1 H), 7.21 (d, J = 5.0 Hz, 1 H), 7.03 (s, 2 H). MS (ESI, pos. ion) *m/z*: 367.0 (M+1).

*6.1.8. 2-(2-Aminopyrimidin-4-yl)-4-(2,4-dichlorophenyl)thiazole-5-carboxamide (**74**).* HATU (211 mg, 0.556 mmol) was added to a mixture of **66-acid** (170 mg, 0.463 mmol) and diisopropylethylamine (242 µl, 1.39 mmol) in DMF (1 ml) and the mixture was stirred at room temperature for 30 min. A 0.5M solution of ammonia in 1,4-dioxane (2.78 ml, 1.39 mmol) was added and the mixture was stirred at room temperature for 2 h. The mixture was diluted with MeOH/CH_2Cl_2, absorbed onto silica gel, and purified by flash chromatography (silica gel, 5% to 10% MeOH/CH_2Cl_2). The resulting yellow solid was further purified by reversed phase HPLC (Phenomenex Gemini-NX 10µ C18 110Å, 100 × 50 mm, 10% to 95% H_2O/MeCN, 0.1% TFA). The product containing fractions were combined, basified with solid $NaHCO_3$, and extracted with CH_2Cl_2 (3 × 20 ml). The combined organic layers were dried ($MgSO_4$) and concentrated under reduced pressure to deliver 2-(2-aminopyrimidin-4-yl)-4-(2,4-dichlorophenyl)thiazole-5-carboxamide (120 mg, 0.328 mmol, 71% yield) as a light yellow solid. ^{1}H NMR (400 MHz, DMSO-d_6) δ ppm 8.44 (d, *J* = 5.0 Hz, 1 H), 7.73 (d, *J* = 1.8 Hz, 1 H), 7.67 (br. s, 2 H), 7.56 (d, *J* = 8.2 Hz, 1 H), 7.53 (dd, *J* = 8.2, 1.8 Hz, 1 H), 7.21 (d, *J* = 5.0 Hz, 1 H), 7.01 (br. s, 2 H). MS (ESI, pos. ion) *m/z*: 365.9 (M+1).

*6.1.9. Ethyl 4-hydroxy-2-(4-pyridyl)-thiazole-5-carboxylate (**1**).* Prepared in 44% yield analogously to **46** using **2** instead of **60**. ^{1}H NMR (400 MHz, DMSO-d_6): δ 12.35 (br. s, 1 H), 8.75 (dd, *J* = 4.5, 1.5 Hz, 2 H), 7.87 (dd, *J* = 4.5, 1.5 Hz, 2 H), 4.26 (q, *J* = 7.0 Hz, 2 H), 1.28 (t, *J* = 7.0 Hz, 3 H). MS (ESI, pos. ion) *m/z*: 251 (M+1).

*6.1.10. Ethyl 4-methoxy-2-(pyridin-4-yl)thiazole-5-carboxylate (**4**).* Iodomethane (267 µl, 4.30 mmol) was added to a mixture of **1** (717 mg, 2.86 mmol) and potassium carbonate (792 mg, 5.73 mmol) in DMF (5 ml) and the mixture was heated in a sealed vial at 80 °C for 18 h. Another 1.5 equiv. iodomethane (267 µl, 4.30 mmol) was added and the mixture was heated in a sealed vial at 80 °C for 6 h. The mixture was cooled to room temperature and partitioned between H_2O (30 ml) and CH_2Cl_2 (20 ml). The layers were separated, and the aqueous layer was extracted with 10% MeOH/CH_2Cl_2 (3 × 30 ml). The combined organic layers were dried ($MgSO_4$) and concentrated under reduced pressure. The crude product was absorbed onto silica gel and purified by flash chromatography (silica gel, 20% to

60% EtOAc/hexanes) to deliver ethyl 4-methoxy-2-(pyridin-4-yl)thiazole-5-carboxylate (199 mg, 0.753 mmol, 26% yield) as an orange solid. ^{1}H NMR (300 MHz, $CDCl_3$) δ ppm 8.75 (dd, *J* = 4.5, 1.5 Hz, 2 H), 7.81 (dd, *J* = 4.5, 1.5 Hz, 2 H), 4.36 (q, *J* = 7.2 Hz, 2 H), 4.25 (s, 3 H), 1.38 (t, *J* = 7.2 Hz, 3 H). MS (ESI, pos. ion) *m/z*: 265.1 (M+1).

*6.1.11. Ethyl 2-(pyridin-4-yl)-4-(trifluoromethylsulfonyloxy)thiazole-5-carboxylate (**5**).* Prepared in 89% yield analogously to **46-triflate** using **1** instead of **46**. ^{1}H NMR ($CDCl_3$, 400 MHz): δ 8.80 (dd, *J* = 4.5, 1.5 Hz, 2 H), 7.78 (dd, *J* = 4.5, 1.5 Hz, 2 H), 4.46 (q, *J* = 7.1 Hz, 2 H), 1.43 (t, *J* = 7.1 Hz, 3 H). MS (ESI, pos. ion) *m/z*: 383.0 (M+1).

*6.1.12. Ethyl 4-amino-2-(pyridin-4-yl)thiazole-5-carboxylate (**6**).* A mixture of **5** (200 mg, 0.523 mmol) and a 0.5 M solution of ammonia in 1,4-dioxane (3.14 ml, 1.57 mmol) was heated in a Biotage® reactor at 120 °C for 1 h and at 160 °C for 1 h and for 3 h. The mixture was cooled to room temperature and concentrated under reduced pressure. The residue was partitioned between saturated aqueous $NaHCO_3$ (20 ml) and EtOAc (20 ml) and the aqueous layer was extracted with EtOAc (2 × 20 ml). The combined organic layers were washed with brine (40 ml), dried (Na_2SO_4), and concentrated under reduced pressure. The crude product was purified by flash chromatography (silica gel, 70% EtOAc/hexanes) to deliver ethyl 4-amino-2-(pyridin-4-yl)thiazole-5-carboxylate (16 mg, 0.064 mmol, 12% yield) as a light yellow solid. ^{1}H NMR (400 MHz, $CDCl_3$) δ ppm 8.73 (d, *J* = 4.5 Hz, 2 H), 7.77 (d, *J* = 5.7 Hz, 2 H), 5.92 (br. s, 2 H), 4.35 (q, *J* = 7.0 Hz, 2 H), 1.39 (t, *J* = 7.0 Hz, 3 H). MS (ESI, pos. ion) *m/z*: 250.1 (M+1).

*6.1.13. Ethyl 4-(methylamino)-2-(pyridin-4-yl)thiazole-5-carboxylate (**7**).* A 2M solution of methylamine in THF (392 µl, 0.785 mmol) was added to a solution of **5** (300 mg, 0.785 mmol) in THF (5 ml) and the mixture was stirred at 75 °C for 1.5 h. The mixture was filtered and H_2O (10 ml) was added to the filtrate whereupon a suspension formed slowly. The solid was collected by filtration and washed with H_2O to deliver ethyl 4-(methylamino)-2-(pyridin-4-yl)thiazole-5-carboxylate (29 mg, 0.110 mmol, 14% yield) as a yellow solid. ^{1}H NMR (400 MHz, $CDCl_3$) δ ppm 8.73 (d, *J* = 5.1 Hz, 2 H),

7.82 (d, *J* = 5.9 Hz, 2 H), 6.72 (br. s, 1 H), 4.32 (q, *J* = 7.1 Hz, 2 H), 3.24 (d, *J* = 5.1 Hz, 3 H), 1.37 (t, *J* = 7.1 Hz, 3 H). MS (ESI, pos. ion) *m/z*: 264.0 (M+1).

*6.1.14. Ethyl 4-(benzylamino)-2-(pyridin-4-yl)thiazole-5-carboxylate (**8**).* Prepared in 41% yield analogously to **7** using benzylamine instead of 2M methylamine in THF. The compound was additionally purified by tituration with MeOH. ^{1}H NMR (400 MHz, DMSO-d_6) δ ppm 8.73 (d, *J* = 5.7 Hz, 2 H), 7.87 (d, *J* = 5.7 Hz, 2 H), 7.61 (t, *J* = 6.3 Hz, 1 H), 7.38–7.43 (m, 2 H), 7.33 (t, *J* = 7.5 Hz, 2 H), 7.20–7.27 (m, 1 H), 4.77 (d, *J* = 6.3 Hz, 2 H), 4.27 (q, *J* = 7.0 Hz, 2 H), 1.28 (t, *J* = 7.0 Hz, 3 H). MS (ESI, pos. ion) *m/z*: 340.0 (M+1).

*6.1.15. Ethyl 4-(phenylamino)-2-(pyridin-4-yl)thiazole-5-carboxylate (**9**).* Prepared in 45 yield analogously to **7** using aniline instead of 2M methylamine in THF. The reaction took 3 d at 75 °C for completion. ^{1}H NMR (400 MHz, DMSO-d_6) δ ppm 9.14 (s, 1 H), 8.78 (d, *J* = 6.1 Hz, 2 H), 7.97 (d, *J* = 6.1 Hz, 2 H), 7.69 (d, *J* = 8.0 Hz, 2 H), 7.37 (t, *J* = 8.0 Hz, 2 H), 7.05 (t, *J* = 7.3 Hz, 1 H), 4.35 (q, *J* = 7.1 Hz, 2 H), 1.33 (t, *J* = 7.1 Hz, 3 H). MS (ESI, pos. ion) *m/z*: 326.0 (M+1).

*6.1.16. Ethyl 4-(dimethylamino)-2-(pyridin-4-yl)thiazole-5-carboxylate (**10**).* Prepared in 93% yield analogously to **7** using dimethylamine instead of 2M methylamine in THF. ^{1}H NMR (400 MHz, DMSO-d_6) δ ppm 8.73 (dd, *J* = 4.5, 1.4 Hz, 2 H), 7.88 (dd, *J* = 4.5, 1.4 Hz, 2 H), 4.21 (q, *J* = 7.0 Hz, 2 H), 3.17 (s, 6 H), 1.27 (t, *J* = 7.0 Hz, 3 H). MS (ESI, pos. ion) *m/z*: 278.1 (M+1).

*6.1.17. Ethyl 2-(pyridin-4-yl)thiazole-5-carboxylate (**13**).* A mixture of 4-pyridylboronic acid (**11**) (3 g, 24.4 mmol), ethyl 2-bromothiazole-5-carboxylate (**12**) (5.76 g, 24.4 mmol), sodium carbonate (7.76 g, 73.2 mmol) in DME/H_2O (3:1, 100 ml) was purged with argon for 10 min. trans-Dichlorobis(triphenylphosphine)palladium (ii) (1.37 g, 1.95 mmol) was added and flushing with argon was continued for 5 min. The mixture was stirred at 80 °C for 3 d, concentrated under reduced pressure, and partitioned between H_2O (100 ml) and EtOAc (100 ml). Celite was added, the layers were separated, and the aqueous layer was extracted with EtOAc (2 × 100 ml). The combined organic layers were washed with brine (150 ml), dried (Na_2SO_4), and concentrated under reduced pressure. The solid was dissolved in MeOH, and the solution was dried (Na_2SO_4) and concentrated under reduced pressure.

The crude product was purified by flash chromatography (silica gel, 100% EtOAc) to deliver ethyl 2-(pyridin-4-yl)thiazole-5-carboxylate (25 mg, 0.107 mmol, 0.4% yield) as a tan solid. ^{1}H NMR (400 MHz, $CDCl_3$) δ ppm 8.77 (d, *J* = 6.1 Hz, 2 H), 8.50 (s, 1 H), 7.85 (d, *J* = 6.1 Hz, 2 H), 4.43 (q, *J* = 7.2 Hz, 2 H) 1.43 (t, *J* = 7.2 Hz, 2 H). MS (ESI, pos. ion) *m/z*: 235.0 (M+1).

*6.1.18. Ethyl 4-methyl-2-(pyridin-4-yl)thiazole-5-carboxylate (**15**).* A mixture of pyridine-4-carbothioamide (**2**) (479 mg, 3.47 mmol) and ethyl 2-chloroacetoacetate (**14**) (575 µl, 4.16 mmol) in EtOH (5 ml) was heated under reflux for 30 h. The mixture was diluted with CH_2Cl_2 (5 ml), absorbed onto silica gel, and purified by flash chromatography (silica gel, 2% to 8% MeOH/CH_2Cl_2) to deliver ethyl 4-methyl-2-(pyridin-4-yl)thiazole-5-carboxylate (628 mg, 2.53 mmol, 73% yield) as a tan solid. ^{1}H NMR (300 MHz, $CDCl_3$) δ ppm 8.74 (d, *J* = 5.3 Hz, 2 H), 7.82 (dd, *J* = 4.5, 1.3 Hz, 2 H), 4.38 (q, *J* = 7.1 Hz, 2 H), 2.81 (s, 3 H), 1.41 (t, *J* = 7.1 Hz, 3 H). MS (ESI, pos. ion) *m/z*: 249.1 (M+1).

*6.1.19. Ethyl 4-phenyl-2-(pyridin-4-yl)thiazole-5-carboxylate (**16**).* Prepared in 66% yield analogously to **66** using **5** and phenylboronic acid instead of **46-triflate** and 2,4-dichlorophenylboronic acid. ^{1}H NMR (300 MHz, $CDCl_3$) δ ppm 8.76 (dd, *J* = 4.6, 1.5 Hz, 2 H), 7.91 (dd, *J* = 4.6, 1.5 Hz, 2 H), 7.84–7.80 (m, 2 H), 7.40–7.53 (m, 3 H), 4.33 (q, *J* = 7.1 Hz, 2 H), 1.32 (t, *J* = 7.1 Hz, 3 H). MS (ESI, pos. ion) *m/z*: 311.0 (M+1).

*6.1.20. Ethyl 4-(2-hydroxyphenyl)-2-(pyridin-4-yl)thiazole-5-carboxylate (**17**).* Prepared in 54% yield analogously to **66** using **5** and 2-(4,4,5,5-tetramethyl-1,3,2-dioxaborolan-2-yl)phenol instead of **46-triflate** and 2,4-dichlorophenylboronic acid. Reaction at 40 °C for 2 h. ^{1}H NMR (300 MHz, DMSO-d_6) δ ppm 8.44 (d, *J* = 4.8 Hz, 1 H), 8.31 (t, *J* = 5.0 Hz, 1 H), 7.72 (s, 1 H), 7.46–7.62 (m, 2 H), 7.21 (d, *J* = 5.0 Hz, 1 H), 6.98 (s, 2 H), 3.16 (d, *J* = 7.0 Hz, 2 H), 1.01 (t, *J* = 7.0 Hz, 3 H). MS (ESI, pos. ion) *m/z*: 281.0 (M+1–EtOH, M+1 of lactone).

*6.1.21. Ethyl 4-(2-chlorophenyl)-2-(pyridin-4-yl)thiazole-5-carboxylate (**18**).* Prepared in 56% yield analogously to **66** using **5** and 2-chlorophenylboronic acid instead of **46-triflate** and 2,4-dichlorophenylboronic acid. ^{1}H NMR (400 MHz, DMSO-d_6) δ ppm 8.76 (d, *J* = 6.2 Hz, 2 H), 7.98 (d, *J*

= 6.2 Hz, 2 H), 7.41–7.64 (m, 4 H), 4.17 (q, *J* = 7.5 Hz, 2 H), 1.11 (t, *J* = 7.5 Hz, 3 H). MS (ESI, pos. ion) *m/z*: 345.0 (M+1).

*6.1.22. Ethyl 4-(2-chloro-4-fluorophenyl)-2-(pyridin-4-yl)thiazole-5-carboxylate (**19**).* Prepared in 55% yield analogously to **66** using **5** and 2-chloro-4-fluorophenylboronic acid instead of **46-triflate** and 2,4-dichlorophenylboronic acid. ^{1}H NMR (400 MHz, DMSO-d_6) δ ppm 8.76 (d, *J* = 6.2 Hz, 2 H), 7.98 (d, *J* = 6.2 Hz, 2 H), 7.53–7.69 (m, 2 H), 7.35 (td, *J* = 8.8, 2.6 Hz, 1 H), 4.18 (q, *J* = 7.4 Hz, 2 H), 1.13 (t, *J* = 7. Hz, 3 H). MS (ESI, pos. ion) *m/z*: 363.0 (M+1).

*6.1.23. Ethyl 4-(2,3-dichlorophenyl)-2-(pyridin-4-yl)thiazole-5-carboxylate (**20**).* Prepared in 80% yield analogously to **66** using **5** and 2,3-dichlorophenylboronic acid instead of **46-triflate** and 2,4-dichlorophenylboronic acid. ^{1}H NMR (400 MHz, DMSO-d_6) δ ppm 8.78 (dd, *J* = 4.7, 1.2 Hz, 2 H), 8.00 (dd, *J* = 4.7, 1.6 Hz, 2 H), 7.80 (dd, *J* = 7.8, 1.7 Hz, 1 H), 7.56 (dd, *J* = 7.8, 1.7 Hz, 1 H), 7.50 (t, *J* = 7.8 Hz, 1 H), 4.20 (q, *J* = 7.1 Hz, 2 H), 1.12 (t, *J* = 7.1 Hz, 3 H). MS (ESI, pos. ion) *m/z*: 379.0 (M+1).

*6.1.24. Ethyl 4-(2,4-dichlorophenyl)-2-(pyridin-4-yl)thiazole-5-carboxylate (**21**).* Prepared in 74% yield analogously to **66** using **5** instead of **46-triflate**. ^{1}H NMR (300 MHz, $CDCl_3$) δ ppm 8.76 (d, *J* = 5.0 Hz, 2 H), 7.86 (dd, *J* = 4.4, 1.2 Hz, 2 H), 7.53 (d, *J* = 1.7 Hz, 1 H), 7.42 (d, *J* = 8.2 Hz, 1 H), 7.37 (dd, *J* = 8.2, 1.7 Hz, 1 H), 4.27 (q, *J* = 7.1 Hz, 2 H), 1.24 (t, *J* = 7.1 Hz, 3 H). MS (ESI, pos. ion) *m/z*: 379.0 (M+1).

*6.1.25. Ethyl 4-(2-chloro-4-methoxyphenyl)-2-(pyridin-4-yl)thiazole-5-carboxylate (**22**).* Prepared in 60% yield analogously to **66** using **5** and 2-chloro-4-methoxyphenylboronic acid instead of **46-triflate** and 2,4-dichlorophenylboronic acid. ^{1}H NMR (400 MHz, DMSO-d_6) δ ppm 8.77 (dd, *J* = 4.7, 1.4 Hz, 2 H), 7.99 (dd, *J* = 4.7, 1.4 Hz, 2 H), 7.49 (d, *J* = 8.5 Hz, 1 H), 7.18 (d, *J* = 2.5 Hz, 1 H), 7.04 (dd, *J* = 8.5, 2.5 Hz, 1 H), 4.21 (q, *J* = 7.1 Hz, 2 H), 3.86 (s, 3 H), 1.16 (t, *J* = 7.1 Hz, 3 H). MS (ESI, pos. ion) *m/z*: 375.8 (M+1).

*6.1.26. Ethyl 4-(pyridin-3-yl)-2-(pyridin-4-yl)thiazole-5-carboxylate (**23**).* Prepared in 22% yield analogously to **66** using **5** and 3-pyridylboronic acid instead of **46-triflate** and 2,4-dichlorophenylboronic acid. ^{1}H NMR (300 MHz, $CDCl_3$) δ ppm 9.06 (s, 1 H), 8.78 (d, *J* = 5.6 Hz, 2 H),

8.69 (d, *J* = 4.9 Hz, 1 H), 8.19 (d, *J* = 7.8 Hz, 1 H), 7.88 (d, *J* = 5.6 Hz, 2 H), 7.42 (dd, *J* = 7.8, 4.9 Hz, 1 H), 4.35 (q, *J* = 7.1 Hz, 2 H), 1.33 (t, *J* = 7.1 Hz, 3 H). MS (ESI, pos. ion) *m/z*: 312.0 (M+1).

*6.1.27. Ethyl 4-(naphthalen-2-yl)-2-(pyridin-4-yl)thiazole-5-carboxylate (**24**).* Prepared in 59% yield analogously to **66** using **5** and 2-naphthylboronic acid instead of **46-triflate** and 2,4-dichlorophenylboronic acid. ^{1}H NMR (300 MHz, $CDCl_3$) δ ppm 9.06 (s, 1 H), 8.78 (d, *J* = 5.6 Hz, 2 H), 8.69 (d, *J* = 4.8 Hz, 1 H), 8.19 (d, *J* = 7.8 Hz, 1 H), 7.88 (d, *J* = 5.6 Hz, 2 H), 7.42 (dd, *J* = 7.8, 4.8 Hz, 1 H), 4.35 (q, *J* = 7.0 Hz, 2 H) 1.33 (t, *J* = 7.0 Hz, 3 H). MS (ESI, pos. ion) *m/z*: 361.1 (M+1).

*6.1.28. Methyl 3-amino-2-bromo-3-oxopropanoate (**26**).* Bromine (0.875 ml, 17.1 mmol) was added portionwise to a solution of methyl 3-amino-3-oxopropanoate (**25**) (2 g, 17.1 mmol) in glacial acetic acid (30 ml) and the mixture was stirred at room temperature until it became colorless. The mixture was partitioned between EtOAc (100 ml) and H_2O (100 ml), the layers were separated, and the organic layer was washed with H_2O (3 × 100 ml), saturated aqueous $NaHCO_3$ (2 × 100 ml), and brine (100 ml). The organic layer was dried (Na_2SO_4) and concentrated under reduced pressure to deliver methyl 3-amino-2-bromo-3-oxopropanoate (1.50 g, 7.65 mmol, 45% yield) as a yellow oil, which used without further purification.

*6.1.29. 4-Hydroxy-2-(pyridin-4-yl)thiazole-5-carboxamide (**27**).* A mixture of **26** (1.50 g, 7.65 mmol), pyridine-4-carbothioamide (**2**) (1.00 g, 7.24 mmol) and pyridine (1.75 ml, 21.7 mmol) in toluene (40 ml) was heated under reflux for 16 h. The mixture was cooled to room temperature, the solvent was decanted and the resulting solid was titurated with hexane. H_2O was added, the solid was collected by filtration and titurated with MeOH to deliver 4-hydroxy-2-(pyridin-4-yl)thiazole-5-carboxamide (50 mg, 0.226 mmol, 3% yield) as a tan solid. ^{1}H NMR (400 MHz, DMSO-d_6) δ ppm 13.04 (br. s, 1 H), 8.74 (d, *J* = 5.9 Hz, 2 H), 7.83 (d, *J* = 5.9 Hz, 2 H), 7.68 (br. s, 1 H), 7.24 (br. s, 1 H). MS (ESI, pos. ion) *m/z*: 222.1 (M+1).

*6.1.30. 4-Hydroxy-2-(pyridin-4-yl)thiazole-5-carboxylic acid hydrochloride (**28**).* A mixture of **1** (700 mg, 2.80 mmol) and lithium hydroxide monohydrate (1.2 g, 50 mmol) in MeOH/THF/H_2O (1:1:1, 30 ml) was stirred at room temperature for 1 h and at 70 °C for 2 h. The volatile solvents were removed

under reduced pressure, H_2O (10 ml) was added, and the solution was acidified by the dropwise addition of 10% aqueous HCl. The resulting solid was removed by filtration and titurated with MeOH to deliver 4-hydroxy-2-(pyridin-4-yl)thiazole-5-carboxylic acid hydrochloride (450 mg, 1.74 mmol, 62% yield) as a tan solid. ^{1}H NMR (400 MHz, DMSO-d_6) δ ppm 10.89 (s, 1 H), 8.67 (d, *J* = 6.1 Hz, 2 H), 7.79 (d, *J* = 6.1 Hz, 2 H), 6.47 (s, 1 H). MS (ESI, pos. ion) *m/z*: 222.9 (M+1).

*6.1.31. 4-Hydroxy-2-(pyridin-4-yl)thiazole-5-carbonyl chloride hydrochloride (**28-acid chloride**).* A 2M solution of oxalyl chloride in CH_2Cl_2 (3.30 ml, 6.60 mmol) was added dropwise to a suspension of **28** (853 mg, 3.30 mmol) in CH_2Cl_2 (7 ml). *N*,*N*-dimethylformamide (50 µl, 3.30 mmol) was added and the mixture was stirred at room temperature for 1 h. The mixture was concentrated under reduced pressure to deliver a yellow solid, which was used without further purification.

*6.1.32. 4-Hydroxy-N-methyl-2-(pyridin-4-yl)thiazole-5-carboxamide (**29**).* A 2M solution of methylamine in THF (0.92 ml, 1.840 mmol) was added to a solution of **28-acid chloride** (170 mg, 0.613 mmol) in DMF (1.5 ml) and the mixture was stirred at room temperature for 2 h. The mixture was filtered and purified by reversed phase HPLC (Phenomenex Gemini-NX 10µ C18 110Å, 100 × 50 mm, 10% to 95% H_2O/MeCN, 0.1% TFA). The product containing fractions were combined, basified with solid $NaHCO_3$, and extracted with CH_2Cl_2 (3 × 20 ml). The combined organic layers were dried ($MgSO_4$) and concentrated under reduced pressure. The resulting solid was taken up in 2N NH_3 in MeOH/CH_2Cl_2, absorbed onto silica gel, and further purified by flash chromatography (silica gel, 2% to 15% MeOH/CH_2Cl_2) to deliver 4-hydroxy-N-methyl-2-(pyridin-4-yl)thiazole-5-carboxamide (11 mg, 0.047 mmol, 8% yield) as an orange solid. ^{1}H NMR (300 MHz, CD_3OD) δ ppm 8.62 (d, *J* = 4.0 Hz, 1 H), 7.88 (d, *J* = 5.7 Hz, 2 H), 2.92 (s, 3 H). MS (ESI, pos. ion) *m/z*: 236.0 (M+1).

*6.1.33. N-Benzyl-4-hydroxy-2-(pyridin-4-yl)thiazole-5-carboxamide (**30**).* Prepared in 13% yield analogously to **29** using benzylamine instead of 2M methylamine in THF. ^{1}H NMR (300 MHz, CD_3OD) δ ppm 8.66 (dd, *J* = 4.8, 1.1 Hz, 2 H), 7.93 (dd, *J* = 4.8, 1.3 Hz, 1 H), 7.30–7.42 (m, 2 H) 7.21–7.30 (m, 1 H), 4.58 (s, 2 H). MS (ESI, pos. ion) *m/z*: 312.0 (M+1).

*6.1.34. 4-Hydroxy-N,N-dimethyl-2-(pyridin-4-yl)thiazole-5-carboxamide (**31**).* Prepared in 10% yield analogously to **29** using 2M dimethylamine in THF instead of 2M methylamine in THF. ^{1}H NMR (300 MHz, CD_3OD) δ ppm 8.66 (d, *J* = 5.9 Hz, 2 H), 7.93 (d, *J* = 5.9 Hz, 2 H), 3.21 (s, 6 H). MS (ESI, pos. ion) *m/z*: 250.1 (M+1).

*6.1.35. 4-Phenyl-2-(pyridin-4-yl)thiazole-5-carboxylic acid (**32**).* Prepared in 82% yield analogously to **66-acid** using **16** instead of **66**. ^{1}H NMR (300 MHz, DMSO-d_6) δ ppm 13.66 (br. s, 1 H), 8.77 (d, *J* = 5.2 Hz, 2 H), 7.98 (d, *J* = 5.2 Hz, 2 H), 7.81 (dd, *J* = 5.6, 2.2 Hz, 2 H), 7.30–7.60 (m, 3 H). MS (ESI, pos. ion) *m/z*: 283.1 (M+1).

*6.1.36. 4-Phenyl-2-(pyridin-4-yl)thiazole-5-carboxamide (**33**).* Prepared in 77% yield analogously to **74** using **32** instead of **66-acid**. ^{1}H NMR (300 MHz, DMSO-d_6) δ ppm 8.76 (d, *J* = 5.3 Hz, 2 H) 7.97–7.82 (m, 6 H), 7.38–7.56 (m, 3 H). MS (ESI, pos. ion) *m/z*: 282.0 (M+1).

*6.1.37. 4-Phenyl-2-(pyridin-4-yl)thiazole-5-carbohydrazide (**34**).* Prepared in 25% yield analogously to **74** using **32** and hydrazine hydrate instead of **66-acid** and 0.5M ammonia in 1,4-dioxane. ^{1}H NMR (400 MHz, DMSO-d_6) δ ppm 9.89 (br. s, 1 H), 8.77 (dd, *J* = 4.5, 1.8 Hz, 2 H), 7.98 (dd, *J* = 4.5, 1.6 Hz, 2 H), 7.85 (dt, *J* = 6.7, 1.6 Hz, 2 H), 7.40–7.53 (m, 3 H), 4.65 (d, *J* = 2.9 Hz, 2 H). MS (ESI, pos. ion) *m/z*: 297.1 (M+1).

*6.1.38. N-Hydroxy-4-phenyl-2-(pyridin-4-yl)thiazole-5-carboxamide (**35**).* Prepared in 11% yield analogously to **74** using **32** and hydroxylamine hydrochloride instead of **66-acid** and 0.5M ammonia in 1,4-dioxane. ^{1}H NMR (400 MHz, DMSO-d_6) δ ppm 11.34 (br. s, 1 H), 9.48 (br. s, 1 H), 8.76 (d, *J* = 5.9 Hz, 2 H), 7.97 (d, *J* = 5.9 Hz, 2 H), 7.85 (d, *J* = 7.0 Hz, 2 H), 7.39–7.58 (m, 3 H). MS (ESI, pos. ion) *m/z*: 298.1 (M+1).

*6.1.39. 4-Methoxy-2-(pyridin-4-yl)thiazole-5-carboxylic acid (**4-acid**).* Prepared in 85% yield analogously to **66-acid** using **4** instead of **66**. ^{1}H NMR (300 MHz, DMSO-d_6) δ ppm 13.07 (br. s, 1 H), 8.75 (d, *J* = 3.9 Hz, 2 H), 7.91 (d, *J* = 3.9 Hz, 2 H), 4.13 (s, 3 H). MS (ESI, pos. ion) *m/z*: 237.1 (M+1).

*6.1.40. 4-Methoxy-2-(pyridin-4-yl)thiazole-5-carboxamide (**36**).* Prepared in 87% yield analogously to **74** using **4-acid** instead of **66-acid**. ^{1}H NMR (300 MHz, DMSO-d_6) δ ppm 8.74 (d, *J* = 5.7 Hz, 2 H),

7.89 (d, *J* = 5.7 Hz, 2 H), 7.77 (br. s, 1 H), 7.11 (br. s, 1 H), 4.17 (s, 3 H). MS (ESI, pos. ion) *m/z*: 236.0 (M+1).

*6.1.41. 4-(2,4-Dichlorophenyl)-2-(pyridin-4-yl)thiazole-5-carboxylic acid (**21-acid**).* Prepared in 88% yield analogously to **66-acid** using **21** instead of **66**. ^{1}H NMR (300 MHz, DMSO-d_6) δ ppm 13.73 (br. s, 1 H), 8.77 (d, *J* = 5.5 Hz, 2 H), 7.97 (d, *J* = 5.5 Hz, 2 H), 7.78 (d, *J* = 1.6 Hz, 1 H), 7.60 (d, *J* = 8.2 Hz, 1 H), 7.55 (dd, *J* = 8.2, 1.6 Hz, 1 H). MS (ESI, pos. ion) *m/z*: 350.9 (M+1).

*6.1.42. 4-(2,4-Dichlorophenyl)-2-(pyridin-4-yl)thiazole-5-carboxamide (**37**).* Prepared in 40% yield analogously to **74** using **21-acid** instead of **66-acid**. ^{1}H NMR (300 MHz, DMSO-d_6) δ ppm 8.75 (d, *J* = 5.5 Hz, 2 H), 7.92 (d, *J* = 5.5 Hz, 2 H), 7.75 (s, 1 H), 7.72–7.52 (m, 4 H). MS (ESI, pos. ion) *m/z*: 350.0 (M+1).

*6.1.43. 4-Phenyl-2-(pyridin-4-yl)thiazole-5-carbonitrile (**38**).* A solution of oxalyl chloride (124 µl, 1.39 mmol) in CH_2Cl_2 (1 ml) was added to a mixture of **33** (261 mg, 0.928 mmol) and dimethyl sulfoxide (132 µl, 1.86 mmol) in CH_2Cl_2 (3 ml) at –78 °C and the mixture was stirred at –78 °C for 15 min. Triethylamine (387 µl, 2.78 mmol) was added dropwise and the mixture was stirred at –78 °C for 15 min. H_2O (10 ml) was added and the mixture was stirred at room temperature for 10 min. It was diluted with H_2O (30 ml) and extracted with CH_2Cl_2 (2 × 50 ml). The combined organic layers were dried (Na_2SO_4) and concentrated under reduced pressure. The resulting yellow solid was titurated with EtOAc to deliver 4-phenyl-2-(pyridin-4-yl)thiazole-5-carboxamide (170 mg, 0.646 mmol, 70% yield) as a yellow solid. ^{1}H NMR (400 MHz, DMSO-d_6) δ ppm 8.84 (dd, *J* = 4.5, 1.8 Hz, 2 H), 8.15 (dt, *J* = 6.5, 1.8 Hz, 2 H), 8.06 (dd, *J* = 4.5, 1.8 Hz, 2 H), 7.54–7.71 (m, 2 H). MS (ESI, pos. ion) *m/z*: 264.0 (M+1).

*6.1.44. 4-Phenyl-2-(pyridin-4-yl)-5-(2H-tetrazol-5-yl)thiazole (**39**).* A mixture of **38** (133 mg, 0.505 mmol), sodium azide (36.1 mg, 0.556 mmol) and zinc bromide (114 mg, 0.505 mmol) in H_2O (2 ml) was heated in a Biotage® microwave reactor at 140 °C for 20 min and at 155 °C for 30 min. The suspension was filtered and the solid was taken up in 0.25 N aqueous NaOH (10 ml). The resulting suspension was stirred for 30 min and filtered. The filtrate was brought to pH = 6.5 by the addition of 10% aqueous HCl and the resulting solid was removed by filtration of deliver 4-phenyl-2-(pyridin-4-yl)-

5-(2H-tetrazol-5-yl)thiazole (42 mg, 0.137 mmol, 27% yield) as a light yellow solid. ^{1}H NMR (400 MHz, CD_3OD) δ ppm 8.79 (dd, *J* = 4.6, 1.4 Hz, 2 H), 8.03 (dd, *J* = 4.6, 1.6 Hz, 2 H), 7.73 (dd, *J* = 6.6, 2.8 Hz, 2 H), 7.43–7.49 (m, 3 H). MS (ESI, pos. ion) *m/z*: 307.1 (M+1).

*6.1.45. 2-(4-Phenyl-2-(pyridin-4-yl)thiazol-5-yl)-1,3,4-oxadiazole (**40**).* A mixture of **34** (260 mg, 0.877 mmol), trimethyl orthoformate (144 µl, 1.32 mmol), and 4-methylbenzenesulfonic acid (2.12 mg, 0.012 mmol) in THF (3 ml) was heated under reflux for 2.5 h. Another 1.5 mol% 4-methylbenzenesulfonic acid (2.12 mg, 0.012 mmol) was added and the mixture was heated under reflux for 1 h. The mixture was concentrated under reduced pressure and partitioned between saturated aqueous $NaHCO_3$ (50 ml) and EtOAc (50 ml). The layers were separated and the aqueous layer was extracted with EtOAc (2 × 50 ml). The combined organic layers were washed with brine (50 ml), dried (Na_2SO_4), and concentrated under reduced pressure. The crude product was taken up in DMSO, filtered, and purified by reversed phase HPLC (Phenomenex Gemini-NX 10µ C18 110Å, 100 × 50 mm, 10% to 95% H_2O/MeCN, 0.1% TFA). The product containing fractions were combined, basified with solid $NaHCO_3$, and extracted with CH_2Cl_2. The combined organic layers were dried (Na_2SO_4) and concentrated under reduced pressure to deliver 2-(4-phenyl-2-(pyridin-4-yl)thiazol-5-yl)-1,3,4-oxadiazole (11 mg, 0.036 mmol, 4% yield) as a yellow solid. ^{1}H NMR (400 MHz, CD_3OD) δ ppm 8.97 (s, 1 H), 8.74 (d, *J* = 5.7 Hz, 2 H), 8.09 (d, *J* = 6.0 Hz, 2 H), 7.78 (dd, *J* = 6.7, 3.0 Hz, 2 H), 7.47–7.54 (m, 3 H). MS (ESI, pos. ion) *m/z*: 307.1 (M+1).

*6.1.46. Ethyl 4-[(2-aminophenyl)amino]-2-(4-pyridyl)-1,3-thiazole-5-carboxylate (**5-amide**).* A solution of **5** (2.01 g, 5.26 mmol) and 1,2-phenylenediamine (1.71 g, 15.8 mmol) in dioxane (10.5 ml) was heated under reflux for 48 h. The solvent was removed under reduced pressure and the resulting residue was purified by flash chromatography (silica gel, 1% to 2% 2M NH_3 in MeOH/CH_2Cl_2) to deliver ethyl 4-[(2-aminophenyl)amino]-2-(4-pyridyl)-1,3-thiazole-5-carboxylate (1.29 g, 3.79 mmol, 72% yield) as a bright-yellow solid. ^{1}H NMR (400 MHz, DMSO-d_6) δ ppm 8.95 (dd, *J* = 4.5, 1.7 Hz, 2 H), 8.79 (s, 1 H), 8.08 (dd, *J* = 4.5, 1.7 Hz, 2 H), 7.38 (dd, *J* = 7.9, 1.1 Hz, 1 H), 7.03–7.12 (m, 2 H),

6.88–6.92 (m, 1 H), 5.04 (br. s, 2 H), 4.54 (q, *J* = 7.1 Hz, 2 H), 1.53 (t, *J* = 7.1 Hz, 3 H). MS (ESI, pos. ion) *m/z*: 341.0 (M+1).

*6.1.47. 2-(4-Pyridyl)-4H,9H-benzo[b]1,3-thiazolo[5,4-f]1,4-diazepin-10-one (**41**).* Trifluoroacetic acid (4.0 ml) was added to a solution of **5-amide** (207 mg, 0.61 mmol) in dioxane (40 ml) and the mixture was heated under reflux for 24 h. The solvent was removed under reduced pressure and the resulting residue was purified by flash chromatography (silica gel, 1% to 2% 2M NH_3 in MeOH/CH_2Cl_2) to deliver 2-(4-pyridyl)-4H,9H-benzo[*b*]1,3-thiazolo[5,4-*f*]1,4-diazepin-10-one (112 mg, 0.38 mmol, 62%) as a rust colored solid. ^{1}H NMR (400 MHz, DMSO-d_6) δ ppm 9.52 (s, 1 H), 9.39 (s, 1 H), 8.79 (dd, *J* = 4.6, 1.6 Hz, 2 H), 7.89 (dd, *J* = 4.6, 1.6 Hz, 2 H), 6.85–6.97 (m, 4 H). MS (ESI, pos. ion) *m/z*: 295 (M+1).

*6.1.48. Ethyl 4-hydroxy-2-(pyridin-3-yl)thiazole-5-carboxylate 2,2,2-trifluoroacetate (**43**).* Prepared in 35% yield analogously to **46** using 3-pyridinecarbothioamide instead of **60**. ^{1}H NMR (300 MHz, DMSO-d_6) δ ppm 12.29 (br. s, 1 H), 9.13 (d, *J* = 2.2 Hz, 1 H), 8.72 (dd, *J* = 4.8, 1.6 Hz, 1 H), 8.28 (dt, *J* = 8.0, 1.6 Hz, 1 H), 7.55 (dd, *J* = 8.0, 4.8 Hz, 1 H), 4.23 (q, *J* = 7.2 Hz, 2 H), 1.27 (t, *J* = 7.2 Hz, 3 H). MS (ESI, pos. ion) *m/z*: 251.0 (M+1).

*6.1.49. Ethyl 4-hydroxy-2-(pyridin-2-yl)thiazole-5-carboxylate (**44**).* Prepared in 17% yield analogously to **46** using 2-pyridinecarbothioamide instead of **60**. ^{1}H NMR (300 MHz, DMSO-d_6) δ ppm 12.10 (s, 1 H), 8.66 (d, *J* = 4.8 Hz, 1 H), 7.97–8.09 (m, 2 H), 7.58 (td, *J* = 4.8, 1.6 Hz, 1 H), 4.23 (q, *J* = 7.2 Hz, 2 H), 1.28 (t, *J* = 7.2 Hz, 3 H). MS (ESI, pos. ion) *m/z*: 251.0 (M+1).

*6.1.50. Ethyl 2-(2-ethyl(4-pyridyl))-4-hydroxythiazole-5-carboxylate (**45**).* Prepared in 58% yield analogously to **46** using ethionamide instead of **60**. ^{1}H NMR (400 MHz, DMSO-d_6) δ ppm 12.39 (br. s, 1 H), 8.64 (d, *J* = 5.2 Hz, 1 H), 7.74 (s, 1 H), 7.68 (dd, *J* = 5.2, 1.6 Hz, 1 H), 4.24 (q, *J* = 7.1 Hz, 2 H), 2.84 (q, *J* = 7.6 Hz, 2 H), 1.22–1.29 (m, 6). MS *m/z*: 279.0 (M+1).

*6.1.51. Ethyl 4-hydroxy-2-(pyrazin-2-yl)thiazole-5-carboxylate (**47**).* Prepared in 42% yield analogously to **46** using 2-pyrazinecarbothioamide instead of **60**. ^{1}H NMR (300 MHz, DMSO-d_6) δ ppm

12.35 (br. s, 1 H) 9.22 (d, *J* = 1.3 Hz, 1 H) 8.82 (d, *J* = 2.5 Hz, 1 H) 8.74-8.77(m, 1 H) 4.24 (q, *J* = 7.2 Hz, 2 H) 1.28 (t, *J* = 7.2 Hz, 3 H). MS (ESI, pos. ion) *m/z*: 252.0 (M+1).

*6.1.52. Ethyl 4-hydroxy-2-phenylthiazole-5-carboxylate (**48**).* Prepared in 18% yield analogously to **46** using benzenecarbothioamide instead of **60**. ^{1}H NMR (300 MHz, DMSO-d_6) δ ppm 12.13 (br. s, 1 H), 7.93 (dd, *J* = 7.9, 1.6 Hz, 2 H), 7.50–7.60 (m, 3 H), 4.25 (q, *J* = 7.2 Hz, 2 H), 1.27 (t, *J* = 7.2 Hz, 3 H). MS (ESI, pos. ion) *m/z*: 249.9 (M+1).

*6.1.53. Ethyl 4-hydroxy-2-(4-methoxyphenyl)-1,3-thiazole-5-carboxylate (**49**).* Prepared in 69% yield analogously to **46** using 4-methoxybenzenecarbothioamide instead of **60**. ^{1}H NMR (400 MHz, DMSO-d_6) δ ppm 12.04 (s, 1H), 7.89 (d, *J* = 8.8 Hz, 2 H), 7.07 (d, *J* = 8.8 Hz, 2 H), 4.21 (q, *J* = 7.1 Hz, 2 H), 3.84 (s, 3 H), 1.26 (t, *J* = 7.1 Hz, 3 H). MS (ESI, pos. ion) *m/z*: 280 (M+1).

*6.1.54. Ethyl 4-hydroxy-2-(thiophen-3-yl)thiazole-5-carboxylate (**50**).* Prepared in 15% yield analogously to **46** using 3-thiophenecarbothioamide instead of **60**. ^{1}H NMR (300 MHz, DMSO-d_6) δ ppm 12.08 (br. s, 1 H), 8.25 (dd, *J* = 2.9, 1.2 Hz, 1 H), 7.73 (dd, *J* = 5.1, 2.9 Hz, 1 H), 7.55 (dd, *J* = 5.1, 1.2 Hz, 1 H), 4.21 (q, *J* = 7.0 Hz, 2 H), 1.28 (t, *J* = 7.2 Hz, 3 H). MS (ESI, pos. ion) *m/z*: 255.9 (M+1).

*6.1.55. Ethyl 2-tert-butyl-4-hydroxythiazole-5-carboxylate (**51**).* Prepared in 15% yield analogously to **46** using 2,2-dimethylpropanecarbothioamide instead of **60**. ^{1}H NMR (300 MHz, $CDCl_3$) δ ppm 9.82 (br. s, 1 H), 4.34 (q, *J* = 7.2 Hz, 2 H), 1.36 (t, *J* = 7.2 Hz, 3 H). MS (ESI, pos. ion) *m/z*: 230.0 (M+1).

*6.1.56. 2-Aminopyridine-4-carbothioamide (**62**).* Prepared in 47% yield analogously to **60** using **59** instead of **57**. ^{1}H NMR (400 MHz, DMSO-d_6) δ ppm 9.94 (br. s, 1 H), 9.52 (br. s, 1 H), 7.92 (d, *J* = 5.3 Hz, 1 H), 6.79 (br. s, 2 H), 6.73 (dd, *J* = 5.3, 1.5 Hz, 1 H), 6.11 (s, 2 H). MS (ESI, pos. ion) *m/z*: 154.1 (M+1).

*6.1.57. Ethyl 2-(2-aminopyridin-4-yl)-4-phenylthiazole-5-carboxylate (**53**).* Prepared in 3% yield analogously to **46** using **62** and **52** instead of **60** and **3**. ^{1}H NMR (400 MHz, DMSO-d_6) δ ppm 12.39 (br. s, 1 H), 8.64 (d, *J* = 5.2 Hz, 1 H), 7.74 (s, 1 H), 7.68 (dd, *J* = 5.2, 1.6 Hz, 1 H), 4.24 (q, *J* = 7.1 Hz, 2 H), 2.84 (q, *J* = 7.6 Hz, 2 H), 1.22–1.29 (m, 6). MS *m/z*: 279.0 (M+1).

*6.1.58. 4-Amino-6-iodopyrimidine (**56-iodide**).* Prepared in 47% yield analogously to **55-iodide** using **56** instead of **55**. ^{1}H NMR (400 MHz, DMSO-d_6) δ ppm 8.04 (d, *J* = 0.8 Hz, 1 H), 7.04 (br. s, 2 H), 6.89 (d, *J* = 0.8 Hz, 1 H). MS (ESI, pos. ion) *m/z*: 221.9 (M+1).

*6.1.59. 6-Aminopyrimidine-4-carbonitrile (**58**).* Prepared in 88% yield analogously to **57** using **56-iodide** instead of **55-iodide**. ^{1}H NMR (400 MHz, DMSO-d_6) δ ppm 8.43 (d, *J* = 0.9 Hz, 1 H), 7.56 (br. s, 2 H), 6.89 (d, *J* = 0.9 Hz, 1 H). MS (ESI, pos. ion) *m/z*: 121.1 (M+1).

*6.1.60. 6-Aminopyrimidine-4-carbothioamide (**61**).* Prepared in 55% yield analogously to **60** using **58** instead of **57**. ^{1}H NMR (400 MHz, DMSO-d_6) δ ppm 10.23 (br. s, 1 H), 9.84 (br. s, 1 H), 8.39 (s, 1 H), 7.45 (s, 1 H), 7.29 (br. s, 2 H). MS (ESI, pos. ion) *m/z*: 155.0 (M+1).

*6.1.61. Ethyl 2-(6-aminopyrimidin-4-yl)-4-phenylthiazole-5-carboxylate (**54**).* Prepared in 7% yield analogously to **46** using **61** and **52** instead of **60** and **3**. ^{1}H NMR (400 MHz, DMSO-d_6) δ ppm 8.45 (d, *J* = 0.9 Hz, 1 H), 7.76 (dd, *J* = 6.6, 3.0 Hz, 2 H), 7.46–7.49 (m, 3 H), 7.31 (s, 2 H), 7.24 (d, *J* = 0.9 Hz, 1 H), 4.25 (q, *J* = 7.1 Hz, 2 H), 1.22 (t, *J* = 7.1 Hz, 3 H). MS *m/z*: 327.0 (M+1).

*6.1.62. Ethyl 2-(2-aminopyrimidin-4-yl)-4-(2-fluorophenyl)thiazole-5-carboxylate (**63**).* Prepared in 73% yield analogously to **66** using 2-fluorophenylboronic acid instead of 2,3-dichlorophenylboronic acid. ^{1}H NMR (400 MHz, DMSO-d_6) δ ppm 8.50 (d, *J* = 4.9 Hz, 1 H), 7.65 (td, *J* = 7.8, 1.8 Hz, 1 H), 7.57 (tdd, *J* = 7.8, 5.5, 1.8 Hz, 1 H), 7.30–7.39 (m, 2 H), 7.27 (d, *J* = 4.9 Hz, 1 H), 7.06 (s, 2 H), 4.23 (q, *J* = 7.1 Hz, 2 H), 1.18 (t, *J* = 7.1 Hz, 3 H). MS (ESI, pos. ion) *m/z*: 345.0 (M+1).

*6.1.63. Ethyl 2-(2-aminopyrimidin-4-yl)-4-(2-trifluoromethylphenyl)thiazole-5-carboxylate (**64**).* Prepared in 50% yield analogously to **66** using 2-trifluoromethylphenylboronic acid instead of 2,3-dichlorophenylboronic acid. ^{1}H NMR (400 MHz, DMSO-d_6) δ ppm 8.45 (d, *J* = 5.3 Hz, 1 H), 7.86 (d, *J* = 7.9 Hz, 1 H), 7.74 (q, *J* = 7.9 Hz, 3 H), 7.56 (d, *J* = 7.5 Hz, 1 H), 7.19 (d, *J* = 5.3 Hz, 1 H), 6.98 (s, 2 H), 4.08 (q, *J* = 7.1 Hz, 2 H), 1.01 (t, *J* = 7.1 Hz, 4 H). MS (ESI, pos. ion) *m/z*: 395.1 (M+1).

*6.1.64. Ethyl 2-(2-aminopyrimidin-4-yl)-4-(2,5-difluorophenyl)thiazole-5-carboxylate (**65**).* Prepared in 73% yield analogously to **66** using 2,5-difluorophenylboronic acid instead of 2,3-dichlorophenylboronic acid. ^{1}H NMR (400 MHz, DMSO-d_6) δ ppm 8.50 (d, *J* = 4.9 Hz, 1 H), 7.65 (td, *J*

= 7.8, 1.8 Hz, 1 H), 7.57 (tdd, *J* = 7.8, 5.5, 1.8 Hz, 1 H), 7.30–7.39 (m, 2 H), 7.27 (d, *J* = 4.9 Hz, 1 H), 7.06 (s, 2 H), 4.23 (q, *J* = 7.1 Hz, 2 H), 1.18 (t, *J* = 7.1 Hz, 3 H). MS (ESI, pos. ion) *m/z*: 363.0 (M+1).

*6.1.65. Ethyl 2-(2-aminopyrimidin-4-yl)-4-(3,5-dichlorophenyl)thiazole-5-carboxylate (**67**).* Prepared in 25% yield analogously to **66** using 3,5-dichlorophenylboronic acid instead of 2,3-dichlorophenylboronic acid. ^{1}H NMR (400 MHz, DMSO-d_6) δ ppm 8.49 (d, *J* = 4.9 Hz, 1 H), 7.86 (d, *J* = 1.8 Hz, 2 H), 7.75 (t, *J* = 1.8 Hz, 1 H), 7.31 (d, *J* = 4.9 Hz, 1 H), 7.05 (s, 2 H), 4.27 (q, *J* = 7.1 Hz, 2 H), 1.25 (t, *J* = 7.1 Hz, 3 H). MS (ESI, pos. ion) *m/z*: 395.0 (M+1).

*6.1.66. Ethyl 2-(2-aminopyrimidin-4-yl)-4-(2-chloro-4-methylphenyl)thiazole-5-carboxylate (**68**).* Prepared in 72% yield analogously to **66** using 2-chloro-4-methylphenylboronic acid instead of 2,3-dichlorophenylboronic acid. ^{1}H NMR (400 MHz, DMSO-d_6) δ ppm 8.47 (d, *J* = 4.9 Hz, 1 H), 7.42 (t, *J* = 3.7 Hz, 2 H), 7.26 (d, *J* = 7.8 Hz, 1 H), 7.22 (d, *J* = 4.9 Hz, 1 H), 7.06 (s, 2 H), 4.17 (q, *J* = 7.0 Hz, 2 H), 2.40 (s, 3 H), 1.14 (t, *J* = 7.0 Hz, 3 H). MS (ESI, pos. ion) *m/z*: 375.0 (M+1).

*6.1.67. Ethyl 2-(2-aminopyrimidin-4-yl)-4-(2-chloro-4-methoxyphenyl)thiazole-5-carboxylate (**69**).* Prepared in 78% yield analogously to **66** using 2-chloro-4-methoxyphenylboronic acid instead of 2,3-dichlorophenylboronic acid. ^{1}H NMR (400 MHz, DMSO-d_6) δ ppm 8.46 (d, *J* = 4.8 Hz, 1 H), 7.44 (d, *J* = 8.8 Hz, 1 H), 7.23 (d, *J* = 5.3 Hz, 1 H), 7.13 (d, *J* = 2.6 Hz, 1 H), 7.02 (dd, *J* = 8.8, 2.6 Hz, 1 H), 6.95 (s, 2 H) 4.16 (quin, *J* = 7.3 Hz, 2 H), 3.67 (s, 3 H), 1.12 (t, *J* = 7.3 Hz, 7 H). MS (ESI, pos. ion) *m/z*: 391.1 (M+1).

*6.1.68. Ethyl 2-(2-aminopyrimidin-4-yl)-4-(dimethylamino)thiazole-5-carboxylate (**70**).* Prepared in 82% yield analogously to **10** using **46-triflate** and dimethylamine instead of **5** and 2M methylamine in THF. ^{1}H NMR (400 MHz, DMSO-d_6) δ ppm 8.45 (d, *J* = 4.9 Hz, 1 H), 7.19 (d, *J* = 4.9 Hz, 1 H), 6.94 (s, 2 H), 4.19 (q, *J* = 7.1 Hz, 2 H), 3.14 (s, 6 H), 1.26 (t, *J* = 7.1 Hz, 3 H). MS (ESI, pos. ion) *m/z*: 294.0.1 (M+1).

*6.1.69. 2-(2-Aminopyrimidin-4-yl)-4-(2-fluorophenyl)thiazole-5-carboxylic acid (**63-acid**).* Prepared in 90% yield analogously to **66-acid** using **63** instead of **66**. ^{1}H NMR (400 MHz, DMSO-d_6) δ ppm 13.61 (br. s, 1 H), 8.47 (d, *J* = 4.9 Hz, 1 H), 7.62 (td, *J* = 7.7, 1.7 Hz, 1 H), 7.53 (tdd, *J* = 7.7, 5.7, 1.7

Hz, 1 H), 7.27–7.37 (m, 2 H), 7.25 (d, *J* = 4.9 Hz, 1 H), 7.04 (s, 2 H). MS (ESI, pos. ion) *m/z*: 317.0 (M+1).

*6.1.70. 2-(2-Aminopyrimidin-4-yl)-4-(2-fluorophenyl)thiazole-5-carboxamide (**71**).* Prepared in 21% yield analogously to **74** using **63-acid** instead of **66-acid**. ^{1}H NMR (400 MHz, DMSO-d_6) δ ppm 8.45 (d, *J* = 4.7 Hz, 1 H), 7.81 (br. s, 1 H), 7.66 (t, *J* = 6.7 Hz, 2 H), 7.51 (q, *J* = 6.1 Hz, 1 H), 7.19–7.40 (m, 3 H), 7.01 (br. s, 2 H). MS (ESI, pos. ion) *m/z*: 316.1 (M+1).

*6.1.71. 2-(2-Aminopyrimidin-4-yl)-4-(2-trifluoromethylphenyl)thiazole-5-carboxylic acid (**64-acid**).* Prepared analogously to **66-acid** using **64** instead of **66**. The crude product (94% yield) was taken on without further purification or characterization. MS (ESI, pos. ion) *m/z*: 367.1 (M+1).

*6.1.72. 2-(2-Aminopyrimidin-4-yl)-4-(2-trifluoromethylphenyl)thiazole-5-carboxamide (**72**).* Prepared in 37% yield analogously to **74** using **64-acid** instead of **66-acid**. ^{1}H NMR (400 MHz, DMSO-d_6) δ ppm 8.43 (d, *J* = 5.0 Hz, 1 H), 7.86 (d, *J* = 7.6 Hz, 1 H), 7.75 (t, *J* = 7.3 Hz, 1 H), 7.69 (t, *J* = 7.6 Hz, 1 H), 7.60 (br. s, 1 H), 7.56 (d, *J* = 7.3 Hz, 1 H), 7.51 (br. s, 1 H), 7.17 (d, *J* = 5.0 Hz, 1 H), 7.01 (s, 2 H). MS (ESI, pos. ion) *m/z*: 366.0 (M+1).

*6.1.73. 2-(2-Aminopyrimidin-4-yl)-4-(2,5-difluorophenyl)thiazole-5-carboxylic acid (**65-acid**).* Prepared in 59% yield analogously to **66-acid** using **65** instead of **66**. ^{1}H NMR (400 MHz, DMSO-d_6) δ ppm 13.79 (br. s, 1 H), 8.48 (d, *J* = 4.9 Hz, 1 H), 7.50 (td, *J* = 6.7, 1.6 Hz, 1 H), 7.34–7.43 (m, 2 H), 7.26 (d, *J* = 4.9 Hz, 1 H), 7.05 (s, 2 H). MS (ESI, pos. ion) *m/z*: 335.0 (M+1).

*6.1.74. 2-(2-Aminopyrimidin-4-yl)-4-(2,5-difluorophenyl)thiazole-5-carboxamide (**73**).* Prepared in 51% yield analogously to **74** using using **65-acid** instead of **66-acid**. ^{1}H NMR (400 MHz, DMSO-d_6) δ ppm 8.45 (d, *J* = 5.0 Hz, 1 H), 7.90 (br. s, 1 H), 7.69 (br. s, 1 H), 7.48 (t, *J* = 7.0 Hz, 1 H), 7.32–7.39 (m, 1 H), 7.26 (d, *J* = 5.0 Hz, 1 H), 7.01 (s, 2 H). MS (ESI, pos. ion) *m/z*: 334.1 (M+1).

*6.1.75. 2-(2-Aminopyrimidin-4-yl)-4-(3,5-dichlorophenyl)thiazole-5-carboxylic acid (**67-acid**).* Prepared in 59% yield analogously to **66-acid** using **67** instead of **66**. ^{1}H NMR (400 MHz, DMSO-d_6) δ ppm 8.38 (d, *J* = 5.1 Hz, 1 H), 8.33 (d, *J* = 2.0 Hz, 2 H), 7.52 (t, *J* = 2.0 Hz, 1 H), 7.28 (d, *J* = 5.1 Hz, 1 H), 6.85 (s, 2 H). MS (ESI, pos. ion) *m/z*: 367.0 (M+1).

*6.1.76. 2-(2-Aminopyrimidin-4-yl)-4-(3,5-dichlorophenyl)thiazole-5-carboxamide (**75**).* Prepared in 14% yield analogously to **74** using using **67-acid** instead of **66-acid**. ^{1}H NMR (400 MHz, CD_3OD) δ ppm 8.42 (d, *J* = 5.1 Hz, 1 H), 7.81 (s, 2 H), 7.47–7.56 (m, 1 H), 7.44 (d, *J* = 5.1 Hz, 1 H). MS (ESI, pos. ion) *m/z*: 365.9 (M+1).

*6.1.77. 2-(2-Aminopyrimidin-4-yl)-4-(2-chloro-4-methylphenyl)thiazole-5-carboxylic acid (**68-acid**).* Prepared analogously to **66-acid** using **68** instead of **66**. The crude product (99% yield) was taken on without further purification or characterization. MS (ESI, pos. ion) *m/z*: 347.0 (M+1).

*6.1.78. 2-(2-Aminopyrimidin-4-yl)-4-(2-chloro-4-methylphenyl)thiazole-5-carboxamide (**76**).* Prepared in 31% yield analogously to **74** using using **68-acid** instead of **66-acid**. ^{1}H NMR (400 MHz, DMSO-d_6) δ ppm 8.44 (d, *J* = 4.9 Hz, 1 H), 7.64 (br. s, 1 H), 7.33–7.49 (m, 3 H), 7.26 (d, *J* = 7.8 Hz, 1 H), 7.21 (d, *J* = 4.9 Hz, 1 H), 7.00 (s, 2 H), 2.38 (s, 3 H). MS (ESI, pos. ion) *m/z*: 346.1 (M+1).

*6.1.79. 2-(2-Aminopyrimidin-4-yl)-4-(2-chloro-4-methoxyphenyl)thiazole-5-carboxylic acid (**69-acid**).* Prepared in 71% yield analogously to **66-acid** using **69** instead of **66**. ^{1}H NMR (400 MHz, DMSO-d_6) δ ppm 13.50 (br. s, 1 H), 8.45 (d, *J* = 4.9 Hz, 1 H), 7.45 (d, *J* = 8.5 Hz, 1 H), 7.22 (d, *J* = 4.9 Hz, 1 H), 7.15 (d, *J* = 2.5 Hz, 1 H), 7.03 (s, 2 H), 7.01 (dd, *J* = 8.5, 2.5 Hz, 1 H), 3.85 (s, 3 H). MS (ESI, pos. ion) *m/z*: 363.0 (M+1).

*6.1.80. 2-(2-Aminopyrimidin-4-yl)-4-(2-chloro-4-methoxyphenyl)thiazole-5-carboxamide (**77**).* Prepared in 46% yield analogously to **74** using using **69-acid** instead of **66-acid**. ^{1}H NMR (400 MHz, DMSO-d_6) δ ppm 8.44 (d, *J* = 5.0 Hz, 1 H), 7.64 (br. s, 1 H), 7.48 (d, *J* = 8.6 Hz, 1 H), 7.34 (br. s, 1 H), 7.21 (d, *J* = 5.0 Hz, 1 H), 7.15 (d, *J* = 2.5 Hz, 1 H), 7.03 (dd, *J* = 8.6, 2.5 Hz, 1 H), 7.00 (s, 2 H), 3.32 (s, 3 H). MS (ESI, pos. ion) *m/z*: 362.0 (M+1).

*6.1.81. 2-(2-Aminopyrimidin-4-yl)-4-(dimethylamino)thiazole-5-carboxylic acid (**70-acid**).* Prepared analogously to **66-acid** using **70** instead of **66**. The crude product (55% yield) was taken on without further purification or characterization. MS (ESI, pos. ion) *m/z*: 366.0 (M+1).

*6.1.82. 2-(2-Aminopyrimidin-4-yl)-4-(dimethylamino)thiazole-5-carboxamide (**78**).* Prepared in 27% yield analogously to **74** using using **70-acid** instead of **66-acid**. ^{1}H NMR (400 MHz, DMSO-d_6) δ ppm

8.41 (d, *J* = 4.9 Hz, 1 H), 7.62 (br. s, 2 H), 7.17 (d, *J* = 4.9 Hz, 1 H), 6.90 (s, 2 H), 2.93 (s, 6 H). MS (ESI, pos. ion) *m/z*: 265.1 (M+1).

6.2. Kinase assays

6.2.1. Assay for Cdc7 activity. A Protein A Amplified Luminescent Proximity Homogenous Assay (AlphaScreen; Perkin Elmer #6760617R) was used to determine inhibition of Cdc7/Dbf4 biochemical activity. Cdc7/Dbf4 enzyme was obtained from Carna Bio (#05-109). Recombinant MCM2 protein (aa1-467) tagged with 6 × His at the amino terminus and avitag at the carboxyl terminus was expressed in E. coli, purified by affinity chromatography, and then biotinylated for use as a substrate. The Alpha Screen reaction contained 3 nM Cdc7/Dbf4 protein, 20 nM MCM2 protein, and 350 nM ATP (approximately 1× the K_m for ATP for Cdc7) in reaction buffer (50 mM Hepes pH7.5, 10 mM $MgCl_2$, 0.05% BSA, 0.01% Tween-20, 2 mM DTT). Phosphorylation of MCM2 by Cdc7/Dbf4 was detected with Protein A-coated acceptor beads bound with antibody to phospho-serine 53 of MCM2 (Bethyl #A300-756A). Chemiluminescence signal resulting from the proximity of streptavidin-coated donor beads and the acceptor beads was used to generate IC_{50} values.

6.2.2. Counter screen assays. A homogeneous time-resolved fluorescence (HTRF) assay was used to counter screen for biochemical inhibition of CDK2/Cyclin E kinase. CDK2/Cyclin E enzyme was obtained from Millipore (#14-475). A ULight peptide for Maltose binding protein (MBP) was used as substrate (Perkin Elmer #TRF0109).

HTRF assays were used to counter screen for inhibition of CDK1/Cyclin B, CDK4/Cyclin D1, Pim1 and Pim2 kinases. CDK9/Cyclin T1 was counter screened with a 4eBP1 ULight HTRF assay, and inhibition of the CK2 tetramer was counter screened using a TopoII ULight HTRF assay (Perkin Elmer). Inhibition of the CK1 isoforms was carried out using Lance TR-FRET assays (Perkin Elmer).

6.3. Cellular assays

6.3.1. Inhibition of MCM2 phosphorylation in HCT-116 cells. A high content imaging assay was used to assess inhibition of MCM2 phosphorylation in cells. HCT-116 cells were treated with Cdc7 inhibitors in a 22-point dose response for 14 h. Cells were then immunostained for phospho-serine MCM2

antibody (Bethyl #IHC-00069), detected with secondary antibody Alexa Fluor 488 (Invitrogen #A11008). Nuclei were counterstained with Hoechst dye (Sigma #14533). The percent of cells with phospho-MCM2 immunostaining above a threshold level was assessed by imaging on a Cellomics ArrayScan (Thermo Fisher) and IC_{50} values were generated in Genedata Screener.

6.3.2. Inhibition of MCM2 phosphorylation in HCT-116 tumor xenografts. MCM2 phosphorylation in tumor xenografts was determined with a meso-scale discovery (MSD) assay. Tumors were homogenized with a Tissue Lyzer (Qiagen) in Tris lysis buffer (150 mM NaCl, 20 mM Tris pH7.5, 1 mM EDTA, 1 mM EGTA, 1% Triton-X-100, containing protease (Roche #11 836 170 001) and phosphatase inhibitors (Sigma #P5726)). Lysates were captured with total MCM2 antibody (Bethyl #A300-122A) on MSD plates (#L15XA-3), and then incubated with antibodies to total MCM2 (Santa Cruz SC-130028) or phospho-serine 53 MCM2 (Bethyl #IHC-00069). Phospho- and total MCM2 proteins were detected by sulfo-tag secondary antibody (MSD) followed by chemiluminescence. Inhibition of phospho-serine 53 MCM2 was calculated as a ratio of phospho-MCM2 to total MCM2.

6.3.3. Determination of DNA content. To determine DNA content, HCT-116 cells treated with Cdc7 inhibitor were collected using Cell Stripper buffer (Invivogen) and fixed in 70% ethanol. DNA was stained with propidium iodide/RNase (Becton Dickinson). Cells were analyzed by flow cytometry using an LSR II cytometer with FACSDiva software (Becton Dickinson).

6.3.4. BrdU incorporation and cell viability. BrdU incorporation and cell viability were assessed in HCT-116 cells treated with a dose range of Cdc7 inhibitor for 4 d. Cells were labeled with 10 µM BrdU for 2 h, and then BrdU incorporation was measured using a colorometric ELISA assay (Roche). Cell viability was measured using a Cell Titer-glo assay (Promega). GraphPad Prism was used to analyze the data.

6.4. Metabolic stability assays

6.4.1. HLM, RLM, and MLM assays. In vitro assays were used to determine *in vitro* metabolic stability of compounds. Human liver microsomes (HLM) (BD Biosciences), rat liver microsomes (RLM) (BD Biosciences), or mouse liver microsomes (MLM) (Xeno Tech) were incubated at 37 °C in

phosphate buffer pH7.4 with 1 mM NADPH and 1 µM of compound. After incubation for 0 or 30 min, the reactions were stopped by addition of MeCN and then analyzed by reverse phase HPLC and tandem mass spectroscopy.

6.5. *In vivo* studies

Rats and mice were maintained and treated in accordance with the Amgen Institutional Animal Care and Use Committee (IACUC) regulations.

6.5.1. Determination of in vivo *pharmacokinetics. In vivo* pharmacokinetics (PK) was determined using male Sprague Darley rats (Harlan) that were dosed intravenously with 2 mg/kg of **74** in DMSO or dosed orally (po) with 5 mg/kg of **74** in 2% HPMC, 1% Tween80, pH2. Blood plasma samples were collected at 0.25, 0.5, 1, 2, 4, 6, 8, 12, 16, and 24 h following compound administration and analyzed by liquid chromatography and mass spectroscopy (LC/MS).

6.5.2. PK/PD relationship in HCT-116 tumor xenografts. The PK/PD relationship of **74** was tested in mice using a HCT-116 tumor xenograft model. Four- to six-week old female, athymic nude mice (NCR/nu; Taconic) were injected subcutaneously with 5×10^6 million cells in Matrigel (BD Biosciences) and maintained until tumors reached approximately 250 mm^3. Mice were dosed iv with **74** formulated in 20% HPbCD, 1% HPMC, 1% PluronicF68, pH7 at 10 mg/ml. Each group consisted of three mice. At the time points indicated, blood plasma and tumor samples were collected. Plasma samples were analyzed by LC/MS, and corrected for unbound plasma concentrations according to percent plasma protein binding in mouse serum. Tumor samples were analyzed by MSD assay for inhibition of MCM2 serine 53 phosphorylation.

7. Acknowledgements

We thank Leeanne Zalameda, Sonia Escobar, and Tisha San Miguel for supporting the SAR assays, and Edward Lobenhofer for coordinating the kinase profiling studies. We thank Marcia Gordon for developing the PD assay, and Jessica Orf for support of *in vivo* studies. We thank Helming Tan for preformulation support, and Dean Hickman and Faye Hsieh for coordinating PK studies. We thank

Tony Polverino, Chris Fotsch, David Powers, and John McCarter for their guidance to the project team. We congratulate the authors of reference 28 on their success in obtaining the co-crystal structure of the Cdc7/Dbf4 – PHA767491 complex.

Appendix A. Supplementary data

Mechanism of Action experiments indicating ATP competitiveness of compounds **1** and **74**. Kinase selectivity data for compounds **1**, **74** and **77**. Determination of the K_m(app) for Cdc7 kinase. Images illustrating compound **74** causing aberrant mitosis.

Figures, Schemes, and Tables

Figure 1: HTS hit thiazole **1**

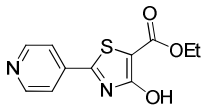

1

Cdc7 IC_{50} = 0.323 μM

CDK2 IC_{50} > 125 μM

Scheme 1

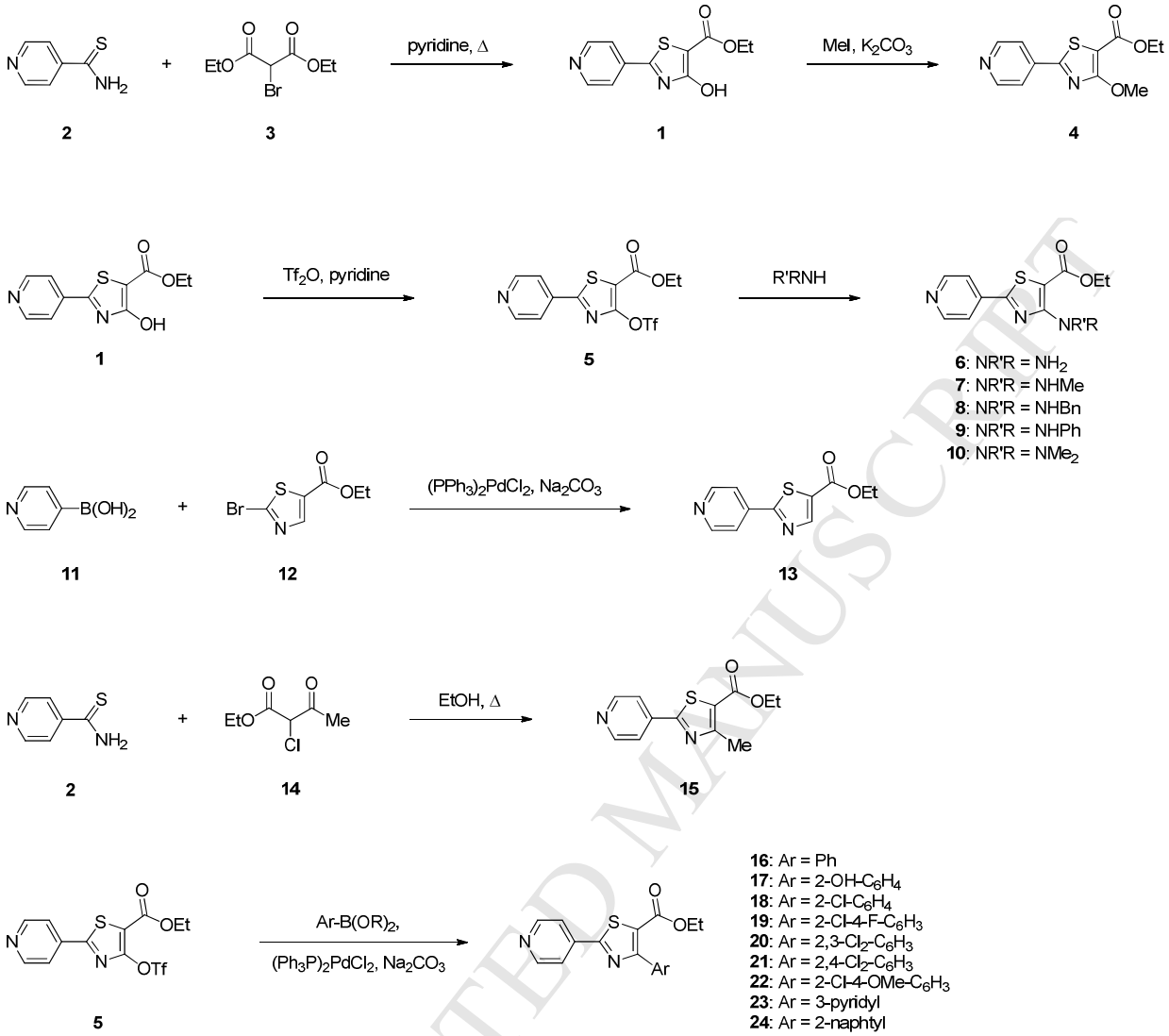

Scheme 2

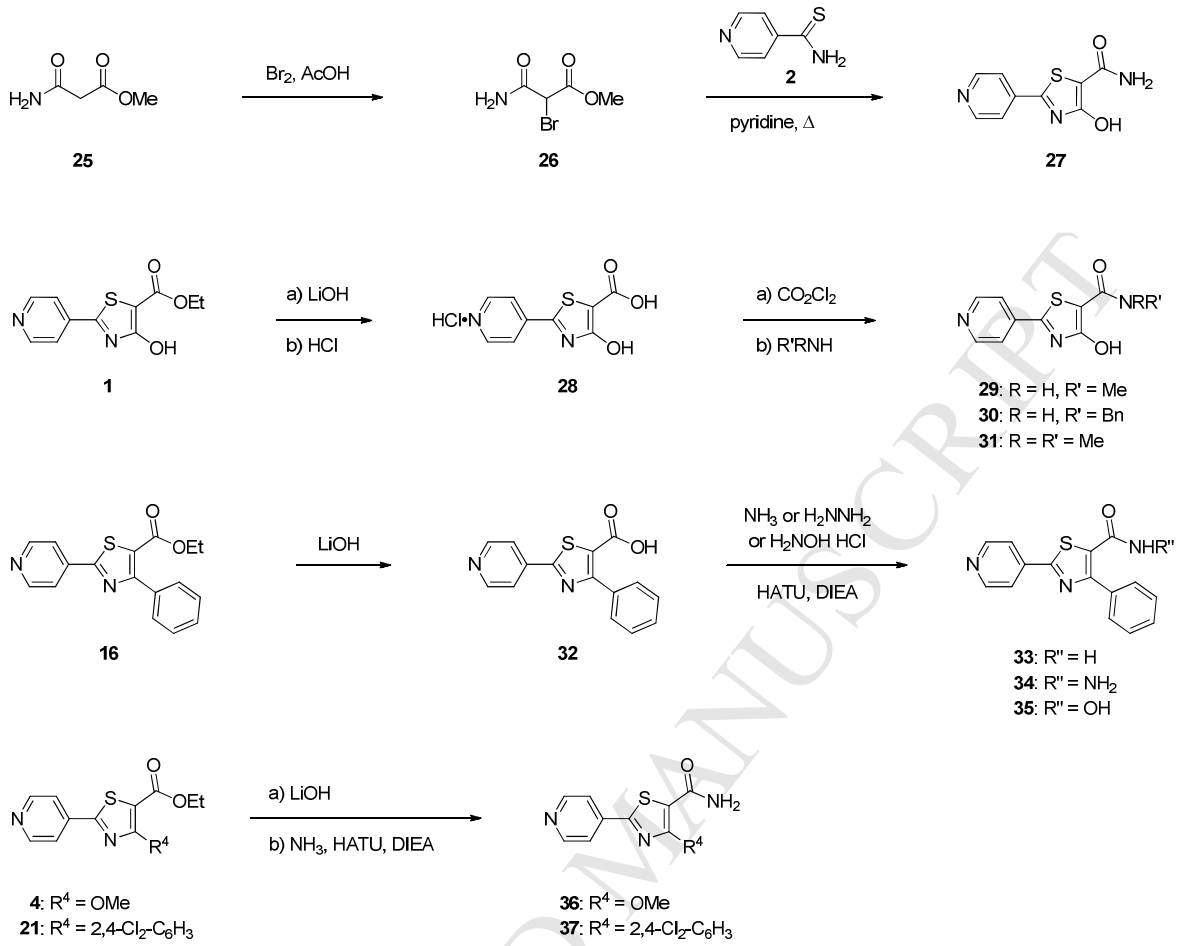

25 | **26** | **2** | **27**

1 | **28**

29: R = H, R' = Me
30: R = H, R' = Bn
31: R = R' = Me

16 | **32**

33: R'' = H
34: R'' = NH_2
35: R'' = OH

4: R^4 = OMe
21: R^4 = 2,4-Cl_2-C_6H_3

36: R^4 = OMe
37: R^4 = 2,4-Cl_2-C_6H_3

Scheme 3

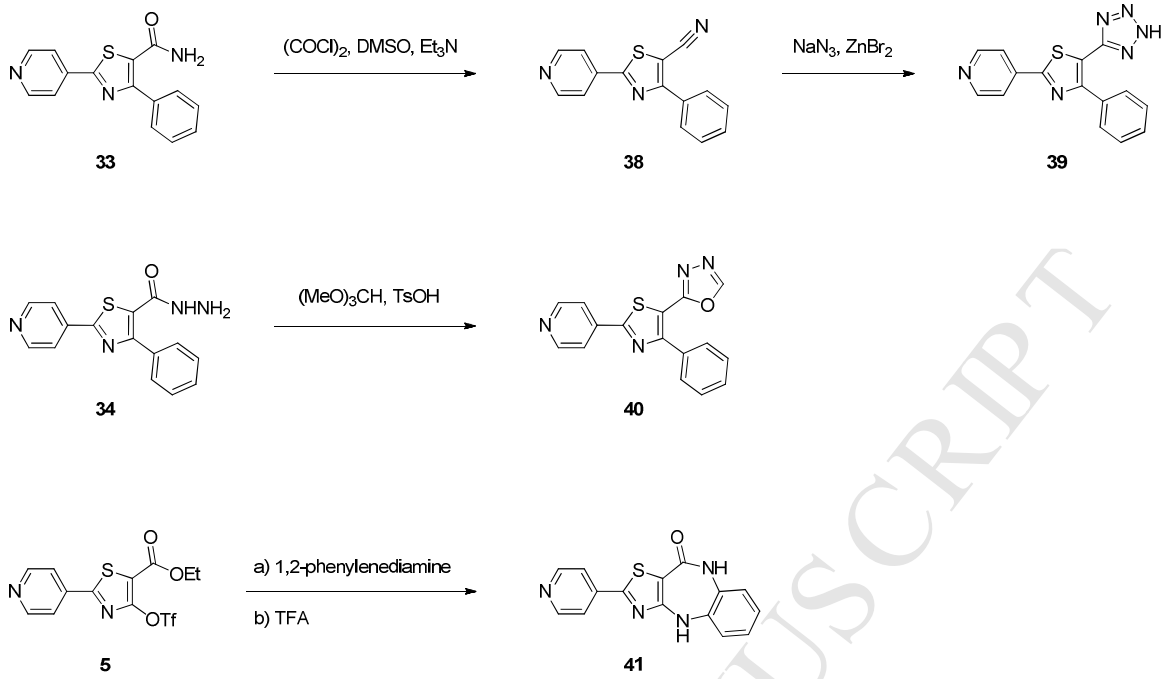

Scheme 4

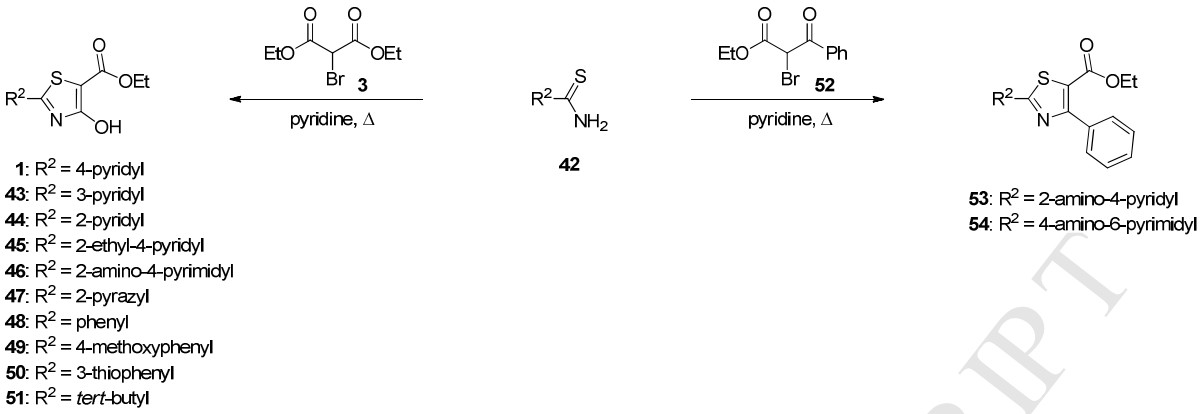

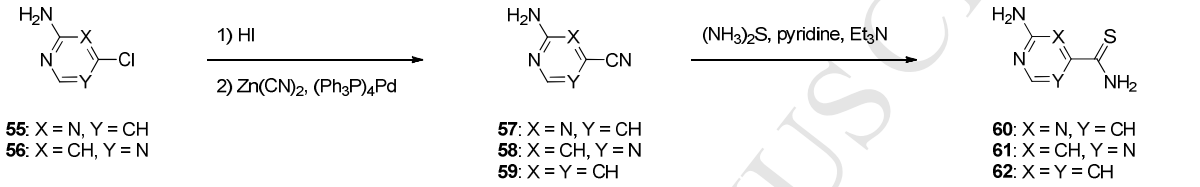

Scheme 5

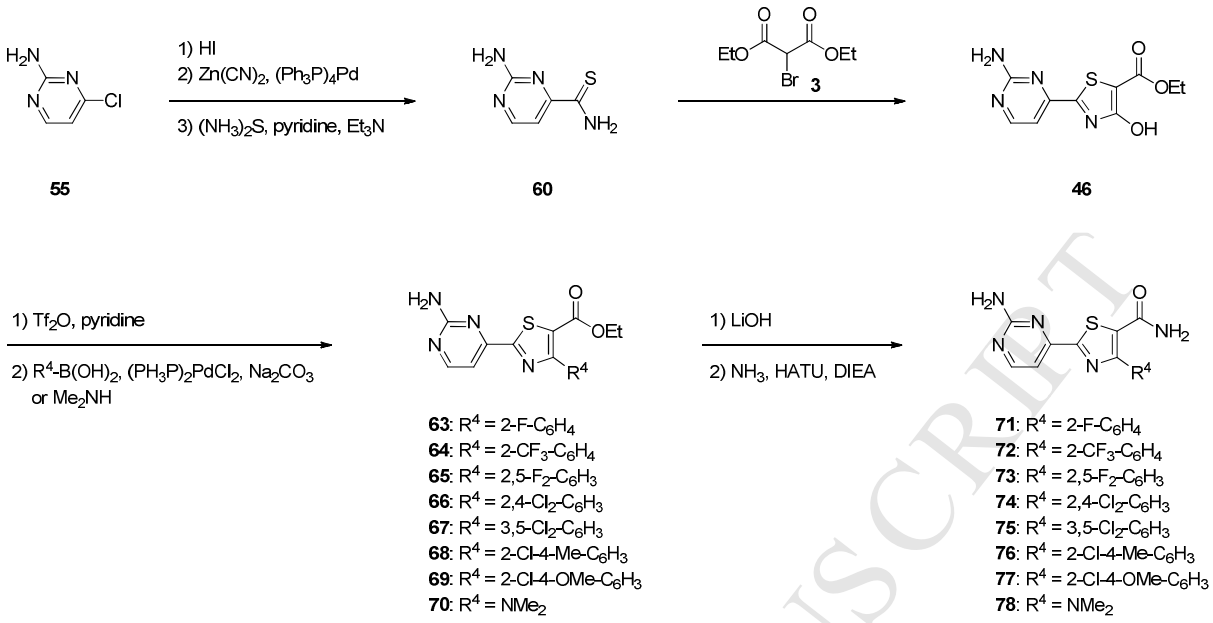

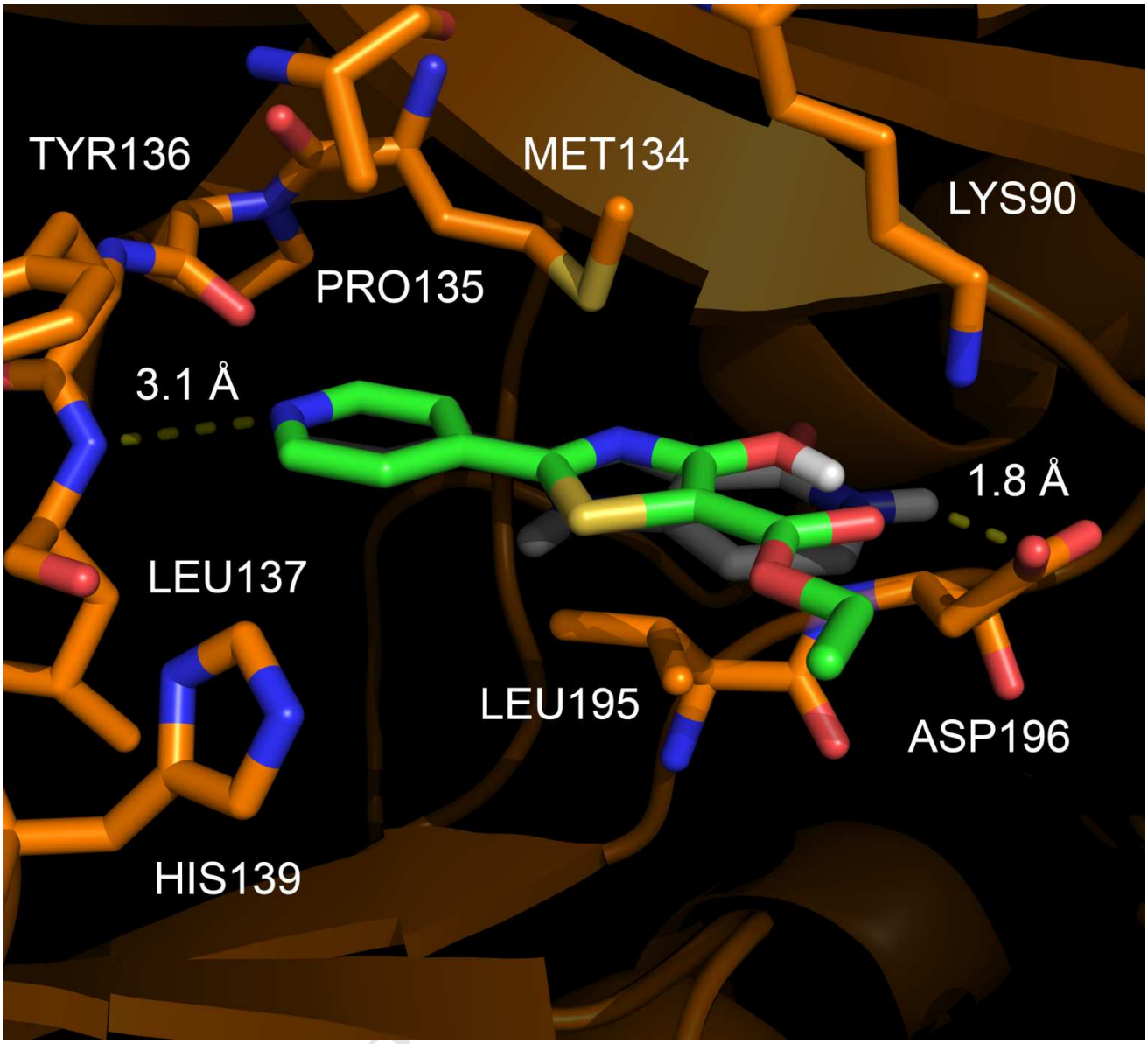

Figure 2: Predicted binding mode of compound **1** (0.343 μM, green) based on the published co-crystal structure (PDB: 4F9B) of Cdc7/Dbf4 (Cdc7 active site shown in orange) with PHA767491 (transparent white).[28] Protein-ligand distances for PHA767491 denoted in Ångstroms. Docked ligand conformation determined from PCM-B3LYP/6-31G* conformational search. See reference 29.

Table 1. SAR of the 4-substituent

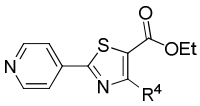

	R^4	Cdc7 IC_{50} [μM][a,b]	CDK2 IC_{50} [μM] [a,b]
1	OH	0.323 ±0.228	>125
4	OMe	17.2 ±6.33	>125
6	NH_2	4.20 ±3.66	>125
7	NHMe	7.35 ±3.78	>125
8	NHBn	38.3 ±13.0	>125
9	NHPh	>125	>125
10	NMe_2	0.669 ±0.364	>125
13	H	24.0 ±5.68	>125
15	Me	25.1 ±5.25	>125
16	Ph	20.5 ±14.0	>125
17	2-OH-C_6H_4	3.22 ±2.13	>125
18	2-Cl-C_6H_4	0.529 ±0.0902	>125
19	2-Cl-4-F-C_6H_3	1.02 ±0.756	>125
20	2,3-Cl_2-C_6H_3	0.451 ±0.103	>125
21	2,4-Cl_2-C_6H_3	0.973 ±0.266	>125
22	2-Cl-4-OMe-C_6H_3	0.855 ±0.516	>125
23	3-pyridyl	8.29 ±3.85	>125
24	2-naphthyl	>125	>125

[a] See the Experimental protocols for experimental details.
[b] Numeric data represents an average of at least three determinations; standard deviations are shown.

Table 2. SAR of the 5-substituent

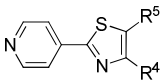

	R^5	R^4	Cdc7 IC_{50} [μM][a,b]	CDK2 IC_{50} [μM][a,b]
1	CO_2Et	OH	0.323 ±0.228	>125
16	CO_2Et	Ph	20.5 ±14.0	>125
28 (HCl)	CO_2H	OH	6.13 ±2.49	>125
32	CO_2H	Ph	0.172 ±0.132	>125
27	$CONH_2$	OH	0.115 ±0.0631	>125
33	$CONH_2$	Ph	0.101 ±0.0845	34.2 ±9.00
29	CONHMe	OH	8.98 ±4.44	>125
30	CONHBn	OH	11.6 ±3.00	52.1 ±13.3
31	$CONMe_2$	OH	24.4 ±3.26	>125
34	$CONHNH_2$	Ph	0.472 ±0.533	>125
35	CONHOH	Ph	1.69 ±1.10	>125
38	CN	Ph	10.3 ±10.1	>125
39		Ph	0.452 ±0.37	>125
40		Ph	3.87 ±2.79	>125
41	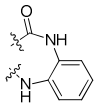		0.104 ±0.159	1.20 ±0.533

[a] See the Experimental protocols for experimental details. [b] Numeric data represents an average of at least three determinations; standard deviations are shown.

Table 3. Cellular activity of 2-(pyridin-4-yl)thiazole-5-carboxamides

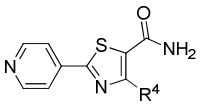

	R^4	Cdc7 IC_{50} [μM][a,b]	CDK2 IC_{50} [μM][a,b]	pMCM2 IC_{50} [μM][a,b]
27	OH	0.115 ±0.0631	>125	>50
36	OMe	0.0955 ±0.0152	5.71 ±0.901	9.93 ±6.33
33	Ph	0.101 ±0.0845	34.2 ±9.00	23.6 ±21.2
37	2,4-Cl_2-C_6H_3	0.0143 ±0.00909	0.700 ±0.375	11.5 ±9.01

[a] See the Experimental protocols for experimental details. [b] Numeric data represents an average of at least three determinations; standard deviations are shown.

Table 4. SAR of the 2-substituent

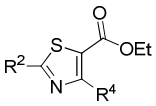

	R^2	R^4	Cdc7 IC_{50} [μM][a,b]	CDK2 IC_{50} [μM][a,b]
1		OH	0.323 ±0.228	>125
16		Ph	20.5 ±14.0	>125
43 (TFA)		OH	32.0 ±12.4	>125
44		OH	>125	>125
45		OH	7.50 ±0.91	>125
53		Ph	19.9 ±16.9	>125
46		OH	0.0415 ±0.0266	>125
54		Ph	>125	>125
47		OH	26.5 ±9.14	>125
48		OH	46.7 ±30.6	>125
49	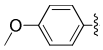	OH	>125	>125
50		OH	29.6 ±6.49	>125
51	*t*-Bu	OH	>125	>125

[a] See the Experimental protocols for experimental details.
[b] Numeric data represents an average of at least three determinations; standard deviations are shown.

Table 5. Potency and stability of 2-(2-aminopyrimidin-4-yl)thiazole-5-carboxamides

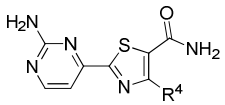

	R^4	Cdc7 IC_{50} [μM][a,b]	CDK2 IC_{50} [μM][a,b]	pMCM2 IC_{50} [μM][a,b]	RLM[a]	HLM[a]
71	2-F-C_6H_4	0.0178 ±0.0203	>125	1.07 ±.348	<14	<14
72	2-CF_3-C_6H_4	0.0184 ±0.00943	34.9 ±17.6	2.04 ±1.00	<14	<14
73	2,5-F_2-C_6H_3	0.0328 ±0.00575	34.8 ±18.3	3.62 ±2.35	28	<14
74	2,4-Cl_2-C_6H_3	0.00377 ±0.0016	1.82 ±0.122	0.501 ±0.519	22	19
75	3,5-Cl_2-C_6H_3	0.0623 ±0.0265	>125	8.50 ±3.81	69	67
76	2-Cl-4-Me-C_6H_3	0.00604 ±0.00303	7.03 ±2.45	1.40 ±1.89	140	<14
77	2-Cl-4-OMe-C_6H_3	0.00681 ±0.00412	10.6 ±3.61	0.862 ±1.08	99	43
78	NMe_2	0.0205 ±0.0238	18.2 ±4.43	1.87 ±1.72	26	23

[a] See the Experimental protocols for experimental details. [b] Numeric data represents an average of at least three determinations; standard deviations are shown.

Table 6. Kinase selectivity of compounds **74** and **77**

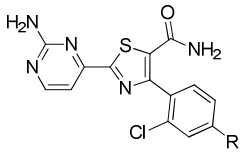

Kinase IC_{50} [μM][a]	**74** R = Cl	**77** R = OMe
Cdc7[b]	0.00377 ±0.0016	0.00681 ±0.00412
CDK1[b]	>50	>50
CDK2[b]	1.82 ±0.122	10.6 ±3.61
CDK4[b]	>50	>50
CDK9[b]	0.749 ±0.364	0.729 ±0.479
CK2	29.1	65.0
CK1α	0.694	0.545
CK1γ	0.760	1.90
CK1δ	0.084	0.104
Pim1	>1	>1

[a] See the Experimental protocols for experimental details. [b] Numeric data represents an average of at least three determinations; standard deviations are shown.

Table 7. Cellular activity of compounds **74** and **77**

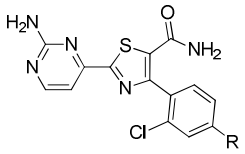

Assay [μM][a,b]	**74** R = Cl	**77** R = OMe
pMCM2 IC_{50}	0.501 ±0.519	0.862 ±1.08
pMCM2 IC_{90}	6.37 ±7.31	>125
BrdU IC_{50}	2.60 ±0.63	6.90 ±0.85
Cell Viability IC_{50}	4.20 ±0.28	4.60 ±0.28
Caspase 3/7 IC_{50}	>50	>50

[a] See the Experimental protocols for experimental details. [b] Numeric data represents an average of at least three determinations; standard deviations are shown.

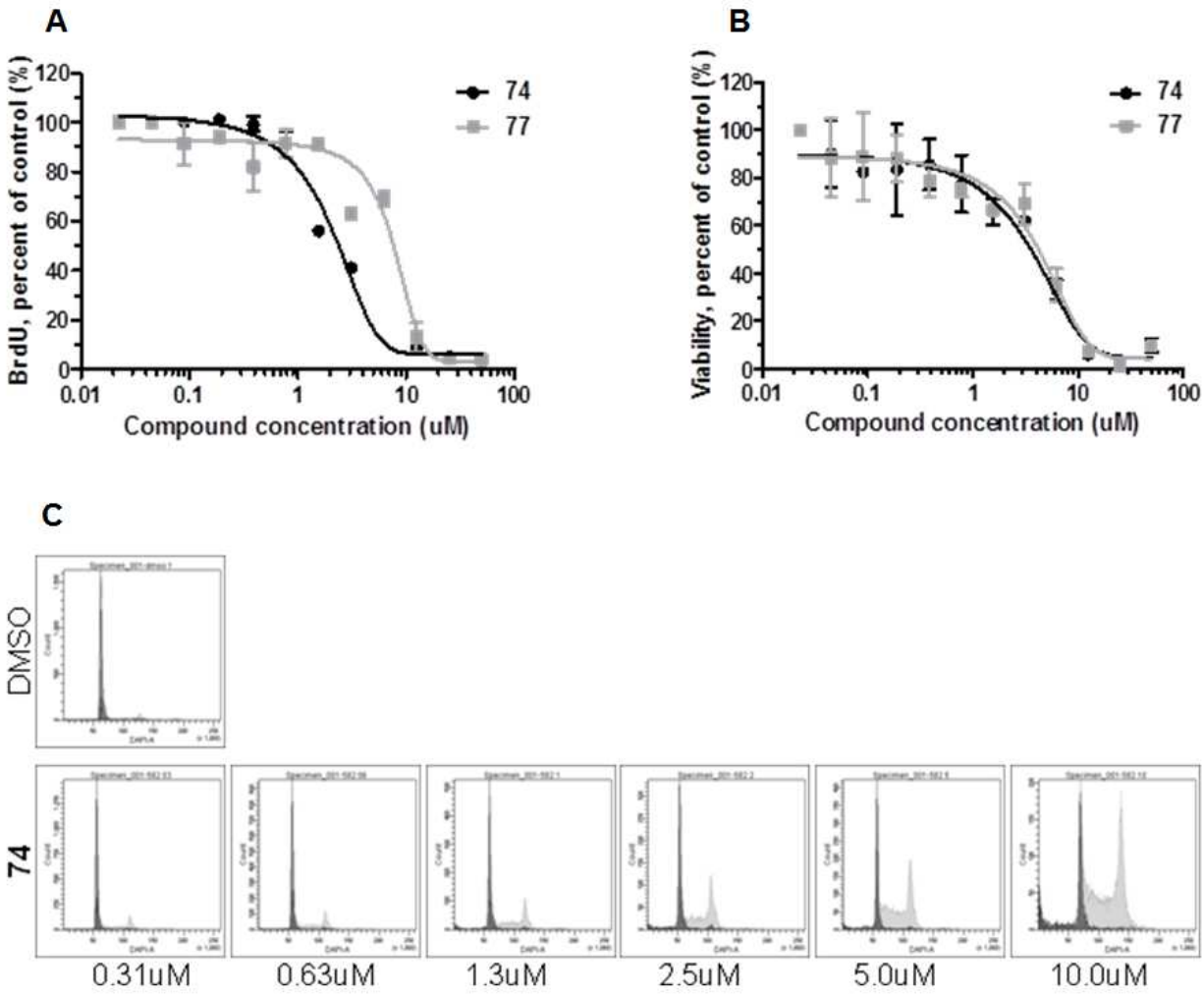

Figure 3. Compounds **74** and **77** inhibit DNA synthesis and cell viability when HCT-116 colorectal cancer cells were treated for 4 d. A) For the DNA synthesis assay, cells were labeled with 10 µM BrdU for 2 h, and then incorporated BrdU was detected using a colorometric ELISA assay. B) Cell viability was measured with a luminescence assay that detected ATP levels as a measure of metabolically active cells. C) DNA content was analyzed by flow cytometry of propidium iodide-stained HCT-116 cells treated with compound **74** for 3 d at the concentrations indicated.

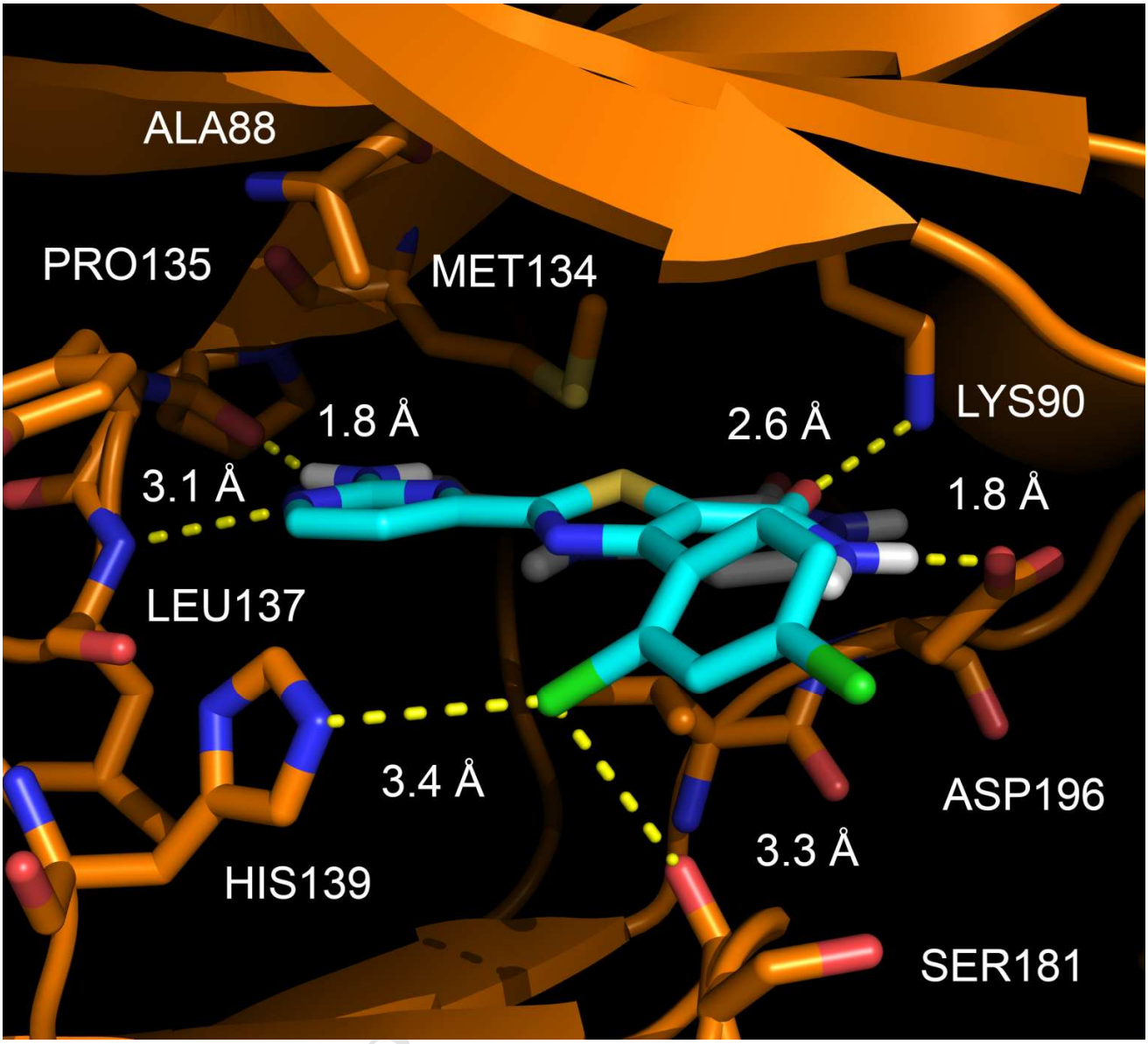

Figure 4: Proposed mode of **74** (cyan) from docking based on the published co-crystal structure (PDB: 4F9B) of Cdc7/Dbf4 (Cdc7 active site shown in orange) with PHA767491 (transparent white).[28] Protein-ligand distances for **74** denoted in Ångstroms. Docked ligand conformation determined from PCM-B3LYP/6-31G* conformational search. (Alternative mode with *ortho*-chloro oriented upward toward P-loop not shown.) See references 29 and 41.

Table 8. In-vivo rat PK of compound **74** in male Sprague Darley rats (Harlan)

2 mpk IV bolus in DMSO

AUC[0-t] (ng*h/ml)	AUC[0-inf] (ng*h/ml)	CL (ml/kg/h)	MRT (h)	T1/2 (h)	Vdss (ml/kg)
518	521	3890	1.15	6.56	4430

5 mpk PO in 2% HPMC, 1% Tween80, pH2 w/MSA

AUC[0-t] (ng*h/ml)	AUC[0-inf] (ng*h/ml)	CL/F (ml/kg/h)	Cmax (ng/ml)	T1/2 (h)	Tmax (h)	F (%)
83.3	85.7	63200	13.0	3.73	2.17	6.58

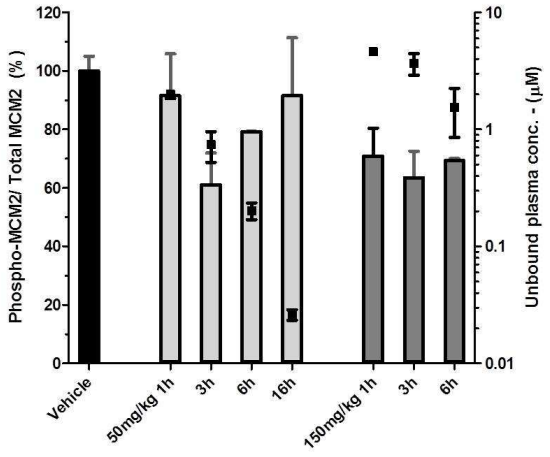

Figure 5. Compound **74** inhibits MCM2 phosphorylation in the HCT-116 tumor xenograft model. NCR/Nu mice (Taconic) bearing HCT-116 tumor xenografts were dosed iv with **74** formulated in 20% HPbCD, 1% HPMC, 1% PluronicF68, pH7. Tumors and plasma were harvested at the indicated time points and PK/PD analyzed. MCM2 phosphorylation was assessed with an MSD assay. Compound levels in plasma were analyzed by LC/MS and corrected for plasma protein binding in mouse serum.

References

[1] H. Masai, K. Arai, Cdc7 kinase complex: a key regulator in the initiation of DNA replication. J. Cell Physiol. 190 (2002) 287–296.

[2] K. Labib, How do Cdc7 and cyclin-dependent kinases trigger the initiation of chromosome replication in eukaryotic cells? Genes Dev. 24 (2010) 1208–1219.

[3] J.M. Kim, N. Kakusho, M. Yamada, Y. Kanoh, N. Takemoto, H. Masai, Cdc7 kinase mediates Claspin phosphorylation in DNA replication checkpoint. Oncogene 27 (2008) 3475–3482.

[4] V. Costanzo, D. Shechter, P.J. Lupardus, K.A. Cimprich, M. Gottesman, J. Gautier, An ATR- and Cdc7-dependent DNA damage checkpoint that inhibits initiation of DNA replication. Mol. Cell 11 (2003) 203–213.

[5] T. Tsuji, E. Lau, G.G. Chiang, W. Jiang, The role of Dbf4/Drf1-dependent kinase Cdc7 in DNA-damage checkpoint control. Mol. Cell 32 (2008) 862–869.

[6] S. Ito, C. Taniyami, N. Arai, H. Masai, Cdc7 as a potential new target for cancer therapy. Drug News Perspect. 21 (2008) 481–488.

[7] A. Montagnoli, J. Moll, F. Colotta, Targeting cell division cycle 7 kinase: A new approach for cancer therapy. Clin. Cancer Res. 16 (2010) 4503–4508.

[8] R. Swords, D. Mahalingam, M. O'Dwyer, C. Santocanale, K. Kelly, J. Carew, F. Giles, Cdc7 kinase - A new target for drug development. Eur. J. Cancer 46 (2010) 33–40.

[9] A. Montagnoli, P. Tenca, F. Sola, D. Carpani, D. Brotherton, C. Albanese, C. Santocanale, Cdc7 inhibition reveals a p53-dependent replication checkpoint that is defective in cancer cells. Cancer Res. 64 (2004) 7110–7116.

[10] A. Montagnoli, B. Valsasina, V. Croci, M. Menichincheri, S. Rainoldi, V. Marchesi, M. Tibolla, P. Tenca, D. Brotherton, C. Albanese, V. Patton, R. Alzani, A. Ciavolella, F. Sola, A. Molinari, D. Volpi, N. Avanzi, F. Fiorentini, M. Cattoni, S. Healy, D. Ballinari, E. Pesenti, A. Isacchi, J. Moll, A. Bensimon, E. Vanotti, C. Santocanale, A Cdc7 kinase inhibitor restricts initiation of DNA replication and has antitumor activity. Nat. Chem. Biol. 4 (2008) 357–365.

[11] E. Lau, G.G. Chiang, R.T. Abraham, W. Jiang, Divergent S phase checkpoint activation arising from prereplicative complex deficiency controls cell survival. Mol. Biol. Cell. 20 (2009) 3953–3964.

[12] S. Tudzarova, M.W. Trotter, A. Wollenschlaeger, C. Mulvey, J. Godovac-Zimmermann, G.H. Williams, K. Stoeber, Molecular architecture of the DNA replication origin activation checkpoint. EMBO J. 29 (2010) 3381–3394.

[13] P.R. Dohrmann, G. Oshiro, M. Tecklenburg, R.A. Sclafani, RAD53 regulates DBF4 independently of checkpoint function in Saccharomyces cerevisiae. Genetics 151 (1999) 965–977.

[14] G.F. Hess, R.F. Drong, K.L. Weiland, J.L. Slightom, R.A. Sclafani, R.E. Hollingsworth, A human homolog of the yeast CDC7 gene is overexpressed in some tumors and transformed cell lines. Gene 211 (1998) 133–140.

[15] D. Bonte, C. Lindvall, H. Liu, K. Dykema, K. Furge, M. Weinreich, Cdc7-Dbf4 kinase overexpression in multiple cancers and tumor cell lines is correlated with p53 inactivation. Neoplasia 10 (2008) 920–931.

[16] M. Choschzick, A. Lebeau, A.H. Marx, L. Tharun, L. Terracciano, U. Heilenkotter, F. Jaenicke, C. Bokemeyer, R. Simon, G. Sauter, J. Schwarz, Overexpression of cell division cycle 7 homolog is associated with gene amplification frequency in breast cancer. Hum. Pathol. 41 (2010) 358–365.

[17] E. Vanotti, R. Amici, A. Bargiotti, J. Berthelsen, R. Bosotti, A. Ciavolella, A. Cirla, C. Cristiani, R. D'Alessio, B. Forte, A. Isacchi, K. Martina, M. Menichincheri, A. Molinari, A. Montagnoli, P. Orsini, A. Pillan, F. Roletto, A. Scolaro, M. Tibolla, B. Valsasina, M. Varasi, D. Volpi, C. Santocanale, Cdc7 kinase inhibitors: Pyrrolopyridinones as potential antitumor agents. 1. Synthesis and structure-activity relationships. J. Med. Chem. 51 (2008) 487–501.

[18] M. Menichincheri, A. Bargiotti, J. Berthelsen, J.A. Bertrand, R. Bossi, A. Ciavolella, A. Cirla, C. Cristiani, V. Croci, R. D'Alessio, M. Fasolini, F. Fiorentini, B. Forte, A. Isacchi, K. Martina, A. Molinari, A. Montagnoli, P. Orsini, F. Orzi, E. Pesenti, D. Pezzetta, A. Pillan, I. Poggesi, F. Roletto, A. Scolaro, M. Tato, M. Tibolla, B. Valsasina, M. Varasi, D. Volpi, C.

Santocanale, E. Vanotti, First Cdc7 kinase inhibitors: Pyrrolopyridinones as potent and orally active antitumor agents. 2. Lead discovery. J. Med. Chem. 52 (2009) 293–307.

[19] M. Menichincheri, C. Albanese, C. Alli, D. Ballinari, A. Bargiotti, M. Caldarelli, A. Ciavolella, A. Cirla, M. Colombo, F. Colotta, V. Croci, R. D'Alessio, M. D'Anello, A. Ermoli, F. Fiorentini, B. Forte, A. Galvani, P. Giordano, A. Isacchi, K. Martina, A. Molinari, J.K. Moll, A. Montagnoli, P. Orsini, F. Orzi, E. Pesenti, A. Pillan, F. Roletto, A. Scolaro, M. Tatò, M. Tibolla, B. Valsasina, M. Varasi, P. Vianello, D. Volpi, C. Santocanale, E. Vanotti, Cdc7 kinase inhibitors: 5-heteroaryl-3-carboxamido-2-aryl pyrroles as potential antitumor agents. 1. Lead finding. J. Med. Chem. 53 (2010) 7296–7315.

[20] A. Ermoli, A. Bargiotti, M.G. Brasca, A. Ciavolella, N. Colombo, G. Fachin, A. Isacchi, M. Menichincheri, A. Molinari, A. Montagnoli, A. Pillan, S. Rainoldi, F.R. Sirtori, F. Sola, S. Thieffine, M. Tibolla, B. Valsasina, D. Volpi, C. Santocanale, Vanotti E., Cell division cycle 7 kinase inhibitors: 1H-Pyrrolo[2,3-b]pyridines, synthesis and structure-activity relationships. J. Med. Chem. 52 (2009) 4380–4390.

[21] C.M. Shafer, M. Lindvall, C. Bellamacina, T.G. Gesner, A. Yabannavar, W. Jia, S. Lin, A. Walter, 4-(1H-indazol-5-yl)-6-phenylpyrimidin-2(1H)-one analogs as potent CDC7 inhibitors. Bioorg. Med. Chem. Lett. 18 (2008) 4482–4485.

[22] C. Zhao, C. Tovar, X. Yin, Q. Xu, I.T. Todorov, L.T. Vassilev, L. Chen, Synthesis and evaluation of pyrido-thieno-pyrimidines as potent and selective Cdc7 kinase inhibitors. Bioorg. Med. Chem. Lett. 19 (2009) 319–323.

[23] K.W. Woods, C. Lai, Y.T. Miyashiro, A.S. Florjancic, E.K. Han, N. Soni, Y. Shi, L. Lasko, J.D. Leverson, E.F. Johnson, A.R. Shoemaker, T.D. Penning, Aminopyrimidinone cdc7 kinase inhibitors. Bioorg. Med. Chem. Lett. 22 (2012) 1940–1943.

[24] E.S. Koltun, A.L. Tsuhako, D.S. Brown, N. Aay, A. Arcalas, V. Chan, H. Du, S. Engst, K. Ferguson, M. Franzini, A. Galan, C.R. Holst, P. Huang, B. Kane, M.H. Kim, J. Li, D. Markby, M. Mohan, K. Noson, A. Plonowski, S.J. Richards, S. Robertson, K. Shaw, G. Stott, T.J. Stout, J. Young, P. Yu, C.A. Zaharia, W. Zhang, P. Zhou, J.M. Nuss, W. Xu, P.C. Kearney, Discovery of XL413, a potent and selective CDC7 inhibitor. Bioorg. Med. Chem. Lett. 22 (2012) 3727–3231.

[25] N. Nakajima, M. Ubukata, Preparation of nitriles from primary amides under Swern oxidation conditions. Tetrahedron Lett. 38 (1997) 2099–2102.

[26] Z.P. Demko, K.B. Sharpless, Preparation of 5-substituted 1H-tetrazoles from nitriles in water. J. Org. Chem. 66 (2001) 7945–7950.

[27] R.M. Rzasa, M.R. Kaller, G. Liu, E. Magal, T.T. Nguyen, T.D. Osslund, D. Powers, V.J. Santora, V.N. Viswanadhan, H.-L. Wang, X. Xiong, W. Zhong, M.H. Norman, Structure-activity relationships of 3,4-dihydro-1*H*-quinazolin-2-one derivatives as potential CDK5 inhibitors. Bioorg. Med. Chem. 15 (2007) 6574–6595.

[28] S. Hughes, F. Elustondo, A. Di Fonzo, F.G. Leroux, A.C. Wong, A.P. Snijders, S.J. Matthews. P. Cherepanov, Crystal structure of human CDC7 kinase in complex with its activator DBF4. Nat. Struct. Mol. Biol. 19 (2012), 1101–1109.

[29] Initial free state conformations were generated via low-mode molecular dyanamics utilizing the MMFF94 force field as implemented in the MOE 2012.10 program suite.[30] Resultant conformations were subjected to quantum mechanical optimization in an implicit aqueous solvent model (PCM-B3LYP/6-31G*) as implemented in *Gaussian 09*.[31] The lowest energy conformers were then aligned to the linker-binding pyridyl moiety of PHA767491 in the active site of Cdc7/Dbf4 and subjected to MM-GBSA refinement using Amber 7.[32]

[30] Molecular *Operating Environment (MOE)* 2012.10; Chemical Computing Group Inc., 1010 Sherbooke St. West, Suite #910, Montreal, QC, Canada, H3A 2R7, 2012.

[31] *Gaussian 09*, Revision D.01, M.J. Frisch, G.W. Trucks, H.B. Schlegel, G.E. Scuseria, M.A. Robb, J.R. Cheeseman, G. Scalmani, V. Barone, B. Mennucci, G.A. Petersson, H. Nakatsuji, M. Caricato, X. Li, H.P. Hratchian, A.F. Izmaylov, J. Bloino, G. Zheng, J.L. Sonnenberg, M. Hada, M. Ehara, K. Toyota, R. Fukuda, J. Hasegawa, M. Ishida, T. Nakajima, Y. Honda, O. Kitao, H. Nakai, T. Vreven, J. A. Montgomery, Jr., J. E. Peralta, F. Ogliaro, M. Bearpark, J. J. Heyd, E. Brothers, K.N. Kudin, V.N. Staroverov, T. Keith, R. Kobayashi, J. Normand, K. Raghavachari, A. Rendell, J.C. Burant, S.S. Iyengar, J. Tomasi, M. Cossi, N. Rega, J.M. Millam, M. Klene, J.E. Knox, J.B. Cross, V. Bakken, C. Adamo, J. Jaramillo, R. Gomperts, R.E. Stratmann, O. Yazyev, A.J. Austin, R. Cammi, C. Pomelli, J.W. Ochterski, R.L. Martin, K. Morokuma, V.G. Zakrzewski, G.A. Voth, P. Salvador, J.J. Dannenberg, S. Dapprich, A.D. Daniels, O. Farkas, J.B. Foresman, J.V. Ortiz, J. Cioslowski, and D.J. Fox, Gaussian, Inc., Wallingford CT, 2013.

[32] D.A. Case, D.A. Pearlman, J.W. Caldwell, T.E. Cheatham III, J. Wang, W.S. Ross, C.L. Simmerling, T.A. Darden, K.M. Merz, R.V. Stanton, A.L. Cheng, J.J. Vincent, M. Crowley, V. Tsui, H. Gohlke, R.J. Radmer, Y. Duan, J. Pitera, I. Massova, G.L. Seibel, U.C. Singh, P.K. Weiner and P.A. Kollman, AMBER 7, University of California, San Francisco, 2002.

[33] A. Montagnoli, B. Valsasina, D. Brotherton, S. Troiani, S. Rainoldi, P. Tenca, A. Molinari, C. Santocanale, Identification of Mcm2 phosphorylation sites by S-phase-regulating kinases. J. Biol. Chem. 281 (2006) 10281–10290.

[34] W.H. Cho, Y.J. Lee, S.I. Kong, J. Hurwitz, J.K. Lee, CDC7 kinase phosphorylates serine residues adjacent to acidic amino acids in the minichromosome maintenance 2 protein. Proc. Natl. Acad. Sci. USA 103 (2006) 11521–11526.

[35] S. Wang, P.M. Fischer, Cyclin-dependent kinase 9: a key transcriptional regulator and potential drug target in oncology, virology and cardiology. Trends Pharmacol. Sci. 29 (2008) 302–213.

[36] A. Natoni, L.S. Murillo, A.E. Kliszczak, M.A. Catherwood, A. Montagnoli, A. Samali, M. O'Dwyer, C. Santocanale, Mechanisms of action of a dual Cdc7/Cdk9 kinase inhibitor against quiescent and proliferating CLL cells. Mol. Cancer Ther. 10 (2011) 1624–1634.

[37] F. Pierre, P.C. Chua, S.E. O'Brien, A. Siddiqui-Jain, P. Bourbon, M. Haddach, J. Michaux, J. Nagasawa, M.K. Schwaebe, E. Stefan, A. Vialettes, J.P. Whitten, T.K. Chen, L. Darjania, R. Stansfield, K. Anderes, J. Bliesath, D. Drygin, C. Ho, M. Omori, C. Proffitt, N. Streiner, K. Trent, W.G. Rice, D.M. Ryckman, Discovery and SAR of 5-(3-chlorophenylamino)benzo[c][2,6]naphthyridine-8-carboxylic acid (CX-4945), the first clinical stage inhibitor of protein kinase CK2 for the treatment of cancer. J. Med. Chem. 54 (2011) 635–654.

[38] C.A. Thorne, A.J. Hanson, J. Schneider, E. Tahinci, D. Orton, C.S. Cselenyi, K.K. Jernigan, K.C. Meyers, B.I. Hang, A.G. Waterson, K. Kim, B. Melancon, V.P. Ghidu, G.A. Sulikowski, B. LaFleur, A. Salic, L.A. Lee, D.M. Miller, 3rd, E. Lee, Small-molecule inhibition of Wnt signaling through activation of casein kinase 1α. Nat. Chem. Biol. 6 (2010) 829–836.

[39] G.J. Yu, C. L. Yoo. B. Yang, M.W. Lodewyk, L. Meng, T.T. El-Idressy, J.C. Fettinger, D.J. Tantillo, A.S. Verkman, M.J. Kurth, Potent *s-cis*-locked bithiazole correctors of DF508 cystic fibrosis transmembrane conductance regulator cellular processing for cystic fibrosis therapy. J. Med. Chem. 51 (2008) 6044-6054.

[40] H. Gökce, S. Bahçeli, Analysis of molecular structure and vibrational spectra of 2-(2'-thienyl)pyridine. J. Mol. Struct. 1005 (2011) 100-106.

[41] An alternative binding orientation of **74** (not shown in Figure 4), arising from the opposite orientation of the pendant 2,4-dichlorophenyl substituent and projecting the *ortho*-chloro functionality upward toward the P-loop, is also accommodated by the Cdc7 structure and presents an additional feasible mode. This alternative substituent orientation maintains the same key anchoring contacts to the linker region, as well as the *syn* orientation of the thiazole sulfur and proximal pyrimidine nitrogen atoms.

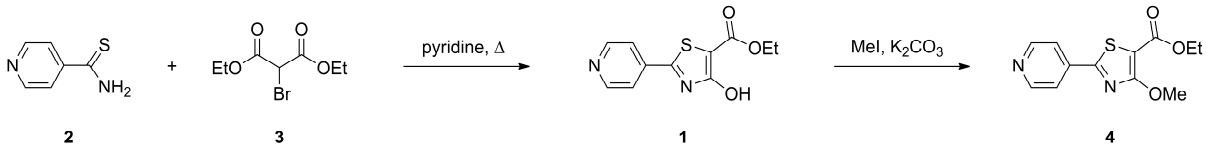

2 **3** **1** **4**

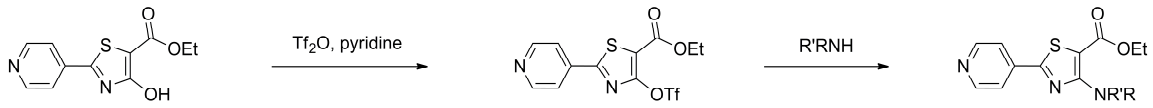

1 **5**

6: NR'R = NH_2
7: NR'R = NHMe
8: NR'R = NHBn
9: NR'R = NHPh
10: NR'R = NMe_2

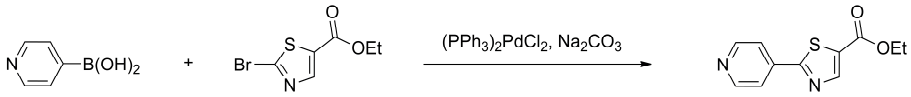

11 **12** **13**

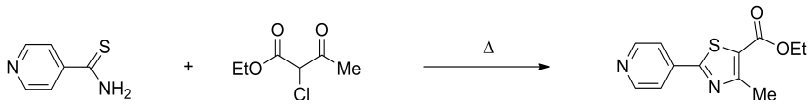

2 **14** **15**

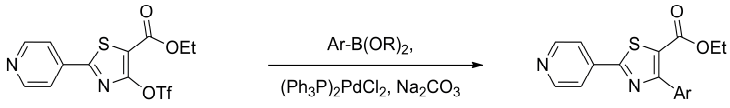

5

16: Ar = Ph
17: Ar = 2-OH-C_6H_4
18: Ar = 2-Cl-C_6H_4
19: Ar = 2-Cl-4-F-C_6H_3
20: Ar = 2,3-Cl_2-C_6H_3
21: Ar = 2,4-Cl_2-C_6H_3
22: Ar = 2-Cl-4-OMe-C_6H_3
23: Ar = 3-pyridyl
24: Ar = 2-naphtyl

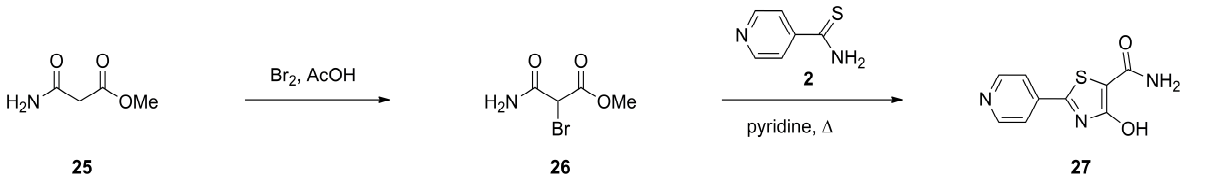

25 **26** **27**

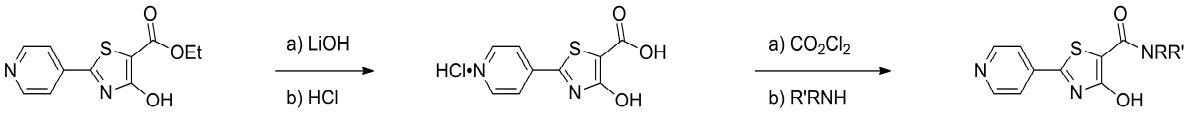

1 **28**

29: R = H, R' = Me
30: R = H, R' = Bn
31: R = R' = Me

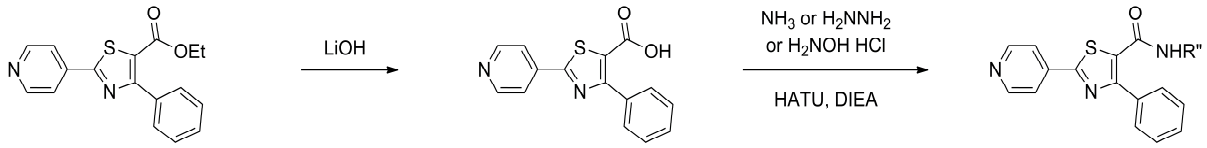

16 **32**

33: R" = H
34: R" = NH_2
35: R" = OH

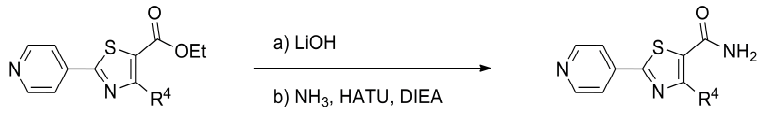

4: R^4 = OMe **36**: R^4 = OMe

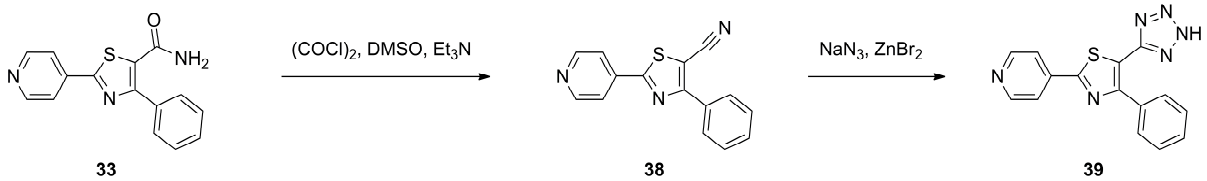

33 38 39

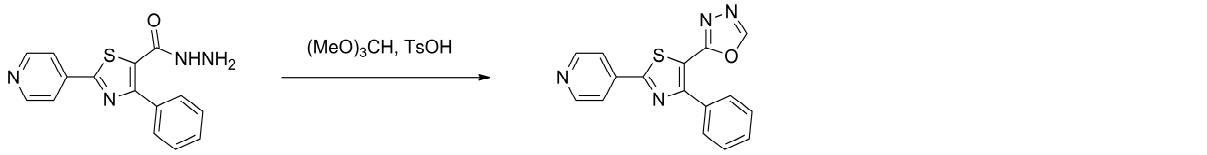

34 40

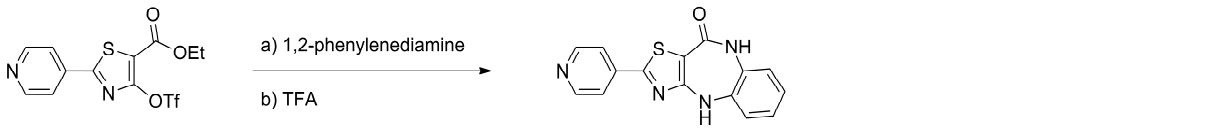

5 41

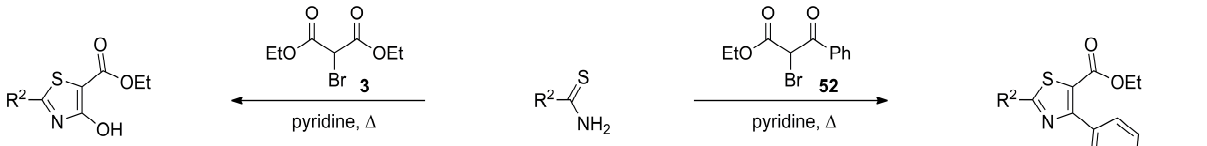

1: R^2 = 4-pyridyl
43: R^2 = 3-pyridyl
44: R^2 = 2-pyridyl
45: R^2 = 2-ethyl-4-pyridyl
46: R^2 = 2-amino-4-pyrimidyl
47: R^2 = 2-pyrazyl
48: R^2 = phenyl
49: R^2 = 4-methoxyphenyl
50: R^2 = 3-thiophenyl
51: R^2 = *tert*-butyl

53: R^2 = 2-amino-4-pyridyl
54: R^2 = 4-amino-6-pyrimidyl

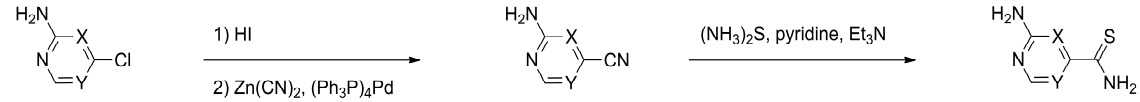

55: X = N, Y = CH
56: X = CH, Y = N

57: X = N, Y = CH
58: X = CH, Y = N

60: X = N, Y = CH
61: X = CH, Y = N

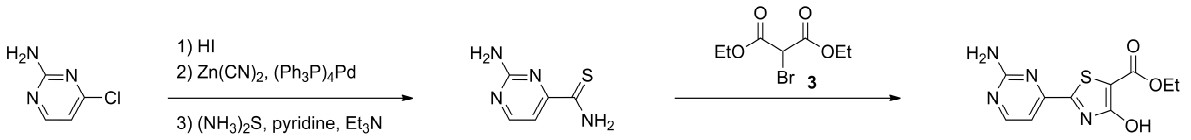

55 **60** **46**

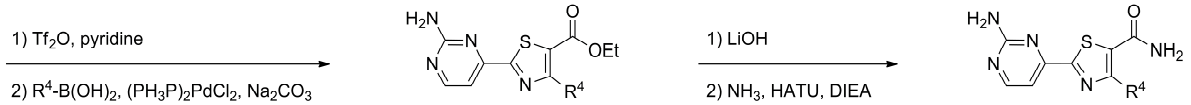

63: R^4 = 2-F-C_6H_4
64: R^4 = 2-CF_3-C_6H_4
65: R^4 = 2,5-F_2-C_6H_3
66: R^4 = 2,4-Cl_2-C_6H_3
67: R^4 = 3,5-Cl_2-C_6H_3
68: R^4 = 2-Cl-4-Me-C_6H_3
69: R^4 = 2-Cl-4-OMe-C_6H_3
70: R^4 = NMe_2

71: R^4 = 2-F-C_6H_4
72: R^4 = 2-CF_3-C_6H_4
73: R^4 = 2,5-F_2-C_6H_3
74: R^4 = 2,4-Cl_2-C_6H_3
75: R^4 = 3,5-Cl_2-C_6H_3
76: R^4 = 2-Cl-4-Me-C_6H_3
77: R^4 = 2-Cl-4-OMe-C_6H_3
78: R^4 = NMe_2

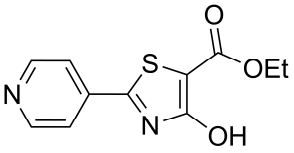

1

Cdc7 IC_{50} = 0.323 μM

CDK2 IC_{50} > 125 μM

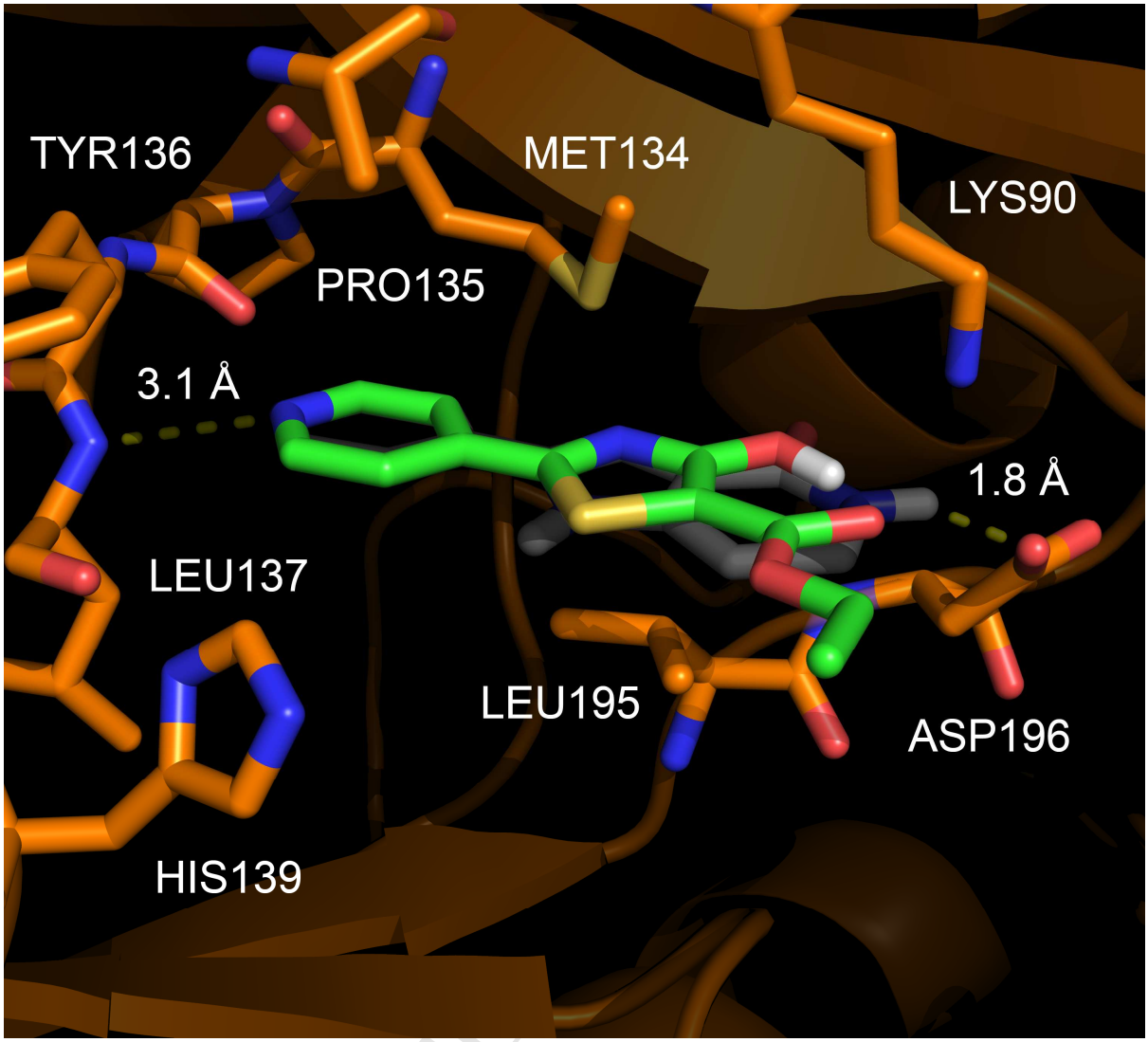

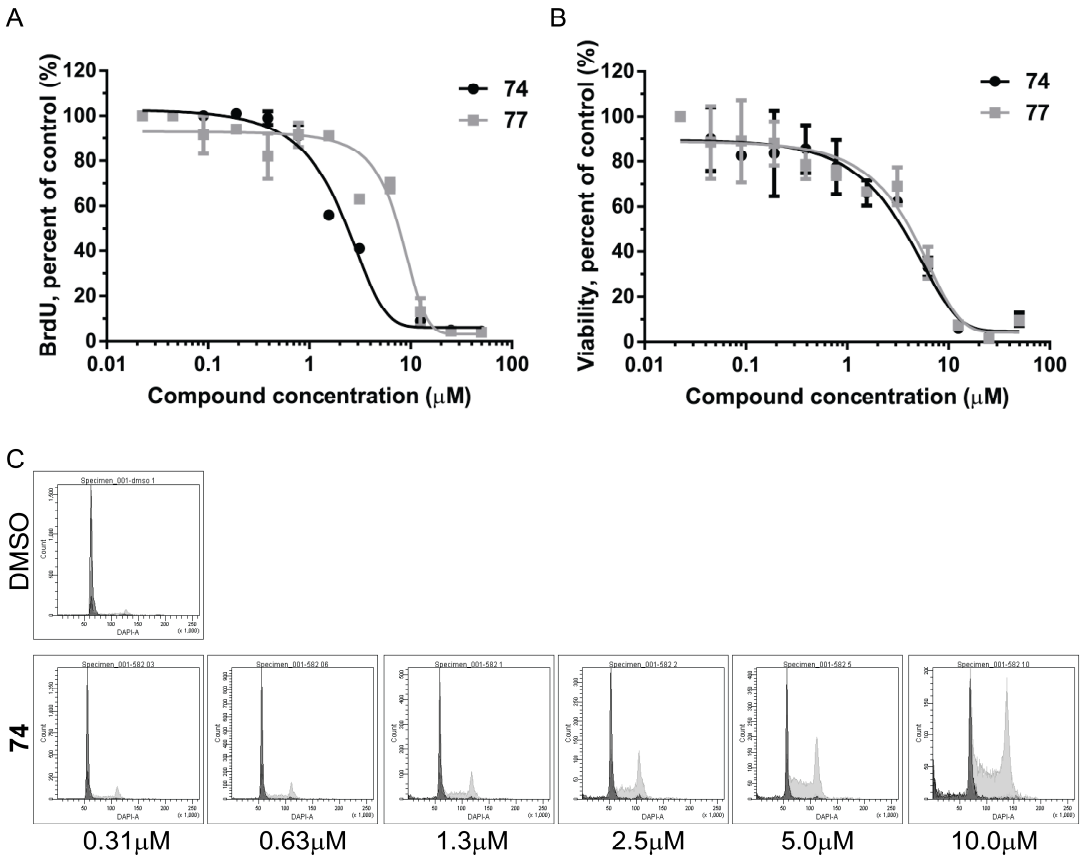

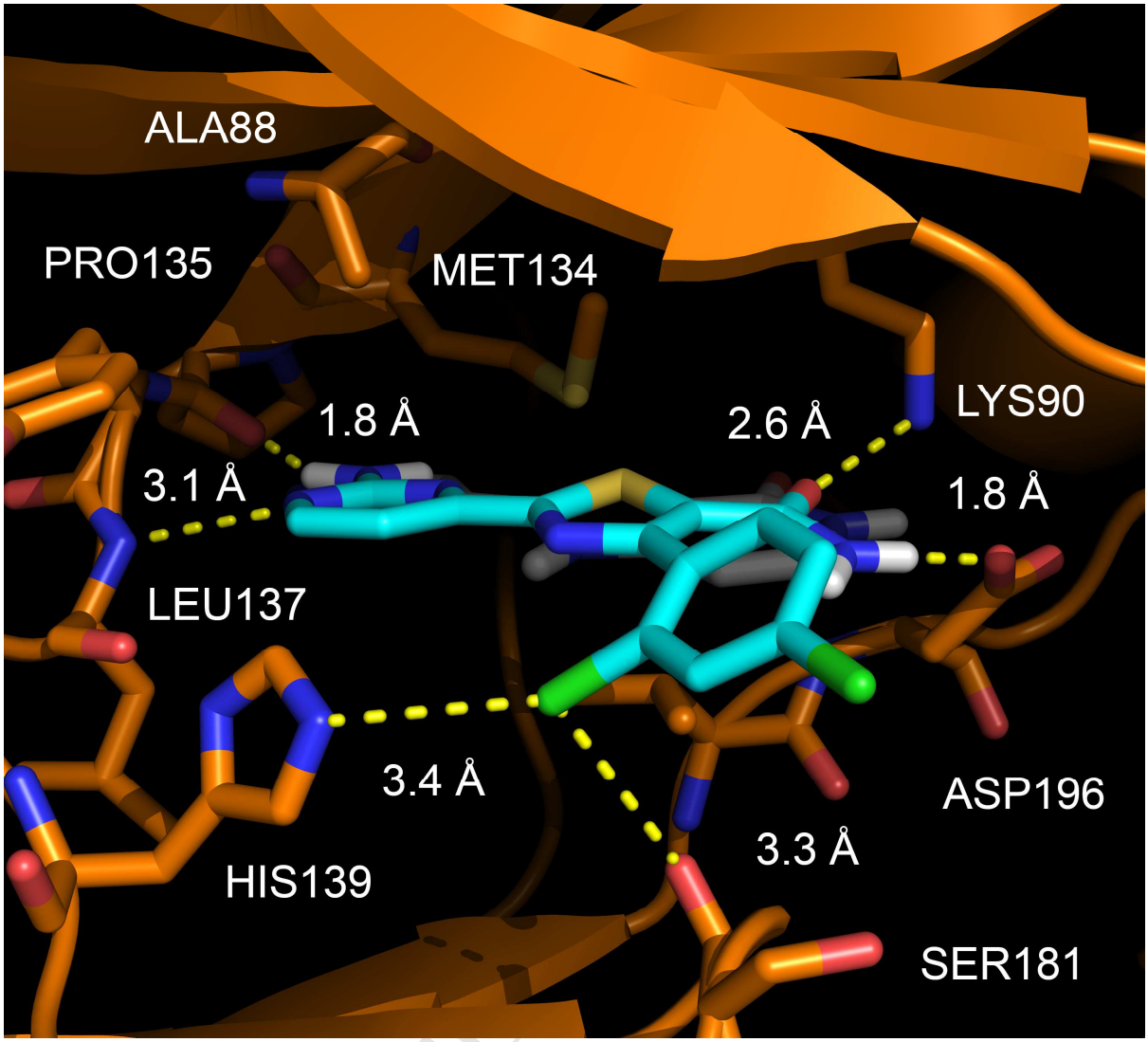

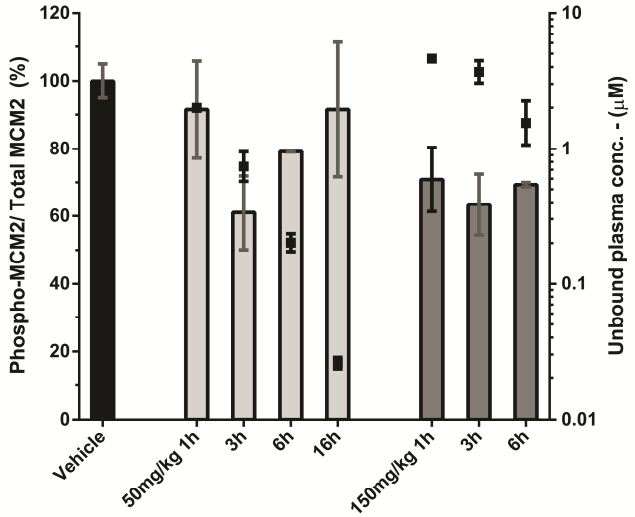

Highlights

of the manuscript

Synthesis and structure-activity relationship of trisubstituted thiazoles as Cdc7 kinase inhibitors

submitted for consideration as an

Original Paper in the *European Journal of Medicinal Chemistry*

1. Inhibition of Cdc7 kinase may not be limited by cytotoxicity to regular cells
2. Compounds with low MW and high binding efficiencies were found in the HTS
3. Our SAR studies systematically explored all substituents on the core of thiazoles
4. We discovered selective Cdc7 inhibitors that showed potency *in vitro* and *in vivo*
5. The synthesis of every compound in this manuscript is illustrated

Supplementary data

Synthesis and structure-activity relationship of trisubstituted thiazoles as Cdc7 kinase inhibitors

Andreas Reichelt[a,], Julie M. Bailis[b], Michael D. Bartberger[c], Guomin Yao[a], Hong Shu[a], Matthew R. Kaller[a], John G. Allen[a], Margaret F. Weidner[b], Kathleen S. Keegan[b], Jennifer H. Dao[c]*

[a]*Departments of Medicinal Chemistry, Amgen, Inc., One Amgen Center Drive, Thousand Oaks, California 91320.* [b]*Oncology Research, Amgen, Inc., 1201 Amgen Court West, Seattle, Washington 98119.* [c]*Molecular Structure and Characterization, Amgen, Inc., One Amgen Center Drive, Thousand Oaks, California 91320.*

Contents

Supplementary Figure 1. Mechanism of Action Studies on Compound **1**

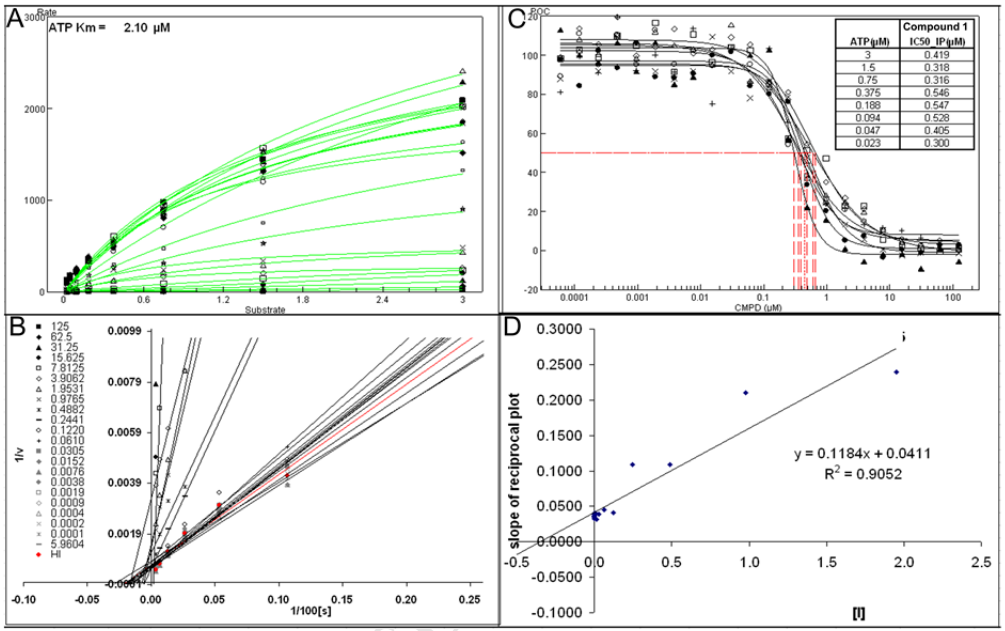

Compound **1** is an ATP-competitive inhibitor. The rate of Cdc7 enzymatic activity was determined from an AlphaScreen assay (see Experimental Procedures) following titration of ATP and compound **1**. The results fit the competitive model for enzyme inhibition. Effects of ATP on Cdc7 enzymatic activity with various concentrations of compound **1** are shown in Michaelis–Menton (**A**) and double-reciprocal plot (**B**) formats. **C**, Compound **1** inhibitor potency was determined in the AlphaScreen assay. **D**, Slope of the double-reciprocal plot versus inhibitor concentration.

Mechanism of action studies to determine whether inhibition of the Cdc7 enzyme was competitive or non-competitive were carried out using an AlphaScreen assay using 6 nM Cdc7/Dbf4 protein, 10 nM MCM2 protein, and varying the concentrations of ATP (from 3 µM in 1:2 titrations) and compounds (from 125 µM in 1:2 titrations). Reaction time was 2 h. Reaction rates, K_m, and K_i were determined as reported previously.[1] The K_m was determined from AlphaScreen assays of Cdc7 enzymatic activity, varying the concentration of Cdc7/Dbf4 protein or the concentration of ATP.

[1] Dao, J. H.; Kurzeja, R. J.; Morachis, J. M.; Veith, H.; Lewis, J.; Yu, V.; Tegley, C. M.; Tagari, P., Kinetic characterization and identification of a novel inhibitor of hypoxia-inducible factor prolyl hydroxylase 2 using a time-resolved fluorescence resonance energy transfer-based assay technology. *Anal. Biochem.* **2009**, *384*, 213–223.

Supplementary Figure 2. Kinase Selectivity of Compounds **1**, **74**, and **77**

Cmpd	Replicate	# with POC <50	ABL1-nonphosphorylated	ABL1-phosphorylated	AKT1	AKT2	ALK	AMPK-alpha1	AURKA	BMPR1A	BRAF	BRK	BTK	CAMK2D	CAMK4	CDK2	CDK4-cyclinD1	CDK8	CHEK1	CLK1	CLK2
1	1	0	88	100	100	96	95	100	100	82	100	100	99	88	100	100	100	94	100	90	89
	2	0	87	100	75	100	86	68	100	88	100	94	92	79	76	100	100	82	100	100	86
74	1	11	100	100	87	100	100	100	77	94	90	68	100	90	100	100	100	98	100	1.3	7.9
	2	10	99	100	80	100	100	100	100	100	80	74	75	100	100	100	100	97	99	1.5	14
77	1	12	100	90	100	100	63	81	61	81	100	80	76	93	100	84	98	84	100	2.3	10
	2	13	100	98	66	100	100	76	55	100	100	98	96	100	100	100	100	86	78	3	11

Cmpd	CLK4	CSNK1D	CSNK1G2	CSNK2A1	DAPK1	DDR1	DMPK	DYRK1A	DYRK1B	EGFR	EPHA2	EPHA4	EPHB3	ERK2	ERN1	FGFR1	FLT3	FYN	GAK	GRK1	GSK3B
1	92	90	77	100	81	98	97	100	93	94	79	96	85	95	100	89	87	100	100	99	100
	100	100	100	50	77	100	88	100	86	78	78	58	71	93	100	99	88	100	97	100	100
74	0	1.4	5	100	100	96	100	0.1	0.4	100	92	72	93	79	100	87	66	76	93	100	9.1
	1.3	0.7	11	66	100	80	100	0.1	0.6	100	88	94	86	98	100	100	84	87	90	75	6.4
77	0.5	0.6	5.2	95	100	100	65	0.2	0.8	81	80	100	97	91	100	100	100	87	88	100	12
	0	0.6	7.3	97	100	84	50	0.1	0.3	97	100	100	100	82	32	100	100	97	100	100	6.8

Cmpd	HPK1	IGF1R	INSR	IRAK4	JAK2 (JH1 domain-catalytic)	JNK3	KIT	LCK	LIMK1	LYN	MAP3K1	MAP4K4	MAPKAPK 2	MARK1	MARK3	MEK3	MEK5	MET	MKNK1	MLK1	MST2
1	92	85	100	100	100	93	100	96	100	81	85	93	94	100	90	100	83	100	100	100	100
	81	99	92	100	100	100	100	76	100	80	86	80	94	100	100	100	100	81	100	90	84
74	64	94	78	100	100	86	80	100	100	85	100	92	96	100	100	25	100	100	85	99	100
	84	100	100	91	100	83	75	99	100	81	97	72	100	100	86	30	79	88	84	100	100
77	100	76	86	100	100	46	78	81	78	92	93	89	100	100	96	35	90	86	55	94	74
	100	94	82	100	100	70	83	74	96	88	100	99	100	100	100	65	80	92	66	100	71

Cmpd	MTOR	NEK4	NEK6	OSR1	p38-alpha	p38-gamma	PAK2	PCTK3	PDGFRB	PIK3CA	PIK3CD	PIM1	PKAC-alpha	PLK1	PLK4	PRKCE	PRKD2	PRKG1	PRKR	RIPK2	ROCK2
1	93	100	85	100	97	100	100	100	100	100	100	88	100	100	100	100	100	100	92	100	92
	96	100	65	100	76	100	99	76	89	100	97	75	100	100	100	100	99	75	100	99	100
74	100	100	81	90	99	65	100	100	57	100	78	83	84	100	99	100	92	88	92	100	43
	93	93	93	82	95	86	100	100	52	78	88	98	69	100	92	73	100	96	68	82	34
77	100	100	100	92	100	100	89	100	62	83	55	99	83	88	100	100	83	85	92	96	27
	74	76	85	100	100	91	93	100	71	100	62	99	70	100	100	100	77	51	100	100	29

Cmpd	RPS6KA5 (Kin.Dom.1-N-terminal)	RSK1 (Kin.Dom.1-N-terminal)	S6K1	SRC	STK33	SYK	TAK1	TAOK2	TBK1	TGFBR1	TIE2	TRKA	TSSK1B	TYK2(JH1 domain-catalytic)	VEGFR2	WEE1	YANK2	YSK4
1	100	98	92	81	100	97	100	100	100	100	100	100	96	100	79	87	100	96
	100	100	83	81	100	100	65	100	100	100	67	100	89	100	74	73	82	97
74	100	94	100	100	100	83	34	55	100	97	88	100	100	100	100	74	100	41
	100	92	75	100	100	72	78	58	85	72	82	100	100	100	56	80	100	38
77	100	67	86	100	100	62	50	25	100	91	99	98	87	96	98	94	100	68
	100	100	42	100	100	56	49	32	100	100	100	92	83	94	92	100	88	34

Compounds at 1 µM concentration were tested in duplicate for inhibition of 100 kinases in competitive binding assays (KinomeSCAN, Ambit Bioscience, Inc.). Percent inhibition of control is indicated; kinases inhibited more than 50% are marked in yellow, and kinases inhibited more than 90% are marked in pink.[2]

[2] Fabian, M. A.; Biggs, W. H., 3rd; Treiber, D. K.; Atteridge, C. E.; Azimioara, M. D.; Benedetti, M.G.; Carter, T.A.; Ciceri, P.; Edeen P,T.; Floyd, M; Ford, J. M.; Galvin, M.; Gerlach, J. L.; Grotzfeld, R. M.; Herrgard, S.; Insko, D. E.; Insko, M. A.; Lai, A. G.; Lélias, J. M.; Mehta, S. A.; Milanov, Z. V.; Velasco, A. M.; Wodicka, L. M.; Patel, H. K.; Zarrinkar, P. P.; Lockhart, D. J., A small molecule-kinase interaction map for clinical kinase inhibitors. *Nat. Biotechnol.* **2005**, *23* , 329–336.

Supplementary Figure 3. Determination of the K_m(app) for Cdc7 kinase

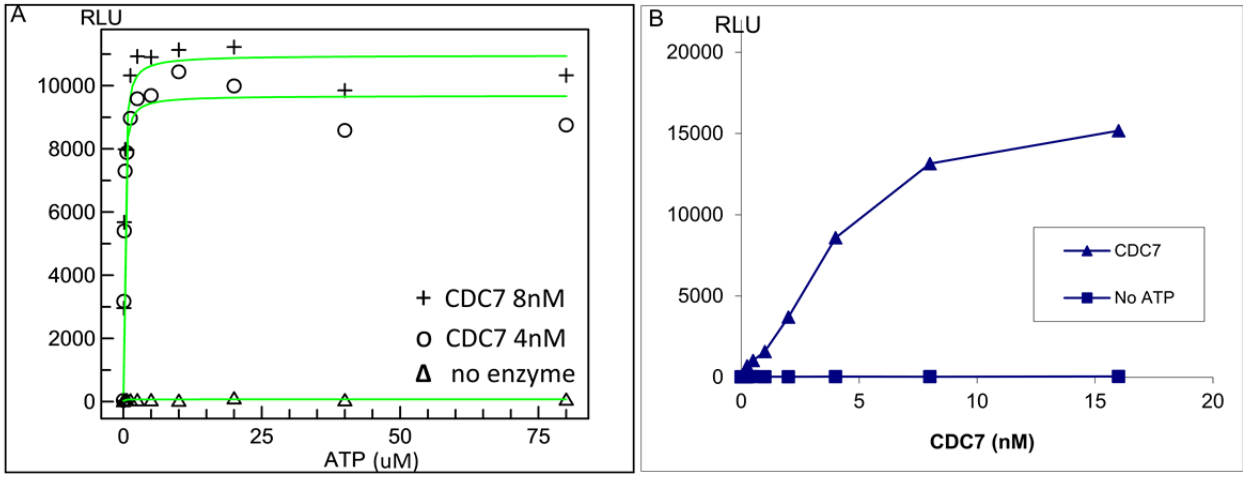

A, Enzymatic activity of Cdc7 kinase was determined by Alpha Screen assay to detect phosphorylation of the serine 53 residue of the MCM2 protein. Cdc7 protein concentrations of 8 nM and 4 nM were assayed. RLU = relative luminescence units.
B, Using a Cdc7 protein concentration of 4 nM, the ATP concentration in the AlphaScreen reaction was then varied to determine the K_m(app) for Cdc7.1

Supplementary Figure 4. Mechanism of Action Studies on Compound **74**

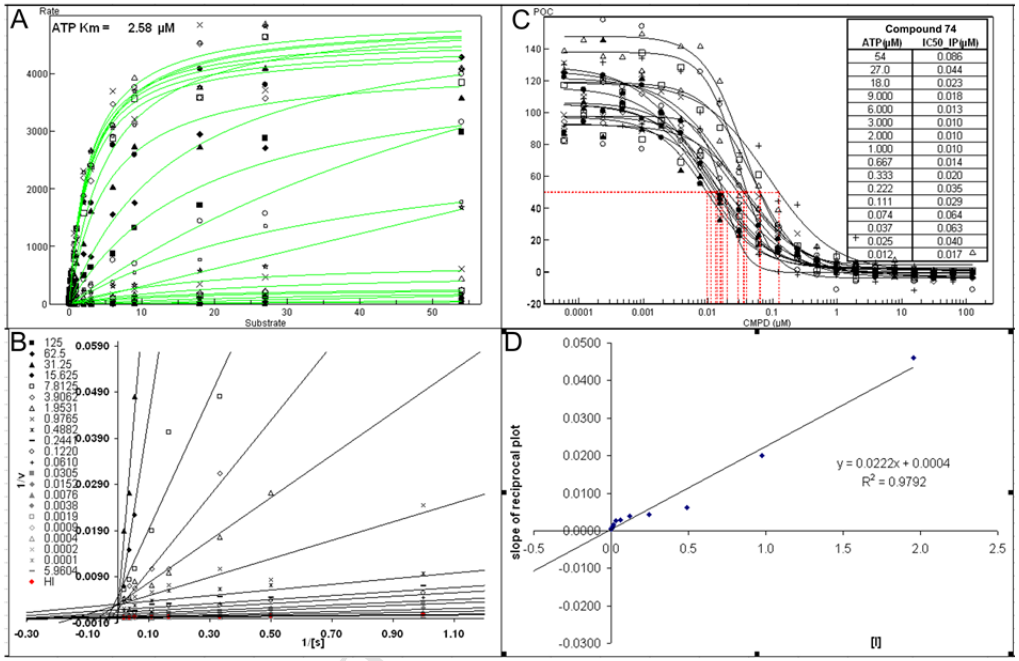

Compound **74** is an ATP-competitive inhibitor. The rate of Cdc7 enzymatic activity was determined from an AlphaScreen assay (see Experimental Procedures) following titration of ATP and compound **74**. The results fit the competitive model for enzyme inhibition. Effects of ATP on Cdc7 enzymatic activity with various concentrations of compound **74** are shown in Michaelis–Menton (**A**) and double-reciprocal plot (**B**) formats. **C**, Compound **74** inhibitor potency was determined in the AlphaScreen assay. **D**, Slope of the double-reciprocal plot versus inhibitor concentration. Mechanism of action studies to determine whether inhibition of the Cdc7 enzyme was competitive or non-competitive were carried out using an AlphaScreen assay using 6 nM Cdc7/Dbf4 protein, 10 nM MCM2 protein, and varying the concentrations of ATP (from 3 µM in 1:2 titrations) and compounds (from 125 µM in 1:2 titrations). Reaction time was 2 h. Reaction rates, K_m, and K_i were determined as reported previously.1 The K_m was determined from AlphaScreen assays of Cdc7 enzymatic activity, varying the concentration of Cdc7/Dbf4 protein or the concentration of ATP.

Supplementary Figure 5. Compound **74** Causes Aberrant Mitosis

DMSO

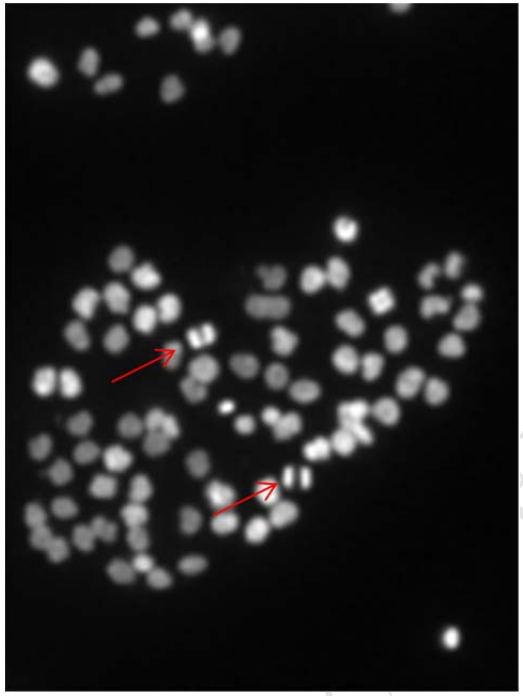

1.25 μM of compound **74**

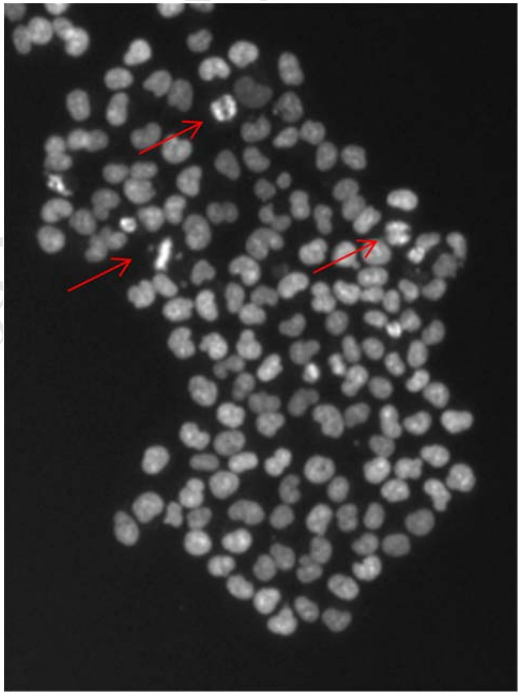

HCT-116 cells were treated with DMSO or with 1.25 μM of with compound **74** for 72 h, and then fixed with 4% formaldehyde in PBS, permeabilized with PBS that contained 0.5% Triton X, and then stained with Hoechst dye to visualize cell nuclei. Images were collected using a Cellomics ArrayScan with 20× objectives. In the cells treated with DMSO only, the nuclei have a regular shape and show equal segregation of chromosomes at mitosis (arrows). In contrast, in the cells treated with compound **74**, mitotic cells (arrows) display defects such as lagging chromosomes (DAPI-positive material that is outside of or in between the main chromosomal mass).

Date	22 Mar 2010 15:12:47		
Date Stamp	22 Mar 2010 15:12:47		
File Name	\\scone\NMR-Archive\jcamp\hshu\2010\110985-49-1_12.dx		
Frequency (MHz)	400.35	***Nucleus***	1H
Number of Transients	16	***Origin***	Bruker BioSpin GmbH
Owner	shr-ato-nmr1	***SW(cyclical) (Hz)***	6410.06
Solvent	DMSO-d6	***Spectrum Offset (Hz)***	2396.0457
Sweep Width (Hz)	6409.86	***Temperature (degree C)***	27.000

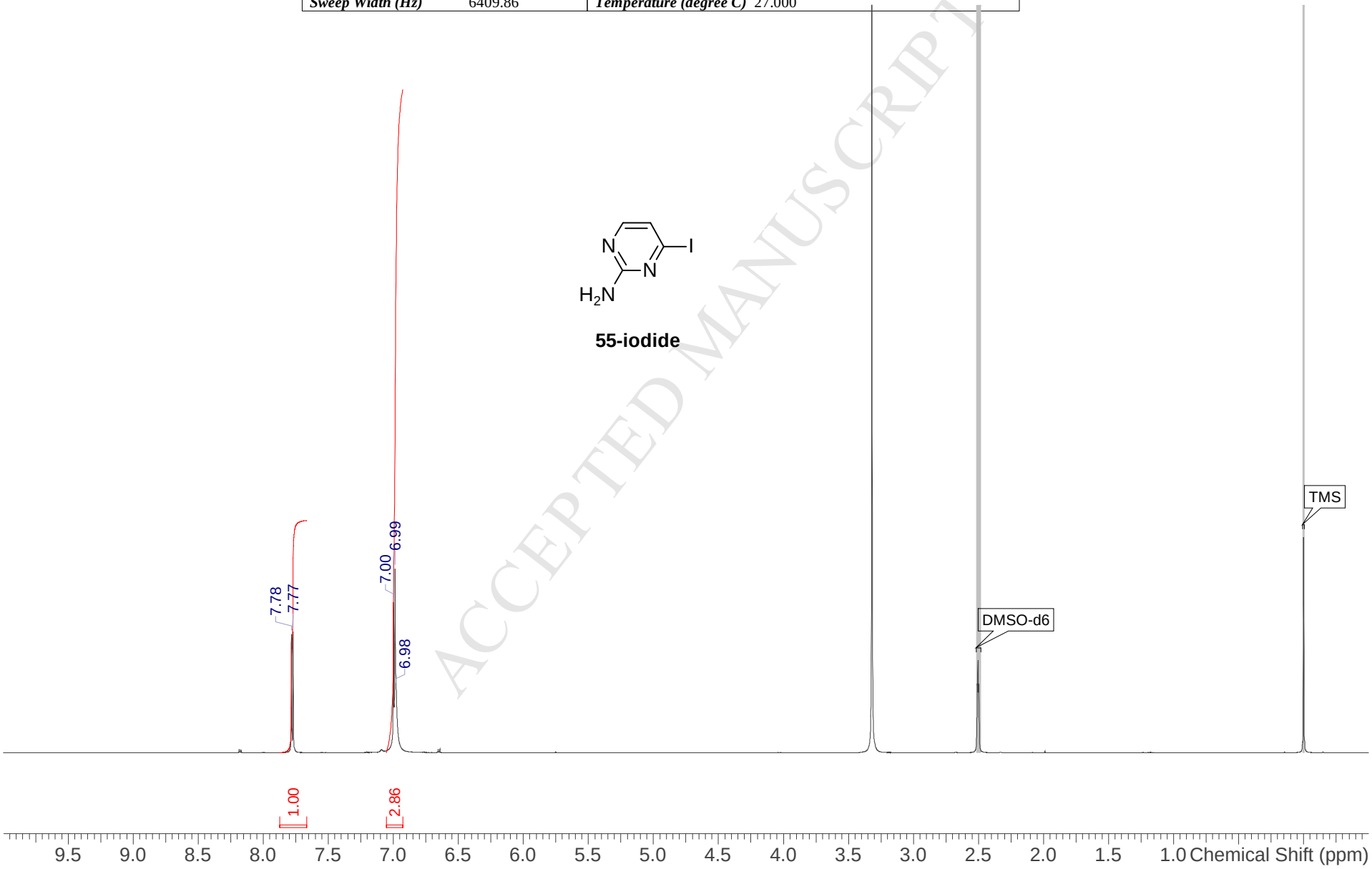

Date	24 Mar 2010 10:08:53		
Date Stamp	24 Mar 2010 10:08:53		
File Name	\\scone\NMR-Archive\jcamp\hshu\2010\111234-3-1_10.dx		
Frequency (MHz)	400.13	***Nucleus***	1H
Number of Transients	16	***Origin***	Bruker BioSpin GmbH
Owner	shr-ato-nmr1	***SW(cyclical) (Hz)***	6410.06
Solvent	DMSO-d6	***Spectrum Offset (Hz)***	2399.5669
Sweep Width (Hz)	6409.86	***Temperature (degree C)***	25.000

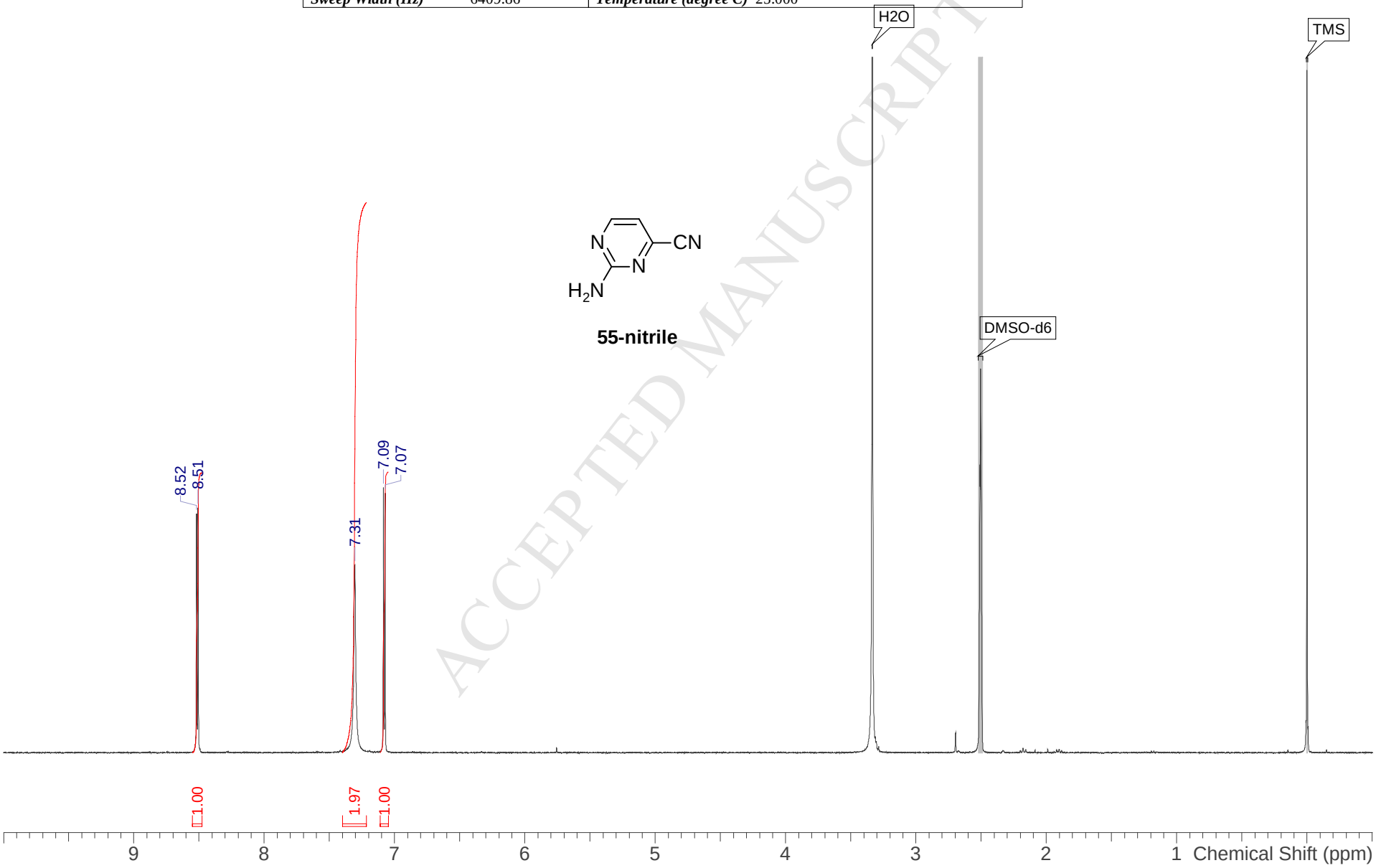

Date	22 Apr 2010 15:10:23		
Date Stamp	22 Apr 2010 15:10:23		
File Name	\\scone\NMR-Archive\jcamp\hshu\2010\111234-20-1_10.dx		
Frequency (MHz)	400.23	***Nucleus***	1H
Number of Transients	16	***Origin***	Bruker BioSpin GmbH
Owner	shr-ato-nmr1	***SW(cyclical) (Hz)***	6410.06
Solvent	DMSO-d6	***Spectrum Offset (Hz)***	2402.4883
Sweep Width (Hz)	6409.86	***Temperature (degree C)***	27.000

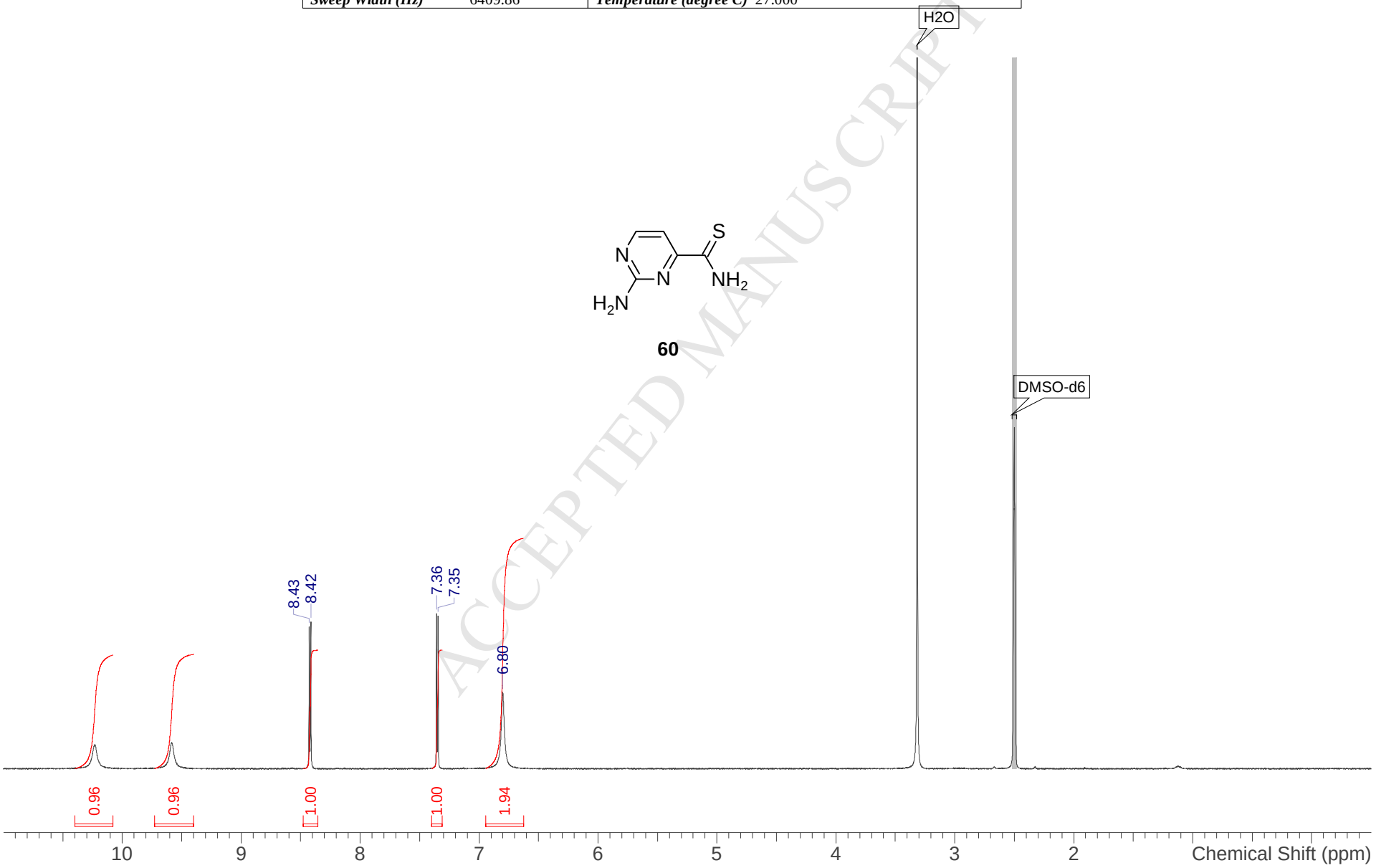

60

Date	14 Dec 2009 18:31:57		
Date Stamp	14 Dec 2009 18:31:57		
File Name	\\scone\NMR-Archive\jcamp\gyao\2009\110742-36-1_10.dx		
Frequency (MHz)	400.23	***Nucleus***	1H
Number of Transients	32	***Origin***	Bruker BioSpin GmbH
Owner	shr-ato-nmr1	***SW(cyclical) (Hz)***	6410.06
Solvent	DMSO-d6	***Spectrum Offset (Hz)***	2403.2837
Sweep Width (Hz)	6409.86	***Temperature (degree C)***	27.000

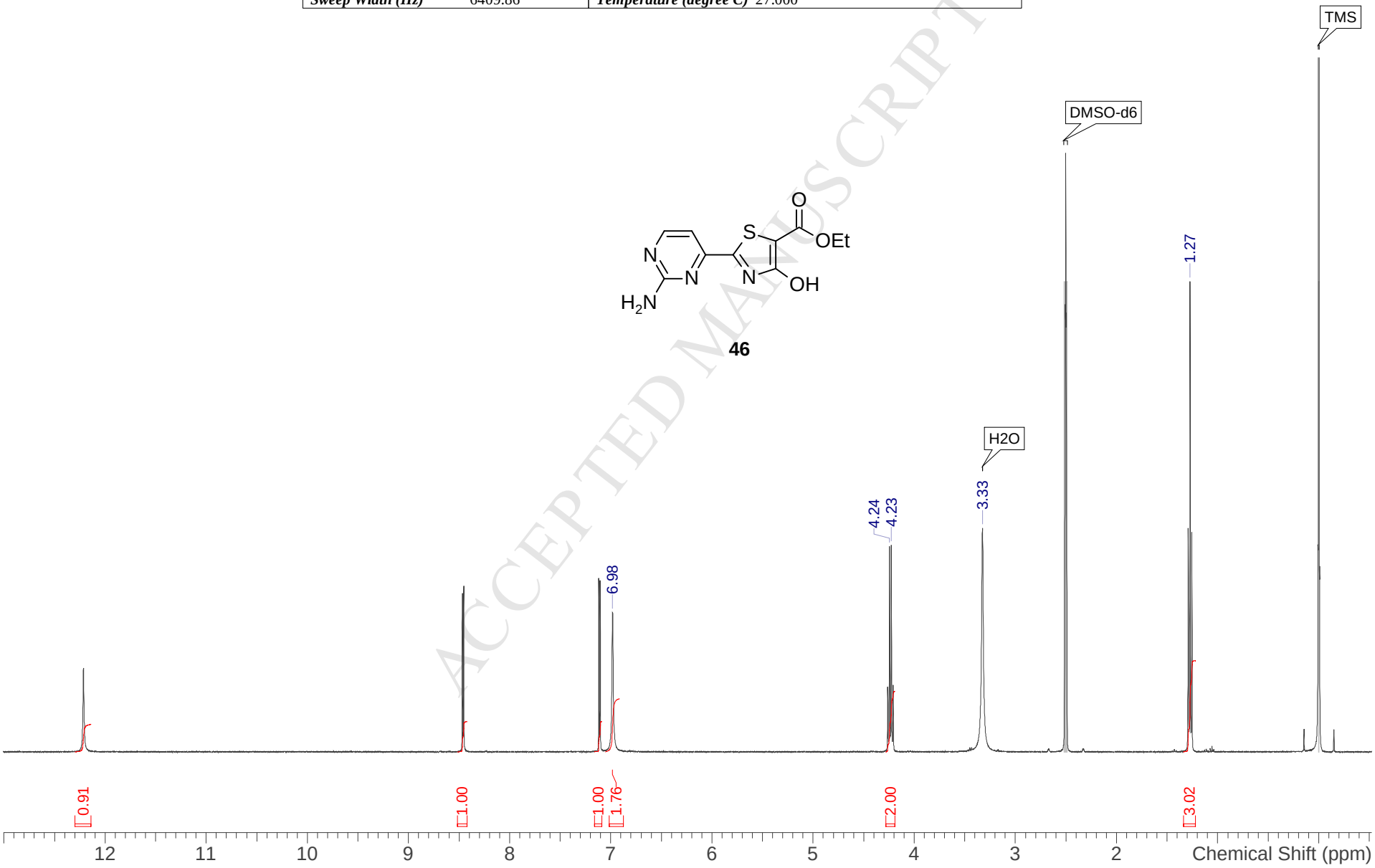

46

Date	12 Apr 2010 10:53:16		
Date Stamp	12 Apr 2010 10:53:16		
File Name	\\scone\NMR-Archive\jcamp\hshu\2010\111234-14-1_11.dx		
Frequency (MHz)	400.13	***Nucleus***	1H
Number of Transients	16	***Origin***	Bruker BioSpin GmbH
Owner	shr-ato-nmr1	***SW(cyclical) (Hz)***	6410.06
Solvent	DMSO-d6	***Spectrum Offset (Hz)***	2397.7390
Sweep Width (Hz)	6409.86	***Temperature (degree C)***	25.000

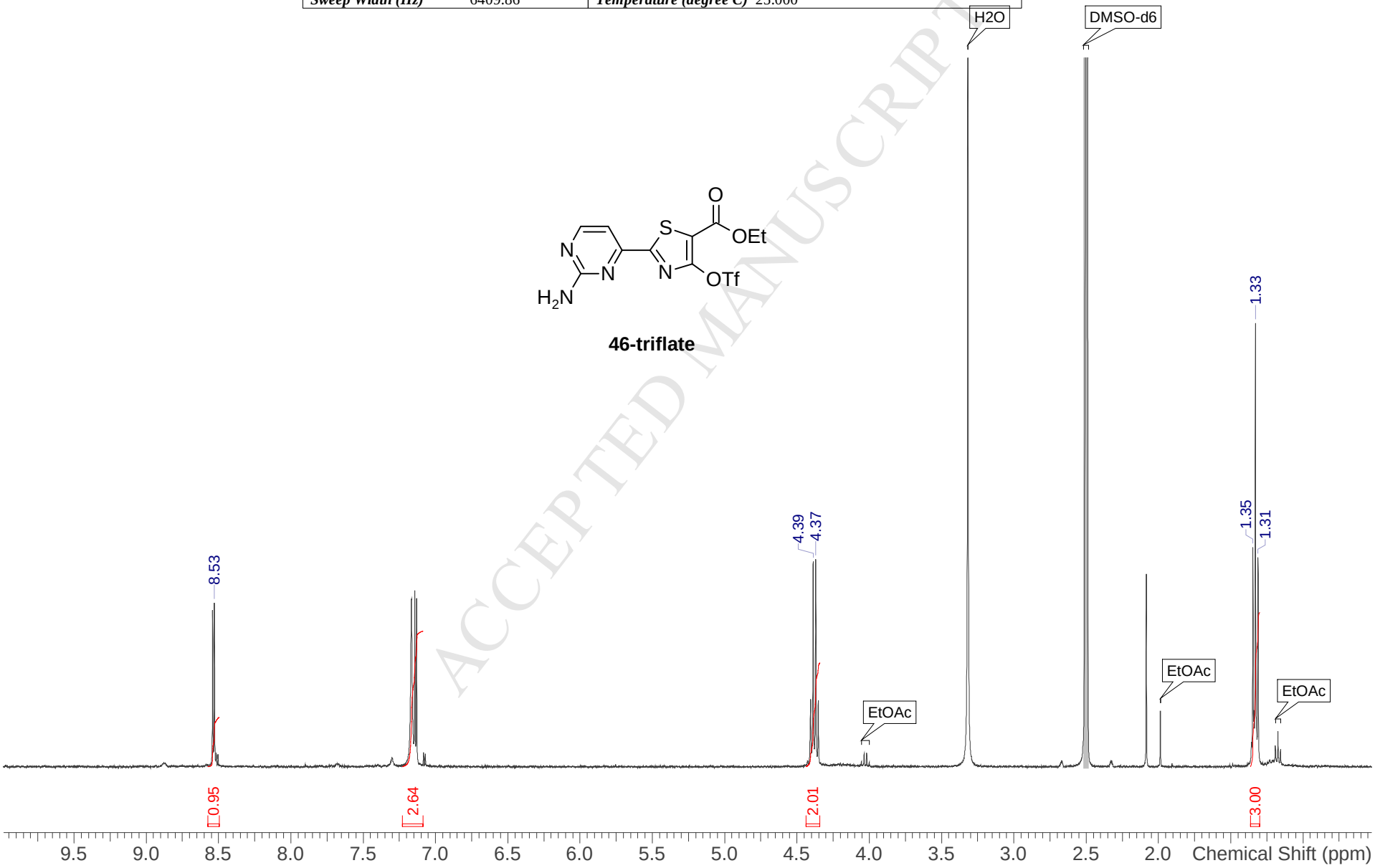

46-triflate

Date	14 Jan 2010 19:40:24		
Date Stamp	14 Jan 2010 19:40:24		
File Name	\\Scone\NMR-Archive\jcamp\andreasr\2010\110727-15-3_10.dx		
Frequency (MHz)	300.13	***Nucleus***	1H
Number of Transients	64	***Origin***	Bruker BioSpin GmbH
Owner	shr-ato-nmr1	***SW(cyclical) (Hz)***	4789.27
Solvent	CHLOROFORM-d	***Spectrum Offset (Hz)***	1795.1732
Sweep Width (Hz)	4789.13	***Temperature (degree C)***	27.000

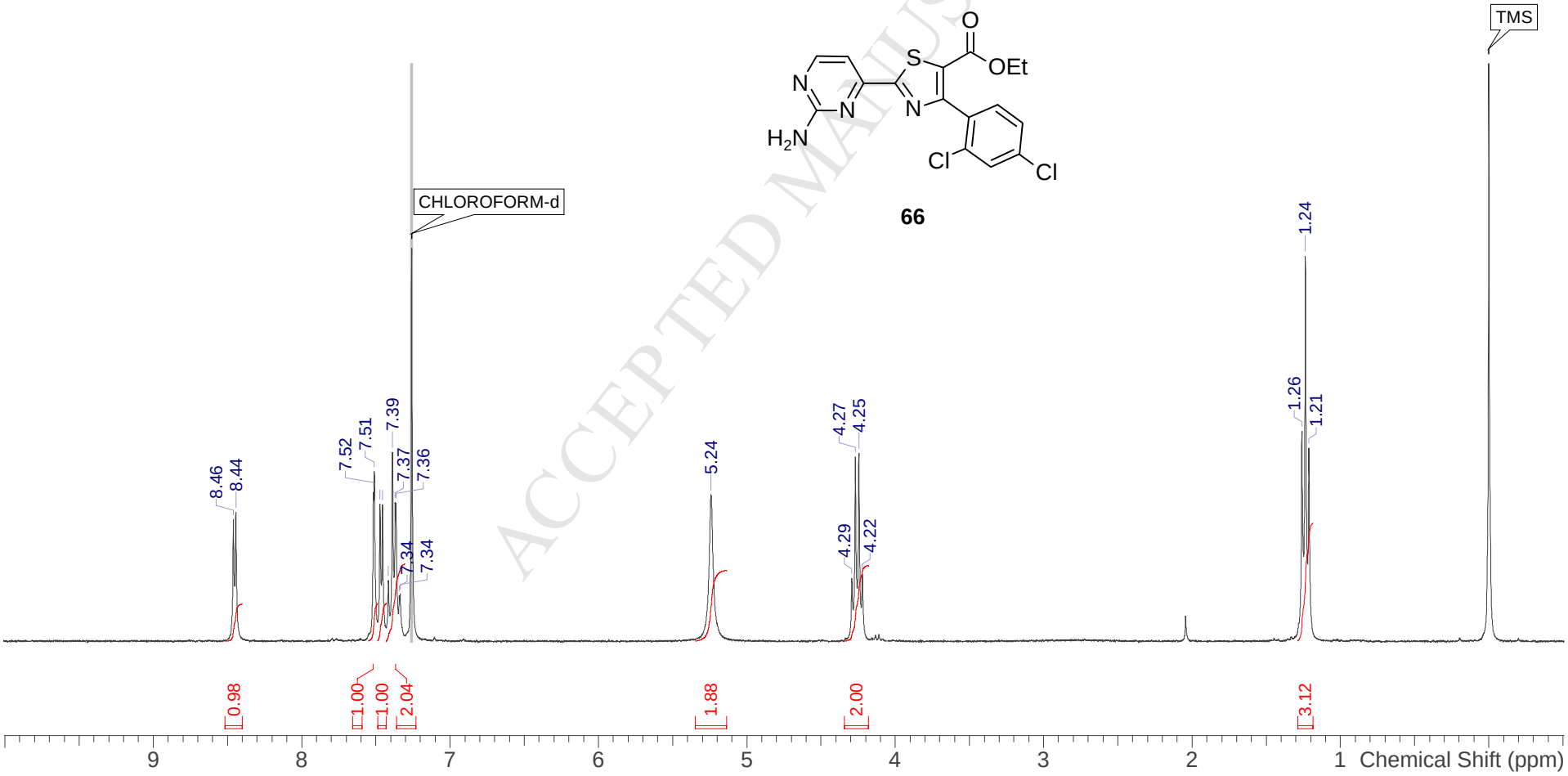

Date	19 Jan 2010 18:30:17		
Date Stamp	19 Jan 2010 18:30:17		
File Name	\\Scone\NMR-Archive\jcamp\andreasr\2010\110727-16-6_10.dx		
Frequency (MHz)	400.23	***Nucleus***	1H
Number of Transients	64	***Origin***	Bruker BioSpin GmbH
Owner	shr-ato-nmr1	***SW(cyclical) (Hz)***	6410.06
Solvent	DMSO-d6	***Spectrum Offset (Hz)***	2402.6838
Sweep Width (Hz)	6409.86	***Temperature (degree C)***	27.000

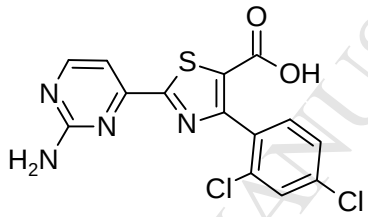

66-acid

Date	25 Jan 2010 16:30:24		
Date Stamp	25 Jan 2010 16:30:24		
File Name	\\Scone\NMR-Archive\jcamp\andreasr\2010\110727-17-6_10.dx		
Frequency (MHz)	300.13	***Nucleus***	1H
Number of Transients	64	***Origin***	Bruker BioSpin GmbH
Owner	shr-ato-nmr1	***SW(cyclical) (Hz)***	4789.27
Solvent	DMSO-d6	***Spectrum Offset (Hz)***	1801.1656
Sweep Width (Hz)	4789.13	***Temperature (degree C)***	27.000

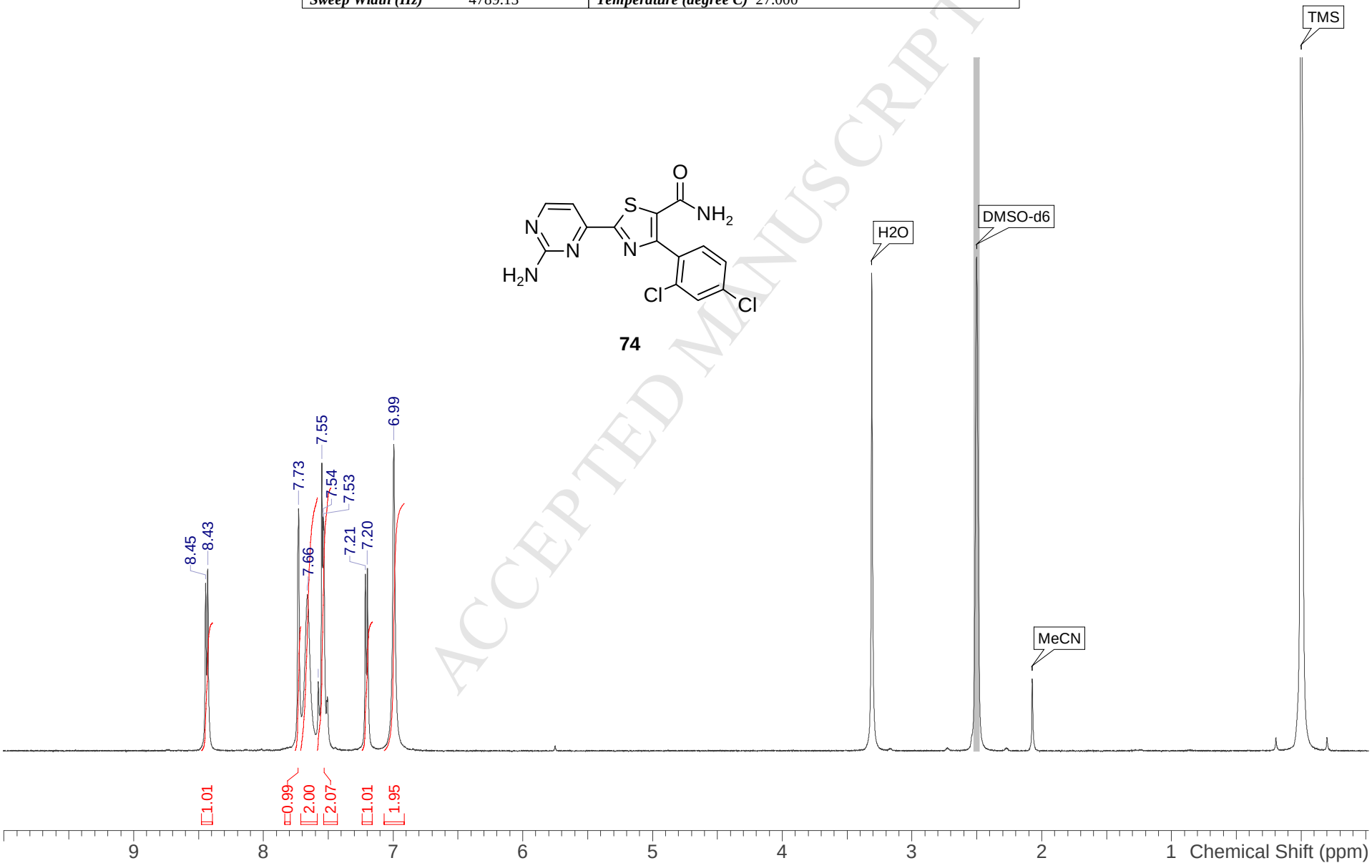

74

Date	25 Mar 2014 22:19:47		
Date Stamp	25 Mar 2014 22:19:47		
File Name	\\scone\NMR-Archive\jcamp\lewisp\2014\121490-8-1_11.dx		
Frequency (MHz)	100.68	***Nucleus***	13C
Number of Transients	2048	***Origin***	Bruker BioSpin GmbH
Owner	shr-ato-nmr1	***SW(cyclical) (Hz)***	23147.44
Solvent	DMSO-d6	***Spectrum Offset (Hz)***	10015.7803
Sweep Width (Hz)	23146.73	***Temperature (degree C)***	27.000